KU LEUVEN

ARENBERG DOCTORAL SCHOOL
Faculty of Engineering Science

Grid Planning for the Future Grid

Optimizing Topology and Technology Considering Spatial and Temporal Effects

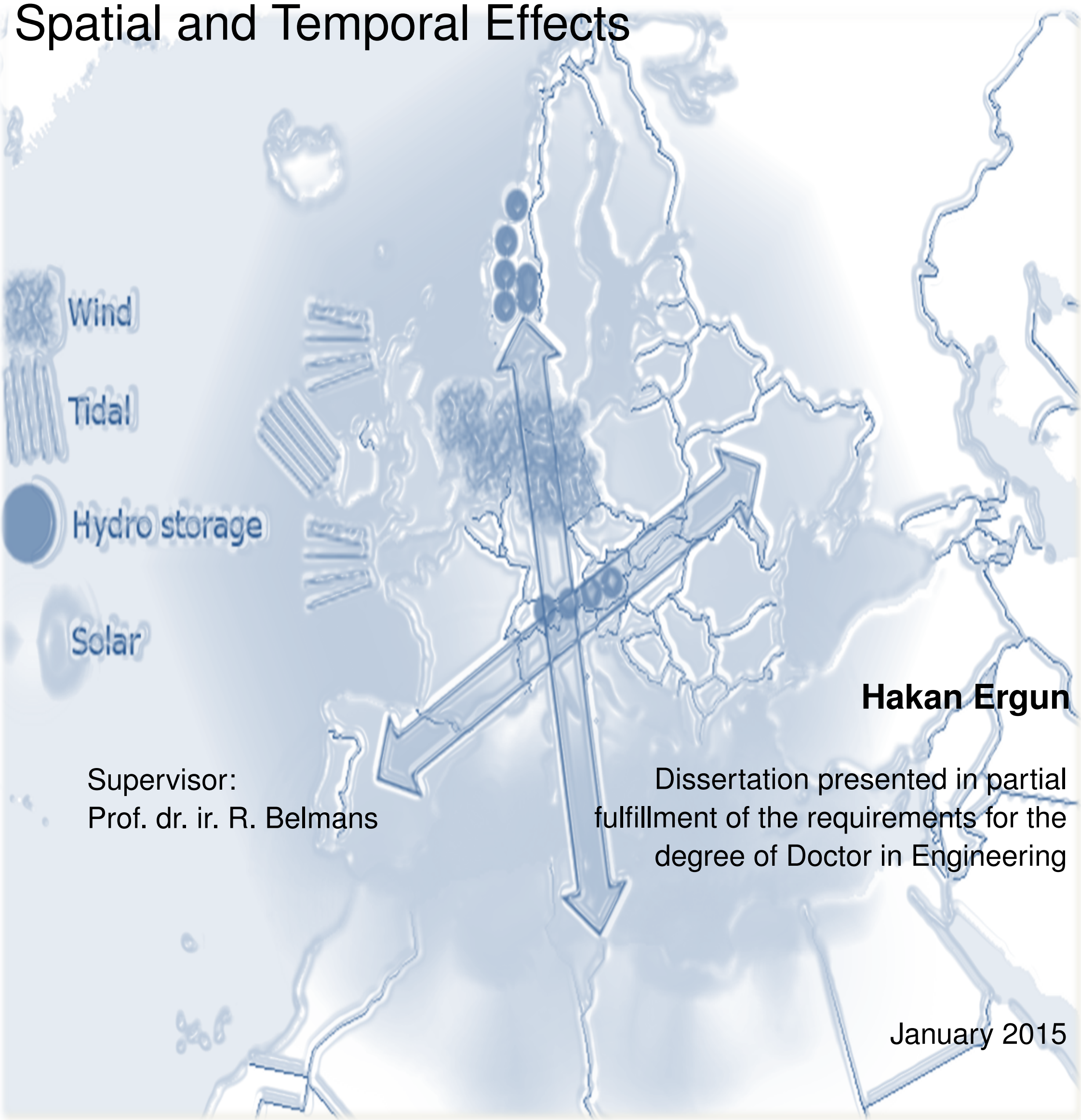

Hakan Ergun

Supervisor:
Prof. dr. ir. R. Belmans

Dissertation presented in partial fulfillment of the requirements for the degree of Doctor in Engineering

January 2015

Grid Planning for the Future Grid

Optimizing Topology and Technology Considering Spatial and Temporal Effects

Hakan ERGUN

Examination committee:
Prof. dr. A. Bultheel, chair
Prof. dr. ir. R. Belmans, supervisor
Prof. dr. ir. W. D'haeseleer
Prof. dr. ir. D. Van Hertem
Prof. dr. ir. N. Hadjsaid
(Technical University of Grenoble)
Prof. dr. Dipl.-Ing. H. Renner
(Graz University of Technology (TUG))
Prof. dr. Dipl.-Ing. A. Sumper
(Technical University of Catalonia (UPC))
Ir. M. Berger
(Elia Grid International)
Dr. ir. A. Oudalov
(ABB Corporate Research Switzerland)

Dissertation presented in partial fulfillment of the requirements for the degree of Doctor in Engineering

January 2015

Uitgegeven in eigen beheer, Hakan Ergun, Kasteelpark Arenberg 10, Bus 2445, B-3001 Heverlee (Belgium)

ISBN 978-94-6018-957-9

D/2015/7515/13

A smile is cheaper than electricity and brings more light - Saint Pierre

Abstract

Increased use of renewable energy sources and the creation of an internal electricity market have resulted in higher and more volatile power flows in the transmission grid. Due to a sustained climate policy, the share of renewable energy sources in electricity generation will increase over the coming decades. To cope with the expected future power flows, new transmission system investments are inevitable. Over the coming decades, in Europe alone, transmission system investments worth several hundred billion Euro are foreseen.

The aim of transmission system planning is to provide an expansion scheme for the transmission network in order to fulfil future grid requirements. Transmission system planning is a complex and multidimensional problem due to the high number of uncertainties and influencing parameters. Therefore, it is difficult to obtain a unique optimal investment plan which satisfies all technical, economical, social and environmental constraints. Many different scenarios regarding generation, demand, market prices, technological and social developments have to be analysed in the planning process in order to assess uncertainties and minimize the investment risks.

This dissertation provides the building blocks of a transmission system investment optimization methodology to assess different future scenarios in a fast and effective way. The methodology consists of different modules which can be combined to a single framework or used separately by transmission system planners. The optimization takes the geographic and demographic properties of the area of interest into account which are not included in existing transmission system investment optimization methodologies. It delivers a stepwise transmission system investment plan containing the optimal time point, power rating, transmission route and transmission technology for new investments. Another new feature of the developed methodology is the determination of strong grid nodes based on probabilistic optimal power flow solutions.

Beknopte samenvatting

Toegenomen gebruik van hernieuwbare energiebronnen en de totstandkoming van een interne markt voor elektriciteit hebben tot hogere en meer volatiele energiestromen in het transmissienet geleid. Het volgehouden klimaatbeleid, zal in de komende decennia het aandeel van hernieuwbare energiebronnen in de elektriciteitsproductie verder doen toenemen. Om met de verwachte toekomstige energiestromen te kunnen omgaan, zijn nieuwe investeringen in het transmissienet onvermijdelijk. In de komende decennia zijn investeringen in het transmissienet ter waarde van enkele honderden miljarden euro voorzien.

Transmissienetplanning heeft tot doel de uitbreiding van het transmissienet uit te werken zodat het transmissienet van alle toekomstige eisen kan voldoen. Transmissienetplanning is een complex en multidimensionaal probleem te wijten aan het groot aantal onzekerheden en beïnvloedende parameters. Daarom is het moeilijk om een optimaal investeringsplan te vinden dat aan alle technische, economische, sociale en milieueisen voldoet. Een groot aantal verschillende scenario's met betrekking tot productie, vraag, marktprijzen, technologische en maatschappelijke ontwikkelingen moeten in de planning geanalyseerd worden om onzekerheden te beoordelen en het investeringsrisico te beperken.

Dit proefschrift levert de verschillende bouwstenen van een transmissiesysteem investeringsoptimalisatie methodologie om verschillende toekomstscenario's op een snelle en effectieve manier te beoordelen. De beschreven methodiek bestaat uit verschillende modules die kunnen gecombineerd worden tot een gloabaalaanpak of afzonderlijk gebruikt door planners. De optimalisatie houdt rekening met de geografische en demografische eigenschappen van het beschouwde gebied die niet zijn opgenomen in de bestaande transmissienet investeringsoptimalisatie methodieken. Zij levert een stapsgewijze transmissienet investeringsplan die het optimale tijdstip, vermogen, transmissie route en transmissie technologie voor nieuwe investeringen bevat. Een ander nieuw element van de ontwikkelde methodiek is het bepalen van de sterke

knooppunten op basis van probabilistische optimale power flow berekeningen.

Acknowledgements

The following chapters are the closing words of a significant chapter of my life. Nearly five years ago, I left Austria to come to Belgium and start my PhD. I had beautiful years, making many new experiences and learning many interesting and exciting things. On this five year journey, I came across many people who guided me and walked along with me helping me to develop different professional and personal skills and shaping me to be the person I am today. I think, this is the right occasion to thank them.

First, I want to thank *Ronnie Belmans*, my promoter. Thank you for being there in case of need and at the same time leaving me the freedom in my research and not being too strict on deadlines or working hours. I am most thankful for challenging me as I know that one can only grow with the challenges he has to master. Just to give an example, since I have been in Erfurt pretty much at the beginning of my PhD, I am not afraid of conferences any more. And of course, I also need to thank you to keep me update about upcoming concerts and broadening my rock music horizon.

My *Leuven experience* started with a skype call I had with *Dirk Van Hertem* in October 2009. The whole decision making process happened quite quickly - somewhat ironically considering the content of this thesis - and we agreed in a couple of weeks that I should do my PhD in Leuven. Eventually, I found myself in Leuven in February 2010 after all the paperwork was done. Dirk, although you were having an intermezzo in Sweden, you sacrificed a lot of precious weekend time to give direction to my research which I highly appreciate. I thank you for all the long discussions we had, for the papers we have written and the work we have done together in the TRIP project in the last five years. It is a pleasure working with you. You have been the perfect guide, being critical and supportive throughout my research. I also need to thank you for teaching me extra curricular things such as life in Belgium, single malt scotch whiskies and Belgian cuisine. I believe that without this supportive information, my working efficiency would have been much lower, as let's face the truth, Belgium is quite depressing in terms of weather.

The day we visited TU Delft or when you came by in Leuven for the first IEEE Energy Sessions, I wouldn't have suspected that we would become colleagues very soon. Suddenly, you were here in Leuven to work with us on the TRIP project. *Barry "the Bear" Rawn*, thank you for all the long discussions we had, eventually leading to the publications which are the basis of this thesis. Also thank you very much for reading this thesis and providing valuable input. And also thank you for coping with my strange kind of humour and making my birthday parties unforgettable!

I am very glad that I could do my research in the course of the *TRIP* project. I want to thank to ABB, Elia and Vattenfall for supporting my research, providing me data and more importantly sharing their experience. I want to thank Magnus Callavik, Johan Ahstrom, Hubert Lemmens, Christoph Druet, Johan Söderbom, Mats Nilsson and Kristian Gustafsson to make the TRIP project happen. I especially want to thank Alexndare Oudalov for hosting me at the ABB Corporate Research Centre in Switzerland and Christoph Druet, Fabian Georges, Peter Van Roy and Thierry Springuel at the grid development department of Elia respectively. I am happy that I could learn many interesting things in a friendly working climate and with excellent coffee!

Well, people who me know that I love the city of Leuven and think that is is a great place to live. In my opinion, a city is a reflection of the people who populate it. In the past five years, I have met wonderful people here most of them being my colleagues. You made me feel home every time, inside and outside the of *Electa* office. That's why I enjoyed coming to office everyday, knowing that my day will at least be fun if it not productive. It is difficult to find such a large research group where the interaction is inside and outside of the office is so close and personal.

First of all, thank you guys of the *Power Group*! Especially, *Jef, David, Stijn, Simon, Patrik, Kristof, Pieter, Steven, Cedric, Willem and Robert* for being more than just a colleague. Thank you for introducing me in the art of barbecuing, teaching me the Dutch language, making me aware of Esperanto music, keeping me up to date with the latest concert agenda, broadening my beer horizon and travelling to the end of the world together. I am sure that we will keep the power spirit alive among the new colleagues as well.

Electa is of course more than just the *Power Group.* Thank you all for coping with my strange kind of humour, the politically incorrect and definitely inappropriate talks we had for lunch and all the fun things we did together. *Frederik, Niels, Jeroen, Juan and Carlos* thank you for your friendship and support. I had a great time in everything we did.

I also want to thank the guys of the *IEEE Student Branch Leuven* for their help and dedication in everything we did. It was a great experience to organize many lectures, symposia, trips, soireé techniques and of course, beer tastings together.

I want to thank the technical staff for not getting mad when I set things on fire in the lab from time to time. I also want to thank the administrative staff, especially *Katleen*, for managing the excessive amount of paper work, being patient with me and setting up all the "Tolintos".

Jan, although we did a lot of insane things together, you are the person who kept me sane during my PhD. I can not thank you enough for always being there, cheering me up in times of sadness, celebrating with me the good times, listening constantly to my complaints and problems and giving me the right advice to solve them. You are the definition of a true friend and it is a privilege being friends with you!

Moving to a new country to and starting a new life can be a scary experience. But somehow, in my family we seem to have it in our genes to be scattered in different parts of the world. Although we are many kilometres apart, I can always count on the support of my family in times of need. Thank you for everything you do for me. In future, I promise to do my best to remember birthdays, as apparently, I can not use the thesis-stress as an excuse any more.

Hakan Ergun
Leuven, January, 2015

List of Abbreviations

AC	Alternating Current
BFC	Brute Force Calculation
CB	Critical Branch
CPTE	Coordination de la Production et du Transport de lÉnergie électrique
DC	Direct Current
DP	Dynamic Programming
ECF	European Climate Foundation
ETSO	European Transmission System Operators
ENTSO-E	European network of transmission system operators for electricity
ERP	European Recovery Program
FACTS	Flexible Alternating Current Transmission Systems
GCCM	Gaussian Component Combination Method
HVAC	High Voltage Alternating Current
HVDC	High Voltage Direct Current
LLF	Line Limit Frequency
LODF	Line Overload Distribution Factor
LP	Linear Programming
MCS	Monte Carlo Simulation
MILP	Mixed Integer Linear Programming
MINLP	Mixed Integer Non-Linear Programming
MIP	Mixed Integer Programming
MPIC	Maximum Power Injection Capability
NLP	Non-linear Programming
OHL	Overhead Line
OPF	Optimal Power Flow
OWF	Offshore Wind Farm
PDF	Probability Distribution Function
PSDF	Phase Shifter Distribution Function

PST	Phase Shifting Transformer
PTDF	Power Transfer Distribution Factor
RES	Renewable Energy Sources
SEDAC	Socio-economic Data and Applications Centre
SSSC	Static Synchronous Series Compensator
TCSC	Thyristor Controlled Series Compensation
TSO	Transmission System Operator
UCPTE	Union for the Co-ordination of Production and Transmission of Electricity
UCTE	Union for the Co-ordination of and Transmission of Electricity
UGC	Underground Cable
VSC	Voltage Source Converter
WWII	World War II

Contents

List of Figures

List of Tables

Chapter 1

Introduction

To get the economy of the electric power, coordination of all the industries is necessary, and the electric power is probably today the most powerful force tending towards coordination, that is cooperation. - Charles P. Steinmetz

1.1 Historic Development of the European Transmission Grid

During the first World War, there has been a large increase in demand for electricity, especially, in the United States of America and in Germany. New factories were built to produce steel and nitrate, the basic component for fertilizers and explosives [1]. To meet the large demand required by such factories, new power plants with higher power ratings than at that time available were needed. In the United States hydro power plants were constructed, whereas in Germany mostly lignite was used. As these power plants were situated near the location of the primary energy, i.e. near rivers, resp. lignite mines, they were not always close to the location of the demand. Therefore, longer transmission distances needed to be bridged to connect load centres and power plants. High voltage transmission lines were used to increase the transmitted power while keeping the voltage drops and the transmission losses sufficiently low over these larger distances.

After World War I, there was an overcapacity in generation as demand crumbled and power plants could only be operated at reduced output. There was an urge to operate the electricity system in a more economic way. Therefore, first high voltage interconnections were built to link thermal and hydro generation units with each other. This way, demand could be met to larger extends by cheaper hydro power plants in seasons where rivers carried sufficient water. During low water seasons or frost, the majority of the electricity could be supplied by thermal units [2].

Another reason for interconnecting different areas was to flatten load profiles. The interconnected areas had their highest and lowest load levels in different hours of the day. By interconnecting these systems thus aggregating the load, flatter profiles could be achieved. The flat load profiles decreased generation costs as the power plants could run at their optimal operating points. In the early 1920s, first connections between Swiss hydro power plants in Gösgen and French thermal power plants in Nancy were established for this purpose [2]. Other interconnections were built to connect the lignite power plants in the Ruhr area in Germany with the hydro power plants in Switzerland and Austria. In 1930, RWE built the hydro storage power plant Vermuntwerk in Austria which was also connected to the thermal power plants in the Ruhr area. For this purpose the substation in Brauweiler has been put in operation 1929 [2]. This substation was the starting point of the *Verbundbetrieb*, which literally can be translated to *connected operation*. In Brauweiler, power plants and loads could be controlled and monitored enabling a more economic operation using complementary technologies.

Although Europe was politically diverging between the years 1930 and 1937, the idea of having an economically unified Europe was put forward by some politicians and scientists. The economic unification would create an internal market such as in the United States of America and help European countries to get out of the economic depression. The economic unification should also bring more peace in the region. As the electrical power supply was one of the major elements of economic growth, the electrical unification of Europe was proposed. Some politicians believed that if Europe was electrically and economically united, a peaceful and prosperous environment could be achieved. In early 1930s several ideas of a Pan-European electricity transmission grid were proposed. The proposed systems used transmission voltages of 220 kV, 400 kV or 660 kV. The most famous proposal was made by Oskar Oliven at the second World Power Conference in Berlin in 1930 (figure 1.1). He proposed a Pan-European 400 kV transmission grid operated at 220 kV until standardization was achieved [2]. The proposed transmission network had two main connection axis. The east-west axis would connect the Iberian peninsula with Turkey and the Ukraine and the north-south axis would connect Scandinavia with northern Italy and Yugoslavia.

The same year, the Belgian government came with a proposal of pursuing the idea of Oliven to establish the European electricity network. In the following

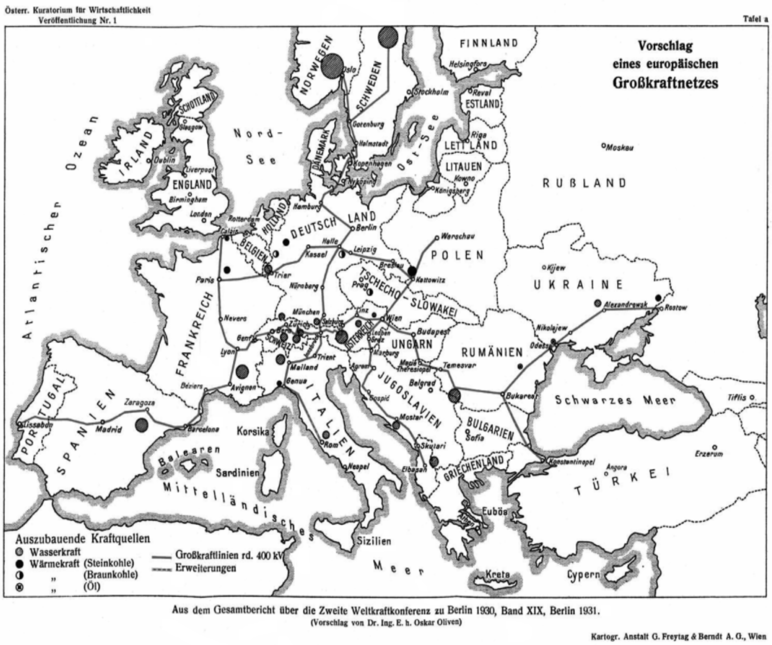

Figure 1.1: Pan-European transmission grid as proposed by Oskar Oliven at the second World Power Conference in 1930 [3]

years the matter was discussed at European level by decision makers, scientists and engineers. Eventually, this idea of a European network was abandoned as the majority of the discussing parties believed that national electricity grids with interconnecting lines to neighbouring countries would be more feasible than a European grid. One of the reasons was that the 400 kV technology was not yet sufficiently developed in the 1930s. Another aspect was that the proposed European grid did not take the underlying transmission grids and the ongoing processes of national network planning sufficiently into account [2].

In the pre WWII years and during the war, most countries developed national networks by connecting internal zones. This also required the installation of central dispatch units to coordinate operation as the latter became more and more complex. Two examples illustrating this are the creation of the Belgian *Coordination de la Production et du Transport de l'Énergie électrique - CPTE* established in 1937 and the German *Zentrallastverteiler* established in 1939.

These dispatch centres could control and monitor power plants and substations countrywide. During WWII, Germany established a number of connections to their neighbouring countries which they occupied or were allied with. One of the interesting ones is the 220 kV connection between Lutterade (Netherlands), Brauweiler (Germany) and Jupille (Belgium) established in 1944 but taken out of service after some months due to the developments in the war [2].

After WWII the European power system was separated mainly for political reasons. There were three separated transmission grids linked to the European Recovery Program (ERP) also known as the Marshall plan. Central and Western European countries who participated in the program, started to rebuild their demolished infrastructure and also established interconnections to other participants of the program wherever needed. Scandinavian and Eastern European countries who did not participate in the program started to build interconnections with neighbours in their own region. At the end of 1940s, ideas were put forward again to establish a European "super" grid as of the Marshall plan zone. By using 400 kV interconnections, the idea was to better coordinate the operation of thermal and hydro power plants and thus achieve higher economic benefits (figure 1.2).

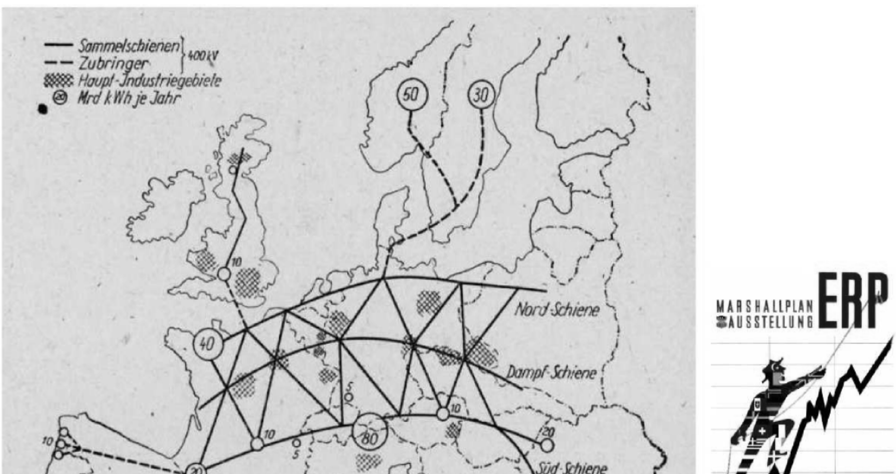

Figure 1.2: Vision of the European supergrid after the second world war

But as in the 1930s, the outcome was that countries should establish their own national networks first and build interconnections to their neighbouring countries only to support each other in case of need. The establishment of interconnections and the operation of tie lines were coordinated bilaterally. Therefore, most countries continued to build 150 and 220 kV connections on a national level as well as links with their direct neighbours.

In the decades following 1950, the European transmission grid grew gradually in a "natural" way. Generally speaking, the transmission system expanded together with the generation capacity needed to satisfy the increasing demand due to the rapidly growing economy. Although the idea of having one European transmission system was abandoned, there was a strong collaboration between different countries in planning and operation. In 1951, the first European power pool, the UCPTE, was established which aimed to coordinate planning and operation. Doing so, unnecessary reserves could be avoided and the economic performance of the electricity system improved. The cooperation in the electricity sector resulted in better connectivity between countries. As a matter of fact, in 1958, the entire UCPTE network was interconnected and operated synchronously at 50 Hz. The European transmission system continued to grow on national and international level using 400 kV transmission lines. In the following years, HVDC connections to non-synchronized regions such as Great Britain and Scandinavia were established. The natural growth of the system resulted in the transmission grid of today (figure 1.3). The cooperation in the electricity sector was further strengthened. In 1999, UCPTE was redefined as UCTE as an association of transmission system operators in the context of the liberalization of the internal energy market where generation, transmission and supply of electricity were unbundled. In 2009, the tasks of UCTE were merged with these of European Transmission System Operators (ETSO) to become the European network of transmission system operators for electricity (ENTSO-E).

1.2 European Grid Today and Future Perspectives

Today, once more the European electricity sector is facing changes and challenges. Driven by the European 20-20-20 targets, the share of generation from renewable energy sources (RES) in the total generation keeps increasing very fast. This has a major impact on the generation mix and the way the transmission grid is operated. Compared to 1990, the share of gross generation from renewable energy sources has increased from 0.5% to $8,8\%$ of total generation in 2010 (figure 1.4). By the end of this decade, the share of renewable energy generation from wind and solar resources is expected to be 18.7% of the total electricity production [5]. If the generation from hydro power plants is included in the calculation, the total share of generation from renewable energy sources is expected to be 34.7% of the total gross electricity

Figure 1.3: The Entso-e transmission grid [4]

production in 2020 [5]. This trend is expected to continue in the decades beyond 2020 in order to further decrease greenhouse gas emissions and dependency on foreign primary energy resources. The fact that especially solar and wind power generation technologies have reached a sufficient level of maturity, larger and more efficient systems are built which further help to decrease the cost of renewable energy.

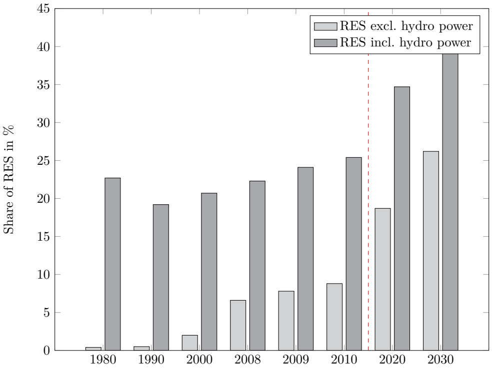

Figure 1.4: Share of generation from renewable energy sources between 1980 and 2030 [5]

While designing the transmission network, the expected power flows are used as basis of the design process. Obviously, the transmission network has to be designed in such a way that it can cope with them in a sufficiently reliable and economic manner. As power flows are the result of all injections and withdrawals, the expected installed capacity becomes more important in system planning than the energy transported over a certain period.

Looking at the installed capacity of generation units from renewable energy sources, a very similar increasing trend compared to the harvested energy is noticed (figure 1.5). By the end of this decade, the total installed capacity of wind power plants is expected to reach 18.9% of the total installed generation capacity in Europe [6]. Including solar generation, hydro generation and other renewable sources, the total expected share of installed generation capacity from renewable energy sources will reach 54.4% by 2030 [6]. In 2013, 72.5% of newly installed generation capacity used renewable energy sources [7].

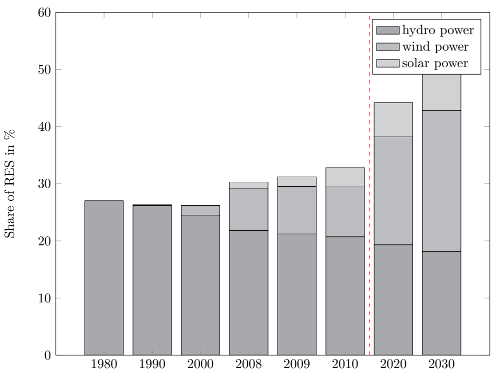

Figure 1.5: Share of installed RES capacity between 1980 and 2030 [6]

The intermittent nature of solar and wind power increases the volatility of flows in the European transmission grid significantly. Volatility is also affected by the liberalization of the European electricity market. The efforts to create a single European electricity market create higher competition on international level. This results in higher flows between countries or regions within a country. Over the last two decades, approximately 80 phase shifting transformers have been installed in the European transmission grid, showing the challenges of controlling such high volatility of power flows.

Ideally, solar and wind power farms should be built where the resources are available in contrary to distributed renewable energy sources. In reality, one of the important decision criteria for the selection of the location is the visual impact. The most favourable locations in terms of wind speed are the Atlantic

Coast, Baltic and North Sea region. For large scale solar power plants, the highest energy yield can probably be achieved around the Mediterranean Sea in southern Europe and Northern Africa (figure 1.6). Most of the new generation facilities using solar and wind power are expected to be installed in these regions. ENTSO-E affirms that there will be more volatile power flows over larger distances in the coming decade, due to the advancing European market coupling within and the relocation of generation facilities further from load centres [8]. The volatility of power flows in the European transmission network will increase both in duration and distance.

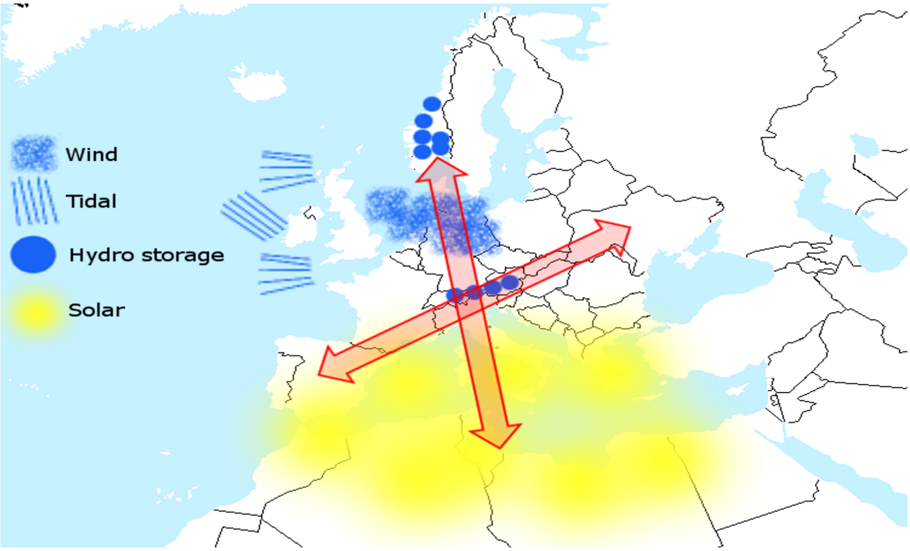

Figure 1.6: Schematic illustration of transmission grid investment needs on European scale

As stated in the 2012 ten year network development plan, ENTSO-E estimates that 52300 km of new or refurbished extra high voltage routes will be required in the coming decade [8]. In monetary terms, the investment need is estimated at 104 G€, equally spread over the coming decade [8]. A significant portion of these new investments will be used for submarine cables as there is a move towards installing large offshore wind farms and increasing the interconnection capacity between non-synchronous zones. Currently, the total amount of installed offshore wind power in Europe is approximately 7 GW. In 2013 alone, 1.3 GW of offshore wind power was installed [7]. If this trend continues, a total of approximately 23.5 GW offshore wind power will be installed by the end of this decade [9].

HVDC submarine connections are primarily used to connect non-synchronous areas but recently they are becoming embedded in systems within synchronous networks. In the future, more (HVDC) interconnections will be needed in order to satisfy the additional need for transmission capacity and further increase the competition and security of supply in Europe. ENTSO-E estimates that in the coming decade 23 G€ will be invested in submarine transmission infrastructure alone [8].

1.3 Motivation

For over more than 80 years, the idea of a European supergrid has been put forward in times of significant changes in the power sector, changes being of political or economical nature. Currently, the idea of a supergrid is put forward again, mainly due to climate policy driven renewable boom and the electricity market structure.

In the past, the maturity of technology has been one of the barriers for the implementation of a European supergrid. Obviously, there has been significant technological progress over the last 80 years and many technical obstacles for a supergrid have been removed. Especially, due to the developments in high voltage direct current and underground transmission technologies, the transmission of several GW of power over hundreds of kilometres has become feasible. However, the maturity of transmission technologies does not imply that such a European supergrid is feasible in all its aspects. The feasibility of such major infrastructure has to be analysed in depth in all technical, social, environmental and economic aspects.

There exist a number of studies investigating a European supergrid from different perspectives [10–16]. They provide rough maps showing different architectures of what such a European supergrid could look like. Nevertheless, there is no study or methodology analysing the European supergrid in all its dimensions [17]. In order to optimally use financial and natural resources, research and development of new transmission system planning techniques are required.

The planning and implementation of the European power system combining renewable energy sources and the transmission infrastructure to connect them, requires major engineering and computing effort. Such a European supergrid would be implemented step by step. The time horizon to realise a supergrid can reach several decades. Such long time horizons make infrastructure projects subject to a large number of uncertainties. Therefore, it is important to analyse a versatile number of scenario's in order minimize the risks.

As elaborated in the previous section, several 100 G€ should be invested in the European transmission grid over the coming decades following ENTSO-E. Using optimization techniques in the planning process, large savings can be achieved which increase the total social welfare making the transition towards more renewable energy more affordable. In case several future scenario's exist, optimal transmission grid architectures for each scenario can be determined. By comparing the optimal grid structure for each scenario, a structure can be derived which suits most scenarios and therefore minimizes investment risks.

1.4 Objectives, context and contribution

Objectives

The aim of this thesis is to provide the building blocks of a methodology to determine optimal grid architectures. If optimal grid architectures can be obtained in a fast and efficient way, a large number of scenarios can be compared. In this way, transmission system operators or independent system planners can analyse different future scenarios regarding generation, demand, available technology, construction delays and equipment prices under different assumptions in order to minimize the risk for future investments. The aim of this thesis is not to make a statement if a European supergrid as proposed in various sources is possible or not. It wants to provide a methodology to make such an assessment possible.

Context

This thesis is developed in the course of the industrial research project ***TRIP***, ***T****ransmission* ***R****emuneration and* ***I****nvestment* ***P****lanning* with the project partners ABB, Vattenfall and Elia, the Belgian transmission system operator. The aim of the *TRIP* project is to investigate and develop new methodologies for long term transmission system planning and regulatory framework design. This thesis focuses only on the first part and aims to develop a new methodology for long term transmission system planning introducing optimization techniques in the process. The regulatory aspects are addressed in the thesis of my fellow colleague Muhajir Mekonnen.

The thesis work has partly been performed at the Corporate Research Centre of ABB in Switzerland, where a new methodology is developed optimizing topology, power rating, technology selection, transmission routing and investment time point of new transmission system investments.

At the grid planning department of Elia, the optimization methodology is further refined and applied to the Belgian transmission grid for verification. The methodology has been used to assess possibilities of transmission grid expansion to enable the integration of offshore wind power in 2030. In the analysis, the optimization methodology is applied to different voltage levels of HVAC and HVDC equipment in order to determine the optimal voltage level of future investments. The methodology has delivered satisfactory results which cannot be published in this thesis due to confidentiality reasons.

The methodology and accompanying software tools are developed in such a way that they can be used by transmission grid planners as an addition to existing planning tools or combined to a single planning tool. They have been developed in a modular way allowing user interaction and interference. This allows the grid planner to include his experience in the optimization process and to analyse a set of scenarios to identify and investigate the most important parameters. The developed methodology and tools aim to provide a set of solutions which can be further analysed by grid planners rather than one optimal solution.

Contributions

The main contribution of this thesis is the study and design of different building blocks of a transmission system investment optimization methodology. Three major building blocks and accompanying software tools are developed.

- Methodology/tool to calculate the maximum power injection capability of the existing network. The methodology combines several techniques in a novel way to quantify how much power can be injected in the transmission grid, taking probabilistic distribution of generation and load, N-1 security and existing power flow controlling devices into account.
- Methodology/tool to determine optimal transmission routes. For a given connection and power rating of a transmission link , its optimal route and technology is determined minimizing investment costs. Taking into account spatial properties and according installation costs, the best technology and cabling option along the transmission route is determined. High voltage alternating current (HVAC) and high voltage direct current (HVDC) are considered as possible technology options whereas overhead lines, underground and submarine cables are considered as possible cabling options.
- Methodology/tool to optimize transmission topology, rating and time point for long term transmission system investments. The tool delivers an

optimal investment sequence minimizing investment costs of new assets over a given planning time horizon. The optimization methodology interacts iteratively with the previous building block in order to account for spatial properties during the optimization process. The methodology includes constraints which can be manipulated by the grid planner in order to investigate possible delays in the investment process.

Combined into a single planning approach, the three building blocks deliver a stepwise investment plan including the optimal transmission route and technology for each new transmission transmission system investments.

Structure of the thesis

The thesis is organized as follows.

Chapter 2 describes transmission system planning in general. Difficulties and uncertainties in the planning process are discussed. The chapter provides the literature study to assess the state of the art of transmission system planning methodologies and discusses their shortcomings. It concludes with the outline of the developed methodology and describes briefly the afore mentioned building blocks.

Chapter 3 describes the first building block of the proposed methodology. It shows how the existing transmission grid can be reduced to a set of possible injections. In order to take the probabilistic nature of generation and demand into account, the reduction is performed using probabilistic optimal power flow techniques. In this chapter, a number of known techniques are combined in a different way to make such a reduction possible. The set of injections serves as input for the investment optimization methodology described in the following chapters.

Chapter 4 provides an optimization methodology to determine the economically most feasible transmission system layout including the determination of transmission routes and technology selection. The chapter shows how the efficiency of the optimization is increased using an iterative combination of mixed integer linear programming and optimal routing algorithms.

Chapter 5 further extends the developed investment optimization methodology by including time point optimization. The extension is achieved by modifying the problem statement of the linear integer program including new constraints. The output of the extended investment optimization is a stepwise investment plan for new transmission system investments.

Chapter 6 shows a case study to demonstrate the practical application of the proposed methodology. Based on it, the effect of variations in input data on the final investment plan and the total costs are discussed.

Chapter 7 provides conclusions and gives recommendations for future research on transmission system investment optimization.

Chapter 2

Transmission Grid Planning

I love it when a plan comes together! - Col. John Hannibal Smith

2.1 Context of Transmission System Planning

There is a continuous demand for electricity which has to be met at all times. Generation and demand vary in two dimensions, time and space. Transmission grids are developed to connect large generation facilities with large consumers or distribution grids over larger distances to ensure cost-effective electricity supply. Transmission grids are the backbone of the electricity system.

The aim of transmission grid planning is to provide a schedule for grid extensions such that it is able to reliably connect generation and demand facilities considering the variation in time and space. The transmission system planning is usually carried out on short ($<$ 5 years), medium ($<$ 10 years) and long term ($>$ 10 years) [18]. The level of detail decreases in time as less information is available and uncertainties become higher. The planning horizon for new connections can reach several decades as the volumes of investments are large and the lifetime of assets built is long.

Besides the technical aspects of the electric power system, also economic aspects have to be taken into account during planning. Therefore, different cost-benefit analysis methods have to be conducted by grid planners in order to assess the total social welfare during planning. Hence, the ultimate goal of transmission grid planners is to find the best possible long term grid expansion scheme in the frame of given investment policies.

The electric power system consists of generation, demand and transmission. One could suggest that the three systems should be planned and optimized as a whole in order to achieve a global optimum while using a minimum of financial and technical resources. In practice, the three systems are planned separately by considering different interactions. Even before market liberalization, planning has been carried out separately as the main drivers for the three systems are different. Generation facilities are most feasible where access to natural resources is easy. Therefore, generation facilities are mostly built directly at the source of the resource such as rivers, lignite mines and LNG terminals or near logistic infrastructure such as harbours, railway hubs or gas grid hubs. Wind and solar power plants are built at locations with high wind speeds and solar radiation. For the electricity demand, different social and economic drivers are decisive yet demand is not definitely planned although policy might influence long term load growth. Especially after liberalization, the level of complexity in these interactions has increased as all three systems are operated by different entities having different goals, policies and agendas.

The long term development of power generation and transmission system is directly linked to energy policy. As such, the long term policy on the use of different primary energy sources has to be optimized as a whole considering security of supply, environmental impact and internal and external costs and according to transmission assets.

Transmission investments can be characterized as [19]:

- A natural monopoly, with only one responsible company for the construction of grids within a given area;
- A capital intensive business, using expensive equipment, occupying considerable space. The investment costs are normally substantially more important than the operational ones;
- Transmission assets have a long life, with expected life ranging from 20 to 40 years, or even longer for transmission lines;
- Most transmission investments are irreversible: it is virtually impossible to move most transmission assets from their original site. Investment decisions made now remain in the system and might become stranded if the rest of the energy system does not develop as anticipated;
- Transmission investments are lumpy, meaning that equipment is normally offered in a limited set of distinct ratings of voltage and power;
- Transmission networks are strongly subject to economies of scale: it is comparatively cheap to build infrastructure with high power capacity.

Overall, transmission system planning is very challenging and complex in nature. Especially for long term planning, with a planning horizon of one or several decades, there are considerable uncertainties in load and generation which need to be accounted for while designing the transmission system. This chapter aims to provide insights in the complex transmission expansion planning problem by pointing out the different aspects and by showing the difficulties. The motivation of transmission system expansion planning is provided. Existing planning methodologies are explained. The chapter is concluded with the brief description of the transmission planning methodology, elaborated throughout this thesis.

2.2 Functionality of grids

Beside connecting generation and demand, electricity grids provide more functions to be considered by the system planner for the future grid. Theoretically, each consumer has the freedom of installing his own generator to cover demand. In such a case there is no need for the transmission of electricity. In fact, the electrification started from isolated load centres. As generation facilities are not always available due to maintenance or unforeseen outages, reserve generation facilities were needed to satisfy the demand in such cases. This resulted in investments which were only needed for a short period of time. Eventually, the isolated load centres were interconnected in order to reduce the need for reserves, resulting in more efficient generation investment and a higher reliability of supply. This is known as the *interconnection function* of the grid. Another advantage of the interconnection function is that there is a common supply of grid users resulting in reduced demand peaks as the demand is aggregated [20].

Obviously, the grid fulfils the *transmission function.* This way, energy can be transported from distant sources to the load centers. In general, large hydro or wind power plants are situated far away. Transmission grids allow the use of such resources by connecting distant generation facilities [20].

The grid has also a *market facilitator function.* It acts as the market place where different parties, such as generators, suppliers and consumers can make transactions. Higher interconnection capacity reduces congestion and increases social welfare. Obviously, not every commercial transaction results in a physical flow. But limited interconnection capacity constrained by the physical flow, also puts a constraint on the market transactions [20].

The system developer has the responsibility of acting in this global context considering the different tasks of the grid. Eventually, the overall goal is to ensure a reliable energy supply taking into account future scenarios. Besides security of supply, also the competitiveness and the social welfare have to be enhanced. As the transmission system investments are expensive, a balance between system wide costs and benefits must be sought while designing the future system [20].

2.3 The four W's of the Transmission Expansion Problem

The goal of transmission system expansion planning is to obtain the optimal transmission expansion plan in a given future by maximizing the social welfare or through a cost-benefit analysis considering future uncertainties. While maximizing social welfare, a number of constraints have to be satisfied to reach a defined level of security of supply. In its most general definition, the transmission expansion plan has to provide an answer to the following four main questions:

- Where to invest?
- What type of investment?
- When to invest?
- Who is going to pay for the investment?

2.3.1 Where to Invest?

The first question to be answered is where the future transmission system investments must be realized: which transmission corridors or regions require new or upgraded transmission infrastructure. The answer to this question depends on the motivation of the transmission expansion. If the motivation is maximization of revenues, e.g. for a merchant line, the optimal location of the line might contradict with that from a TSO perspective.

Locating new transmission infrastructure is a problem with different geographical scales. Firstly, it is important to determine which transmission zones (e.g. countries) to connect, in order to achieve the maximum social benefit in a regional (multi-zonal) perspective. Optimization of investments needs between multiple zones is mostly carried out using a market model and simplifying the transmission grid typically to one or two nodes per zone (figure 2.1 - left). The generation and demand within the countries are aggregated and the interconnecting lines are reduced to one line per border using equivalent impedances and transfer capacities. This way the optimization problem is simplified and the calculations are typically carried out with a large number of generators and loads over a time period of one or several years on an hourly basis. Such a calculation delivers the additional capacity need between the considered zones, allowing a regional optimum of social welfare.

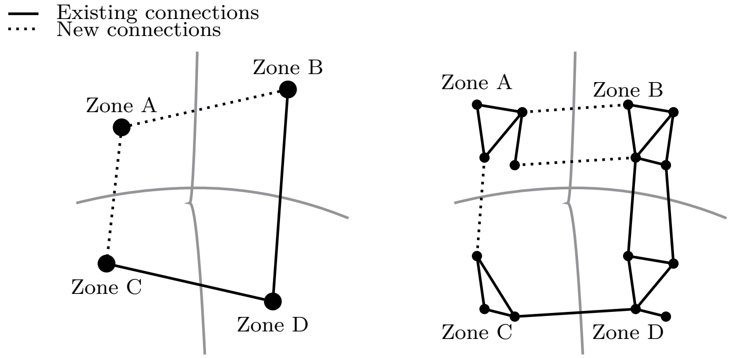

Figure 2.1: Determination of investment needs on a regional (left) and on substation (right) level

If the investment need in the regional context is determined, the system can be designed in such a way that the additionally required transmission capacity between zones is reached. In order to achieve an optimal system design, the question has to be answered, where to place actual lines and how to select their rating, considering a number of technical, economic, social and environmental constraints (figure 2.1 - right).

From purely technical perspective, the optimal location and rating of new lines depend on the spatial and temporal distribution of generation and demand. These distributions can be predicted accurately in the operational domain or short term planning. In long term planning, their prediction is very difficult due to uncertainties.

In case of demand, the spatial distribution mainly depends on the population density and the concentration of heavy industry. The highest demand is concentrated in large urban areas with high population density. Therefore, the future spatial distribution can be predicted rather easily as it can take several decades or even centuries until such demand centres are developed. The temporal distribution of demand is mainly determined by the consumption behaviour. On short and medium term, it is unlikely to change fundamentally. The overall increase and decrease in consumption is related to the change in

GDP, which is a matter of several years. Nevertheless, there is a possibility of extreme events (e.g. the mortgage crisis of 2008 or natural catastrophes), causing sudden drops or increase in consumption. In a time frame of coming decades, the consumption behaviour can change due to increased usage of demand response and demand side management or increased use of electrical vehicles. During the calculation of future transmission need, the behavioural change should be modelled. In order to obtain robust scenarios for future generation and demand, different policy measures leading to behavioural change in electricity consumption should be considered.

In case of generation, the spatial and temporal distribution are linked. The spatial distribution depends on the availability of energy resources. Conventional power plants are ideally located near a supply point, where the infrastructure allows easy transportation of primary energy resources (e.g. lignite power plants near lignite mines or gas power plants near major pipelines). In case of renewable generation, e.g. hydro, wind and solar energy, the favourable locations are determined by the availability of the energy flows to be harvested. As such, wind farms are ideally installed where the wind speeds are high and less fluctuating. Although the best locations from a geographic point of view are known, the actual location of future generation infrastructure is still difficult to predict. Generation assets may be forced to be built at different locations due to public opposition.

The choice of the primary energy resources is driven strongly by (geo-)political, economic and environmental drivers. The temporal distribution of generation depends as such on the decision of which energy resources to use. Conventional generators can deliver power on demand. Except hydro or biomass, renewable power generation depends on the availability of intermittent sources. As such, the fluctuation in renewable generation causes uncertainty. Figures 2.2 and 2.3 show the predicted and actual wind infeed in the 50Hertz Transmission zone in Germany for the first five months of 2014 [21] on an hourly basis. The installed capacity of wind farms in that zone is approximately 14 GW. Although the error between forecasted and actual wind in feed is in a band of ± 1000 MW, it is clearly visible that the difference can reach values higher than 3 GW which is more than 20 % of the installed wind capacity.

Another uncertainty in the temporal distribution is the market price for electricity as well as the market prices for the primary energy sources, mainly coal and gas [1]. Eventually, these prices determine together with demand, the commitment of the power generating units. Power plants located in different geographic regions are committed and de-committed in the market at different

[1] It should be noted that different support schemes and regulations might influence or disturb normal economics

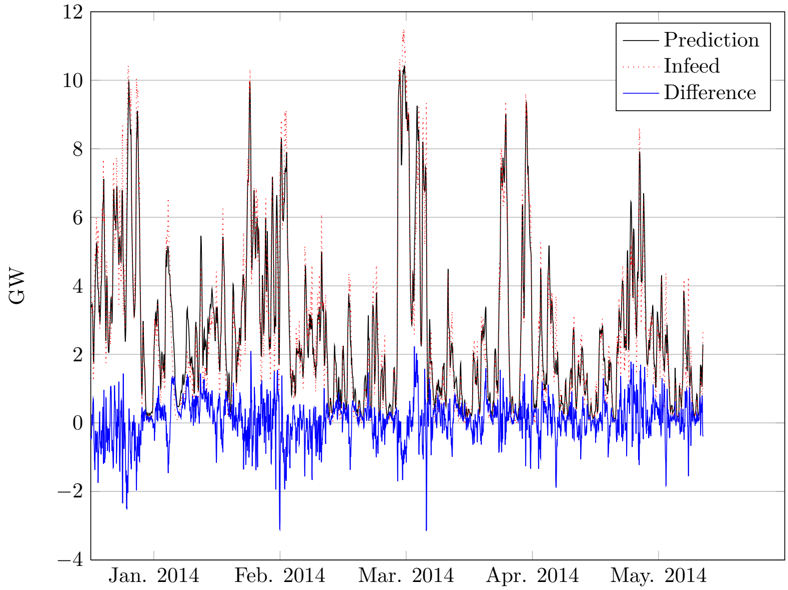

Figure 2.2: Predicted and actual wind in feed in the 50Hertz Transmission zone January 2014 to May 2014 on an hourly basis. Installed wind capacity ca. 14 GW

points in time. As such, the temporal distribution of generation results in a changing spatial distribution. Uncertainties in the temporal and spatial distribution as well as their correlation have to be adequately considered by the grid planner to allow a secure system design. In general, this happens using different generation and demand scenarios or probabilistic power flow calculations.

The right-of-way is another important decision criterion for the actual location of transmission lines and cables. The route selection of new transmission corridors may be coupled to other types of infrastructure such as railways, roads, shipping routes and gas and oil pipelines while prohibited zones are known such as natural reserves, water reservoirs or military installations. Additionally, social acceptance of transmission system expansion is one of the major influencing factors. Such decision criteria are very much case specific and can decide if a transmission line (or cable) can be built or not and at which price. In many cases, this leads to major delays in expansion projects. Such issues are very difficult to be considered in generic transmission planning tools and require expertise of the grid planner.

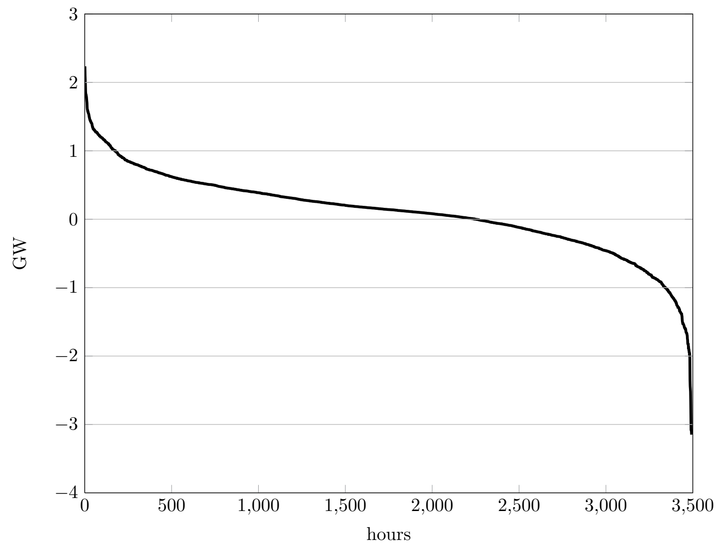

Figure 2.3: Difference between predicted and actual wind in feed in the 50 Transmission zone January 2014 to May 2014 hourly sorted. Installed wind capacity ca. 14 GW

2.3.2 What type of investment?

The system planner can make two fundamental choices during system design in terms of technology. The first is whether to use AC or DC transmission and the second one being the use of overhead lines or cables. Additionally, the power rating and the voltage level have to be determined.

In classical transmission system planning, high voltage AC overhead lines were the technology considered first. High voltage AC overhead lines are a mature, reliable and economic technology. However, underground cabling and HVDC technology have gained a higher importance in today's power system. In Asia, South Africa and North and South America, HVDC links have been used for long distance transmission to avoid stability issues and decrease losses. In Europe where distances are relatively short, HVDC links were mainly used for submarine connections between non-synchronous areas. Nevertheless, current projects such as the Swedish south-west link, the Spain-France connection, the Belgium-Germany connection or the British west link show that embedded HVDC links are an attractive option for new transmission system investments even within a synchronous area.

In the context of renewable energy goals of the European Union, HVDC technology plays an important role. HVDC technology has virtually no length limitation which enables the connection of distant offshore wind farms with high power ratings to the existing onshore electricity system. Beyond that, with the development of VSC technology and the possibility of multi-terminal operation, HVDC connections can be operated in a meshed grid. Meshed HVDC configurations connecting large offshore wind farms and several countries can serve as a first step towards a pan-European super grid.

The choice of the type of investment depends mainly on the distance and the desired power rating. The distance is a limiting factor for high voltage AC transmission. For long (>500 km) overhead lines stability issues and losses become a limiting factor. In case of underground cables, the high cable capacitance and the resulting charging currents limit the feasible transmission distance to some 10 to 100 km without intermediate compensation.

Besides the transmission distance, also the installation site can affect the technology selection. Installation costs of transmission equipment are a considerable part of the total investment. They depend on the spatial properties of the area as well as land acquisition costs for the right of way. Using one single installation cost for transmission equipment does not reflect reality and can lead to suboptimal solutions in terms of routing and technology choice. A key contribution of this thesis is that the developed methodology uses area dependent installation costs to reflect spatial properties, land acquisition and other social and environmental factors.

Another issue to be considered during technology choice is the lumpiness of transmission investments. Installation costs can be considered as fixed in a specific installation area (same altitude, same population density etc.), whereas the investment costs depend on the power rating of the equipment. If the total costs consisting of installation and investment are illustrated as a function of the rating of the transmission system, an inverse dependence is obtained (figure 2.4). The cost function has discontinuities at the maximum power rating of one circuit of transmission equipment. If two different technologies are considered (e.g. HVAC vs. HVDC technology), the location of the discontinuities varies as different technologies have typically different maximum power ratings for one circuit. Depending on the installation and investment costs for both technologies as well as the power rating per circuit, different technologies can be economically viable in a certain power range (figure 2.4). This can also result in multiple break-even points between two technologies to be considered in the technology selection. Therefore, the optimization of location, technology and power rating should be performed together to avoid suboptimal transmission grid layouts. This also means that any optimization result can be challenged as small deviations from the initial assumptions can lead to different results.

Therefore, it is necessary to vary initial assumptions and perform sensitivity analysis in order to obtain the most suitable result.

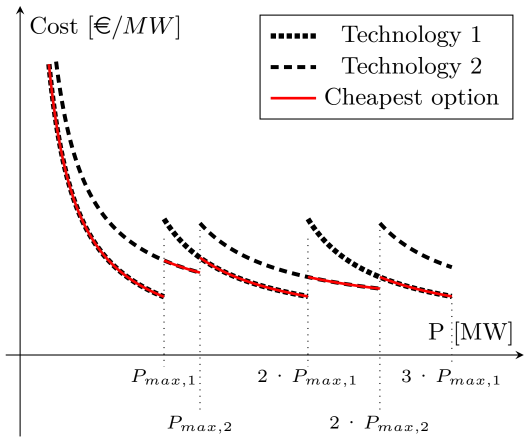

Figure 2.4: Transmission system investment costs [€ /MW] for two different technologies on the same transmission route [22]

2.3.3 When to Invest?

Every time a new transmission investment is done, the grid layout changes. As a consequence of the change in impedances, the power flows in the transmission system change as well. The part of the transmission system that is most congested or which is the most prone to disturbances may shift to other locations. As such, every transmission system investment affects future investments.

Next to the topology change, there is an economic benefit of delaying investments. As investments which can be realised at a later point in time are economicly more beneficial, there is an incentive of postponing investments as much as possible. From an economic point of view, investments can only be postponed as far as security of supply is not jeopardized.

On the other hand, the process of investing in a new transmission asset can take multiple years. Therefore, the decision to delay investments can be a very difficult task given the uncertainties of future scenarios. As such it is required to optimize the timing of transmission system investments, especially in the long term, taking into account a number of uncertainties. Some of the scenario uncertainties are:

- Generation
  - Location
  - Type
  - Profile (including correlation with other sources)
- Demand
  - Location
  - Growth
  - Profile
  - Flexibility
- Technological developments
- Primary energy prices
- Raw material prices

There is an interdependency between location, type and timing of the investment. As such, it is important to optimize the three parameters at the same time while searching for the best expansion plan. Neglecting one of them can result in a suboptimal system design.

2.3.4 Who pays for the investment?

The remuneration scheme for transmission system investments is an important decision criterion as each investor expects sufficient return on investment. There must be a correct financial incentive to invest. In case of investment projects where more parties with different remuneration schemes are involved, it can be difficult to find a compromise which can satisfy all. Also cases where the benefits of the investment are not directly linked to the investor (e.g. when a given investment mainly benefits a third country) require the correct incentives in order to be built.

A clear example can be seen in the number of offshore investments in a given country when comparing the connection charging regime. Depending on the regulatory regime, it is the generator company (deep connection charges) or the system developer (shallow or super shallow connection charges) that is responsible to pay for the grid reinforcements. Depending on the "depth" of the regulatory schemes, different grid layouts are obtained as the optimal solution. In case of interconnecting systems, a harmonisation of the regulatory schemes is needed to facilitate such investments.

Cross Border Investments

Cross border investments deserve special attention in transmission expansion planning. As different TSOs of different countries are involved in the investment decision, the decision making process is complicated. In principle, the goal of such an investment is to maximize the overall social welfare. In most cases, the maximum overall social welfare does not correspond with the sum of the maximum welfare of both countries separately. For instance, a line maximizing the welfare of country A does not maximize the welfare of country B and the other way around. Therefore, investment decisions in inter-connectors may result in a sub-optimum in terms of overall social welfare [23].

2.3.5 Other Influencing Factors

Besides the four “W’s” of transmission system planning, there are a number of influencing factors putting additional constraints on the transmission investment problem.

Security Constraints

There are two classes of security constraints, which have to be taken into account in transmission grid planning. The first class deals with long term security of supply related to investments to secure energy sources for a specific area. The objectives of long term security of supply are decided on the political level. For grid planners, the long term security of supply is rather an input than a constraint. For instance, the connection of north African solar power plants to Europe via sub-Mediterranean HVDC links could help to supply Europe with renewable energy on the long term and reduce its dependency on fossil fuels [12–14]. At the same time Europe’s dependence on resources outside Europe will increase which might result in a security of supply problem in return. The same holds for the connection of large scale wind power from the North Sea [11]. The decision to realize such major investment projects have to be made following a long term vision. The task of the grid planner is to develop an investment sequence to enable the integration of these energy sources into the existing system.

Security constraints play a major role during the selection of location, rating and type of new investments. Currently, different deterministic criteria such as the N-1, N-1-1, N-2 criteria are applied in transmission ssytem planning. The N-1 criterion states that the transmission system is still operable after the failure of one critical element, e.g. a transmission line or a large generator.

The N-1-1 criterion refers to common mode failures, where a second failure as a consequence of a previous failure can be tolerated by the system. The N-2 criterion states that two independent failures can be handled by the transmission system. In future, diverse probabilistic security criteria can be used in the planning process. The choice of the security constraint(s) influences the final layout of the system. The stricter the security criteria, the more redundancy is required, resulting in a higher number of parallel paths or a higher degree of meshing.

Technology Development

On the very long term there might be considerable changes and developments in available technology. Technology options such as storage, super conductivity, unconventional renewable energy (geothermal, wave energy, etc.) might change the way the electricity system is built and operated. Here, no technological developments are taken into account. In section 6 of this work, the effects of using higher power ratings of transmission technology on the final grid topology and the total system costs is analysed qualitatively.

Social Constraints

One of the biggest hurdles for new transmission infrastructure projects is the public opposition mostly related to the visual impact and electromagnetic field exposure. In many cases, TSOs are forced to put new transmission assets underground increasing the costs significantly. Another reason for undergrounding can be that there is no suitable right-of-way available without violating the limits for electric and magnetic field exposure. The requirement to use underground cables affects the technology selection as high voltage AC underground cables have a limited transmission distance and capacity.

It is very important to incorporate the public opposition in the initial phase of the planning where technology selection and line routing are determined. Belated changes in transmission technology or line routing delay the permission, construction and commissioning process significantly which eventually results in additional costs and may lead to failure of the whole project in some cases.

2.3.6 Transmission Grid Planning in the Liberalized Context

Before the liberalization of the electricity markets, transmission planning and generation expansion planning were carried out by a common planning entity.

In the classical scheme, the objective was the minimization of investment and operational costs while fulfilling security constraints as the benefits were fixed.

In the liberalized market, where generation and transmission companies are different entities, planning is done separately. The main difference is that the objective of the planning is the maximization of profits as opposed to minimization of costs in vertically integrated monopolies. This puts additional complexity and uncertainty in the transmission planning. On hand generation companies try to maximize their profits. Transmission system operators have the responsibility to minimize their costs in order to increase social welfare. On the other hand, if listed on the stock market, transmission system operators need to fulfil their responsibilities towards their shareholders as well. As a third dimension, the revenues of TSOs are determined by national regulating bodies who might have again different objectives, incentives and agendas, further complicating the decision making process of transmission investments.

On top of the involved parties having different objectives, there is additional uncertainty for generation as well as transmission companies. As transmission companies are obliged[2] to connect new generation units in their zone, they risk stranded investments, in case the generation project is severely delayed or not realized. A similar risk exists for the generation company, in case the construction and commissioning process for the transmission system is delayed. In that case, the generation company loses revenues due to lack of transmission capacity. Therefore, in current transmission system planning risk assessment gains increasing importance.

2.4 Transmission Expansion Optimization Methodologies

Transmission expansion planning is an optimization problem which can be formulated in different ways depending on the objective of the optimization and the level of abstraction. Due to its complexity, generally, the optimization problem is defined as a two step problem (figure 2.5). The upper level, also called investment or master problem, determines the topology of the expansion. The optimization algorithm determines which nodes in the network should be connected or which lines reinforced. The objective of the investment problem is the minimization of the investment costs. In the lower level called operational or slave problem, usually the power ratings of the connections proposed by the investment problem are optimized with the objective of minimizing operational

[2]This "obligation" can differ in different zones and is subjected to generator connection requirements

costs. In the operational problem, grid constraints such as voltage magnitude and angle limits as well as security constraints can be taken into account. By feeding back the solution of the operational problem, the investment problem is updated until convergence between both sub-problems is reached.

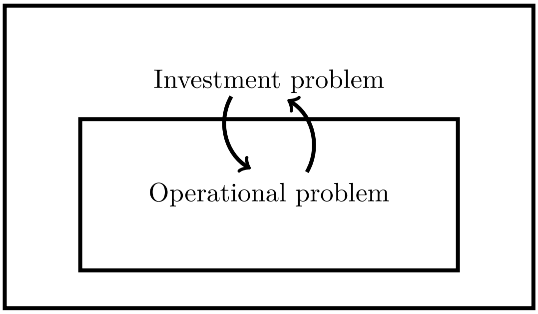

Figure 2.5: Structure of transmission expansion optimization problem

The formulation of the transmission expansion optimization problem depends on the desired objective and the solution methodology. In general, the transmission expansion problem can be classified according to solution methods, planning time horizon and structure of the analysed power system [24]. Additionally, each transmission expansion problem can be formulated in a deterministic or a probabilistic way.

2.4.1 Classification by Solution Method

In general, the transmission expansion problem can be solved using mathematical or heuristic optimization techniques. The combination of mathematical optimization and heuristics are the so called meta-heuristics frequently used for transmission expansion optimization.

Mathematical Optimization Methods

Mathematical solution methods require the description of the optimization problem by a closed set of equations. The formulation consists of an objective function and a set of constraints, which reflect imposed technical, economic and reliability criteria. The problem is solved using classical methods of optimization such as linear programming (LP) [25–30], dynamic programming (DP) [31], non linear programming (NLP) [32], mixed-integer programming

(MIP) [33–40], Benders' decomposition [41–44] and hierarchical decomposition methods [45].

The above mentioned solution methods have different properties in terms of convergence and computational efficiency. As such, it is important to choose the solution methodology which suits the abstraction level of the defined problem. If an LP optimization is used, either a transportation model is chosen [25] or the power flow equations are linearised. Using a transportation model, the investment problem is decoupled from the network equations. In that case, the flows on new built lines are considered as known without having to account for the network impedances. Using non-linear optimization methods, the non-linear network equations can be accounted for, such that voltage magnitude limits and transmission losses can be represented. Additionally, non-linearities in the cost function can be taken into account leading to a more accurate cost representation.

On the other hand, non-linear mathematical solution methods have often convergence problems due to the non-convex nature of the transmission expansion problem. Using an appropriate solver for the problem is essential in mathematical optimization methods. Often, a reformulation or simplification of the problem statement is needed in order to use commercial solvers. Another issue is that high computation times are required as there can be several local optima in the search space. To limit the high computational burden, the optimization problems usually must be simplified. As such, the obtained solutions have to be verified for feasibility in a more complete model.

Transmission system investments are lumpy by nature. First of all, transmission lines or cables can only be built by using a discrete number of circuits. Additionally, the number of conductors per phase as well as the available cross-sections of conductors are of discrete nature. To represent the lumpiness of transmission investments, integer optimization variables are used. In general, integer optimization performs worse in terms of convergence and computational speed compared to continuous optimization and many solvers can't deal with such problems or need to revert to slower computation routines. Therefore it is popular to define the optimization problem as a continuous one and approximate the power rating to the closest discrete value after obtaining the solution.

Heuristics

Heuristic methods are based on the step-by-step solution of the transmission expansion problem using a predefined set of rules. To do so, at each iteration new expansion alternatives are generated, evaluated and selected. This can be done with or without user interaction. These heuristic methods use local searches based on logical or empirical rules and sensitivities to limit the search space [24]. The search is performed until no better solutions are found. Optimization methods based on heuristics mostly consider investment costs, operational costs and energy not served in the objective function.

There are several heuristic methods, such as adjoin network [46], sensitivity analysis [47–53], overload networks [25, 26, 28], decision trees [54], genetic algorithms [55–61], simulated annealing [62, 63], expert systems [64–66], fuzzy set theory [67], greedy randomized adaptive search [41], tabu search [68–70], particle swarm optimization [71] and multi objective meta heuristics [72, 73]. Game theory [74–77] based methods can also be seen as heuristic. In game theory-based methods, the interaction of different agents based on predefined rules are mimicked. This way, it is possible to find solutions acceptable for all agents.

2.4.2 Classification by Planning Horizon

Transmission expansion problems can generally be separated into two classes regarding the planning horizon: static and dynamic. Static problems are solved only for one specific point in time, intermediate time points being neglected. All aforementioned methods can be used for this kind of optimization problem. Referring to section 2.3, these kind of expansion problems only answer the questions where to invest and what type of investments to choose.

The expansion problem gets dynamic, if multiple time steps are considered. In this case, next to sizing of new investments also timing along the whole planning horizon is optimized [24]. Methods to solve such problems are currently sufficiently developed and often require significant simplifications or have serious restrictions [78]. In [30–32, 38, 39, 79, 80], such problems are described.

To simplify dynamic problems, the algorithm can be performed for multiple sequential (and discrete) steps. This way, a pseudo-dynamic problem is created. Such pseudo-dynamic problems can be solved with two natural decompositions: forward and backward methods. In the forward method [81], the problem is sequentially solved, where the starting point is the first year of the planning horizon considered. In the backward methods, first an optimization is performed for the last year of the planning horizon. To solve the problem in the intermediate years the information of the "future" investments are used. The backward method delivers in general better results [24]. The forward and backward method can be combined when the problem at every time step is solved in both directions.

Dynamic and pseudo-dynamic problems require large computational effort due to the large number of variables, growing with the length of the planning horizon. In general, heuristic methods are used to solve dynamic and pseudo-dynamic problems.

2.4.3 Classification by Market Structure

Before the liberalization of the electricity markets, the objective of the transmission expansion planning had been to minimize the life cycle costs of the generation and transmission system while considering security constraints. After liberalization, the electricity market structure has changed, causing multiple and potentially competing objectives.

As mentioned in the previous section, generation and transmission planning can have contradicting objectives which complicates the decision making process. In that context different entities can have different view points in the following issues [24].

- Definition of the objective function (minimum transmission system operation costs, maximum cost-benefit ratio, global welfare, lowest congestion etc.)
- Interaction between transmission and generation expansion planning
- Definition of criteria to choose a specific expansion plan
- Assessment of different expansion options
- Flexibility requirements of the transmission planning process
- Relation between investments and pricing
- Optimization of existing network utilization
- Introduction of flexible transmission devices
- Definition of the highest uncertainty level for the planning
- Review of reliability, security and quality criteria

2.4.4 Deterministic vs. Non-Deterministic Expansion Problems

The classical transmission expansion planning is performed in a deterministic way. In general, several worst case scenarios are created and the transmission system planning is carried out such that security criteria are fulfilled during when the worst case occurs. Such approaches might lead to overinvestments as the the probability of occurrence of such a scenario is very low. On the other hand, the quality of the expansion plan heavily depends on the quality of the worst case scenario. The negation of important scenarios may lead to under investments and to curtailment of load if these cases occur.

Due to increasing number of uncertainties such as renewable generation and flexible loads, probabilistic transmission expansion planning gains popularity. Instead of using fixed load and generation values in certain scenarios, both are modelled with probability density functions. The probability of exceeding line limits in certain expansion plans can be determined and monetized.

Using those techniques, also security criteria can be redefined in a probabilistic way to replace the classical (N-1) security criterion. Using proper risk assessment the costs to avoid low probability failures and the economic consequences in case of occurrence can be compared to each other. This way, over investments in assets which do not significantly contribute to system security can be avoided.

Monte Carlo simulation is the current "standard" for probabilistic planning approaches. It requires large computational effort due to the large number of sample cases. Therefore, it is mostly applied for conceptual study cases in small grids. Especially for large grids with a high number of nodes, the definition of the probability density functions for load and generation as well as the definition of security criteria play a major role and deserve research priority to develop more efficient modelling techniques.

2.5 Transmission system planning in practise

In practise, the identification of investment needs in transmission systems is an iterative process (figure 2.6). In the first step, a market based assessment is made optimizing the dispatch of power generation units on an hourly basis. In the market based assessment, usually a DC load flow approximation with a small number of nodes or a one node per country approach is used [82, 83]. The one node country approach assumes that there is no internal congestion within a zone (country or region) such that all generation and demand can be aggregated to one node. Between the zones, a limited grid transfer capacity is used which is calculated using the capacities of cross-border lines and important lines within the zones. Based on the marked analysis, inter-zonal investment needs care determined. The market analysis takes availability and flexibility of generation units into account as well as wind, solar and load profiles [78,82–85].

Based on the outcome of the market analysis, a network study is performed, where a simplified representation of demand and generation profiles are used [82, 83]. Network studies take internal congestion and loop flows into account such that investment needs within the transmission zones can be identified. In network studies, a number of specific planning cases are used representing the most problematic situations in the transmission grid [82, 83]. Based on the network studies, grid planners propose possible reinforcements to solve the identified problems. The potential costs and benefits of proposed solutions are determined in order to find the most suitable grid investments. Eventually, new grid transfer capabilities are determined including the best reinforcements and used as input for the next iteration (figure 2.6). The best transmission grid reinforcements are determined through further iteration of the process until the proposed solutions prevent all critical situations.

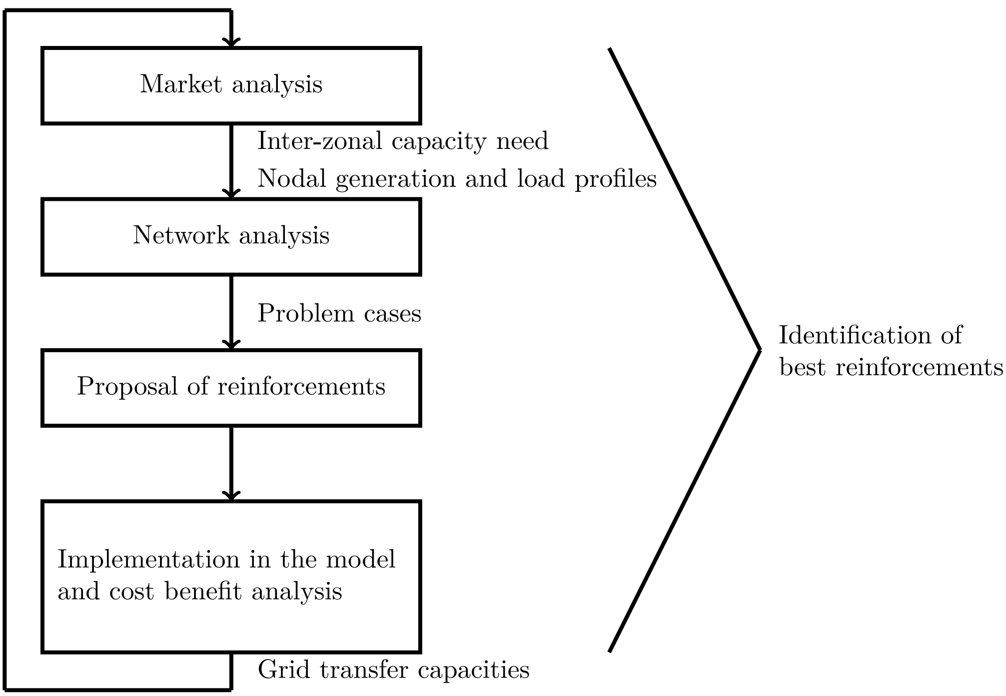

Figure 2.6: Structure of transmission system planning in practise

2.6 Structure of the Proposed Transmission Expansion Optimization Methodology

As elaborated in the previous sections, transmission expansion planning has to deal with a large number of variables, influencing factors and uncertainties. In order to find the global optimal investment sequence for the considered planning horizon and a considered area, a complete transmission expansion optimization methodology has to account for:

- Temporal distribution of generation and demand in the entire network for the entire planning horizon
- Spatial distribution of generation and demand in the entire network for the entire planning horizon
- Long term and short term security of supply
- All current and future technologies for grid expansion
- Spatial, social and environmental aspects of the entire considered area (e.g. Europe)

A key shortcoming of available planning methodologies is that the probabilistic nature of renewable generation and demand is not considered. For large transnational investments, robustness is essential. If the transmission system planning is scenario based, both over- or underinvestment may occur as scenario studies may easily overestimate future generation capacities. At the same time, they could miss extreme cases of flow that require specific reinforcement [86]. This thesis introduces a long term transmission system expansion optimization methodology where the probabilistic nature of generation and demand are taken into account. In this thesis an investment optimization methodology is introduced taking spatial aspects and different technology options for new investments and their interdependency into account. The spatial aspects are important to monetize social and environmental impact of new investments to allowing a direct comparison and transparent cost benefit analysis of different projects [86].

This would require that the optimization methodology is able to model all generators and all lines in a time period of several decades together with a set of possible expansion technologies and a full social-environmental representation. This would result in a huge number of optimization and state variables. Therefore, it is necessary to divide the optimization problem into several virtually decoupled layers. Each layer can be solved in a more simplified and efficient way. Eventually, these layers have to interact with each other and exchange some dedicated information and solve the expansion problem iteratively. In this way the influence of different parameters on different layers and also on the final optimization result can be analysed.

The structure of the proposed long term transmission expansion optimization methodology is shown in figure 2.7. To allow easy integration in existing planning tools and allow user interaction, this specific structure is chosen. The first step of the planning methodology consists of the market analysis (Interconnection Level) as it is common practise. The market analysis delivers the necessary input for a probabilistic network analysis (Network Abstraction) and investment optimization (Substation Level). In classical transmission system planning methodologies the identification of necessary investments is carried out by the grid planner. In the proposed methodology, new investments are identified using optimization techniques such that different technology options and spatial properties can be taken into account. This extends the search space for identification beyond the experience of the grid planner while accelerating the identification process for new investments.

The different building blocks are described briefly in the following sections. The scope of this thesis is the network abstraction and the substation level marked grey in figure 2.7.

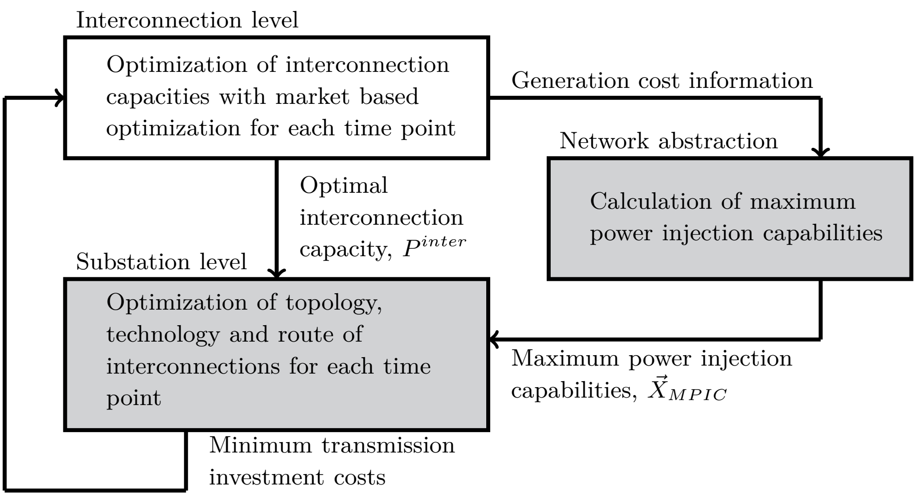

Figure 2.7: Structure of the proposed long term transmission expansion optimization methodology

2.6.1 Interconnetion level

The interconnection level determines the capacity needs between multiple zones, considering future generation and demand scenarios to enable the long term security of supply. The objective of the optimization is to find the best interconnection capability between multiple zones maximizing overall social welfare. Based on expected generation, demand and cost information, the optimal inter-zonal transmission capacities are calculated (figure 2.8).

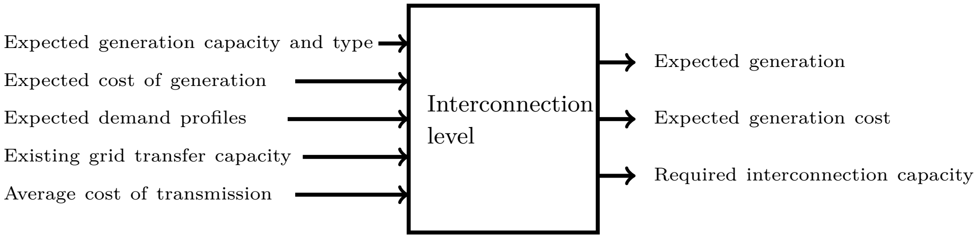

Figure 2.8: Main input and output parameters of the interconnection level

In general, a high number of generation and demand profiles are analysed, e.g hourly profiles over multiple years. Hence, the optimization problem should be defined as simply as possible in order to avoid convergence problems and long calculation times. In such market based optimization methods, zones (e.g. countries) are mostly modelled using one aggregated node, neglecting the internal power flows and possible contingencies. The existing interconnections between the zones are modelled using a transport model or actual equivalent impedances between the zones to account for actual flows. Investment costs in transmission systems are modelled using simplified cost functions. The average costs used are mostly given in €$/MW$, €$/(MW \cdot km)$ or €$/(MW \cdot km \cdot a)$ depending on the chosen level of detail and time horizon.

The output of the interconnection level is the optimal interconnection capacity used as input in the substation level and generation cost information used in the network abstraction level. In case a (pseudo) dynamic approach is chosen, the interconnection capabilities for all considered investment time points have to be provided. The interconnection level is not in the scope of this thesis as a large number of such market based tools exist to address it [78, 87].

2.6.2 Network Abstraction

Using the input coming from the interconnection level, an optimization algorithm can be written to determine optimal placement and rating of new assets to achieve the desired interconnection power. Nevertheless, if the existing transmission system is modelled with its full detail, the number of optimization and state variables increases significantly. If technology selection, route and timing of the investments are optimized, the large number of variables become a burden. As such, an abstraction from the existing network is created to decouple the optimization of technology, topology, routing and timing of new investments from the existing network.

The principle of the network abstraction and the main input and output parameters is shown in figures 2.9 and 2.10 respectively. In the network, the existing network is presented as a possible set of allowable injections and absorptions. They are determined considering probabilistic distribution of generation and demand as well as existing line limits. The determined injection capabilities indicate the maximum amount of power which can be injected or absorbed at a single node of the system without causing any overload. Based on the maximum power injection capabilities, a set of strong nodes can be selected which are used for the further optimization at substation level, rather than the entire set of nodes in the transmission system. The set of nodes can be chosen depending on the injection capability itself as well as on geographic or other constraints. This reduces the number of optimization variables drastically resulting in better convergence and faster computation. The determination of the injection capabilities are elaborated in chapter 3.

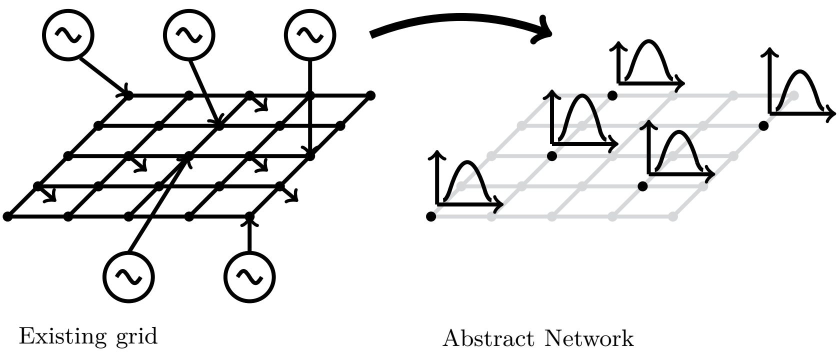

Figure 2.9: Principle of network abstraction

2.6.3 Substation level

Using the required inter-zonal transmission capacities as well the maximum power injection capabilities, the optimization of investments on the substation

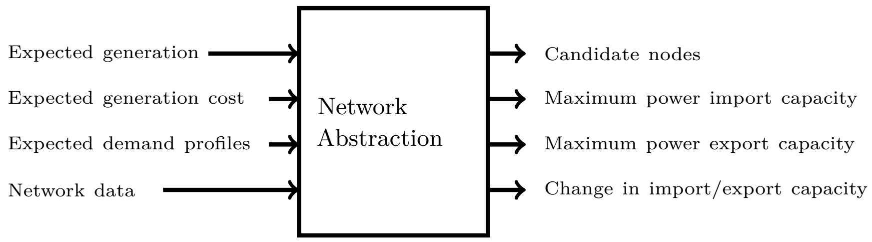

Figure 2.10: Main input and output parameters of the network abstraction

level can be carried out. In this optimization it is determined which substations have to be connected to achieve the desired interconnection capabilities in the most economic way. Therefore, the technology (AC, DC, overhead lines, underground cables) and rating (number of circuits, conductors and their cross sections) of each connection are optimized. Figure 2.11 shows the main input and output parameters.

The optimization considers area dependent installation costs and finds the cheapest transmission route in combination with the chosen technology. This way soft constraints such as social and environmental impact can be included in these area dependent costs. When multiple investment time steps are considered, the investment time point of each connection is determined. Using additional constraints, the impact of construction delays and availability of multi-terminal HVDC operation is analysed.

As averaged transmission investment costs are used at the interconnection level, it is important to iteratively combine the substation and the interconnection level. After determining the minimal costs on the substation level over the entire planning horizon, these costs can be averaged, annualized and used in the interconnection level. Depending on the updated costs, in the next iterations, the interconnection capability might change in such a way that several iterations have to be performed between both. As the generation profiles might change, maximum power injection capabilities have to be recalculated for each iteration between the interconnection and the substation level (see figure 2.7).

The optimization on substation level as well as the iteration between levels is studied in chapters 4 and 5.

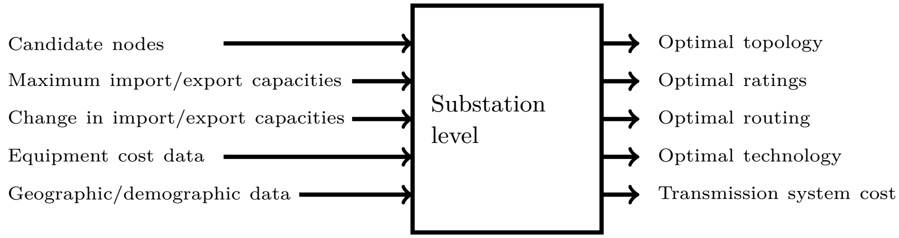

Figure 2.11: Main input and output parameters of the substation level

Chapter 3

Maximum Power Injection Capabilities

I believe that we do not know anything for certain, but everything probably - Christiaan Huygens

3.1 Introduction

New transmission system investments have to be compatible with the existing transmission network. This means that no new overload situations should occur in the network if a new transmission connection is built. The search space for transmission system investment optimization consists of scenarios for investment options. To optimize transmission grid investments on a regional level (e.g. continental), a representation of the entire system is required to make sure that new investments are compatible with the existing grid. This results in a very large number of variables as the power flow equations for the entire network have to be solved during each optimization step. Therefore, it is helpful to reduce the grid investment options by a pre-selection of candidate nodes by determining the effects of power injections and off-takes in these candidate nodes on the rest of the network. This way, the optimization problem can be defined independent of the existing network simplifying the problem. This chapter provides a methodology to pre-select candidate nodes and to represent them as a set of possible injection capabilities.

The connection of a large wind farm to the existing grid is depicted in figure 3.1.

The injected power is distributed among the transmission lines of the grid according to the demand in each node, injections from other generation units and the impedance of transmission lines. The optimal connection point for the wind farm would be a strong node nearby, which allows the maximum amount of power injected without causing congestion. Not every substation is able to cope with such high amounts of injected power. First of all, the additional power injection may require additional equipment such as transformers, FACTS devices or switchgear or the replacement of existing equipment to fulfil short-circuit power requirements. In case sufficient space is available, such extensions can be installed easily. More importantly, the power injected or withdrawn in a specific node has to be transported by the existing transmission grid in order to supply loads. Investing to reinforce local existing transmission lines can be difficult and expensive [88]. This can be a reason to connect new generators not necessarily to the closest connection point but further away, where no additional investments would be needed or less problems are foreseen.

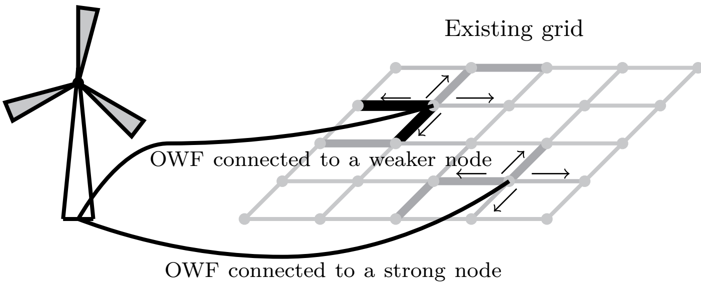

Figure 3.1: Effect of connecting a large offshore wind farm to the existing grid (darker colour indicates higher power flow)

By calculating the amount of power injected in each node, a set of candidate nodes can be chosen depending on the power injection capability and transmission distance. The identification of such strong nodes is not trivial, as several factors such as different demand and generation profiles, the location of generation and demand, import and export situations or line outages influence the maximum power injection capability in nodes and the reserves on transmission lines for additional transport of power.

In case the dispatch of future generation units and hourly load profiles are provided, the maximum power injection capability can be determined using power flow calculations. In this chapter a calculation methodology is developed which identifies the maximum power injection capability (MPIC) based on a probabilistic optimal power flow for the case that future generation and load information is not provided as a time series. Next to identification of strong nodes, also weak links are identified, as these are the most likely to show congestion and therefore the first candidates for future reinforcements. This chapter is based on [89] and is structured as follows. The overall structure of the developed methodology is provided. A formulation for the optimal power flow calculation (OPF) is provided which is used in the remainder of the chapter. Next, a comparison between AC and DC OPF in terms of accuracy is provided. The application of the Gaussian Component Combination Method (GCCM) is shown to take the probabilistic nature of demand and renewable generation into account and compared to Monte Carlo Simulation in terms of accuracy. Further, the effects of considering the N-1 security criterion and power flow controlling devices, namely phase shifting transformers (PST) and HVDC links are discussed.

The methodology is developed and implemented in Matlab and all power flow and optimal power flow calculations are performed using Matpower [90].

3.2 Calculation of maximum power injection capabilities

The developed methodology aims to calculate the maximum power injection capability to serve as input for the optimization of transmission system investments. It is calculated such that no overload situations can occur in the existing network. During the procedure the probabilistic nature of generation and demand is taken into account.

The aim of the developed methodology is to deliver two vectors $\vec{P}^{+}_{MPIC}$ and $\vec{P}^{-}_{MPIC}$ which contain the maximum power injection and absorption capabilities of investigated nodes. $\vec{P}^{+}_{MPIC}$ and $\vec{P}^{-}_{MPIC}$ express how much power can be imported into a node and exported from a node without causing any overload situations in the existing transmission grid. As larger injections or absorptions than $\vec{P}^{+}_{MPIC}$ and $\vec{P}^{-}_{MPIC}$ cause overload in the existing grid, the power injection and absorption capabilities can be seen as capacity limits for new connected transmission lines, generation units or loads.

Every injection in a particular node influences the power flows in the grid and therefore the maximum power injection capability of other nodes. This effect has to be considered during the optimization of line ratings for future investments. Therefore, a matrix Δ_{MPIC} is calculated which represents the change in the maximum power injection capability in each selected node in dependence of injections in each selected node. During the operation of the power system, the injection in a node x can take any value between zero and its power injection capability. As such, the matrix

$$\Delta_{MPIC} = \begin{bmatrix} \Delta_{1,1,1} & \Delta_{1,2,1} & \dots & \Delta_{1,N,1} & \dots & \Delta_{1,N,M} \\ \Delta_{2,1,1} & \Delta_{2,2,1} & \dots & \Delta_{2,N,1} & \dots & \Delta_{2,N,M} \\ \vdots & \vdots & \vdots & \vdots & \vdots & \vdots \\ \Delta_{N,1,1} & \Delta_{N,2,1} & \dots & \Delta_{N,N,1} & \dots & \Delta_{N,N,M} \end{bmatrix} \tag{3.1}$$

has to be defined for multiple power injections. $\Delta_{i,j,k}$ indicates the change in power flow. N is the number of selected nodes, whereas M is the chosen number of different power injections. The size of Δ_{MPIC} is $(N \times N \cdot M)$. The columns of Δ_{MPIC} indicate nodes where power is injected, whereas its rows indicate affected nodes.

The power injection capability is bidirectional. Therefore, four matrices have to be calculated in order to describe the change in power injection and absorption capabilities as a result of injections and absorptions in other nodes (figure 3.2). The definition of the four matrices is as follows:

- $\Delta^{i,i}_{MPIC}$: change in the power injection capability due to injections in other nodes,
- $\Delta^{i,a}_{MPIC}$: change in the power injection capability due to absorptions in other nodes,
- $\Delta^{a,i}_{MPIC}$: change in the power absorption capability due to injections in other nodes,
- $\Delta^{a,a}_{MPIC}$: change in the power absorption capability due to absorptions in other nodes,

As the power injections in the transmission grid vary, $\vec{P}^{+}_{MPIC}$ and $\vec{P}^{-}_{MPIC}$ can have different values for each injection pattern. Therefore, probabilistic methods have to be used in order to calculate a range for $\vec{P}^{+}_{MPIC}$ and $\vec{P}^{-}_{MPIC}$. Figure 3.2 shows the general structure of the developed methodology. First, generation and load data is processed where samples to approximate the probabilistic nature of generation and demand are created. Also possible power flow controlling devices are added to the system and modelled according section 3.6. Secondly, a pre-selection of candidate nodes is performed by calculating their connection capability as elaborated in section 3.4.4. Next, the line overload distribution factors of the system are calculated used for the N-1 calculation (section 3.5). Eventually, the maximum power injection and absorption capability is determined using the Gaussian component combination method (see section 3.4.2) taking into account N-1 security and possible power flow controlling devices.

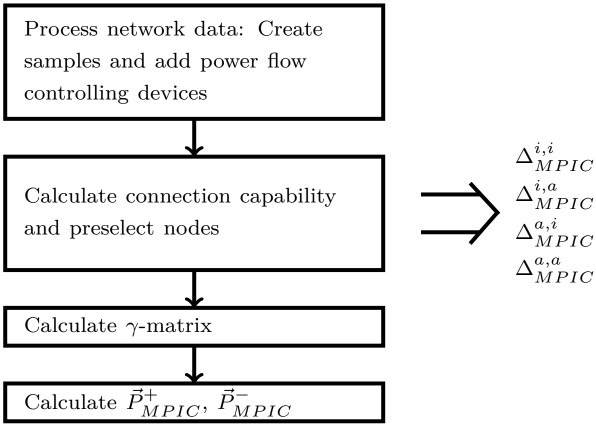

Figure 3.2: Structure of methodology to calculate maximum power injection capabilities

3.3 Optimal power flow formulation

Optimal power flow calculations are used to determine the optimal state of the system minimizing a given objective function. The power flow equations, Kirchhoff's current and voltage laws have to be satisfied. Although the objective function can be virtually anything, in most applications, the objective is the minimization of operational costs, consisting of generation costs, costs for losses and cost of energy not served. In the unbundled system, the typical objective is maximization of profits. Typical additional optimization constraints are current and voltage limits of equipment, stability limits in the grid and security constraints.

In this chapter the OPF formulation is used where the sum of active and reactive power generation costs in the considered area is minimized

$$min \sum_{i=1}^{ng} f_p^i(p_g^i) + f_q^i(q_g^i) \tag{3.2}$$

where ng is the number of generators in the system, $f_p^i(p_g^i)$ the active power generation cost of generator i, p_g the active power injection, $f_q^i(q_g^i)$ the active power generation cost of generator i and q_g the reactive power injection [90].

The optimization is subject to the load balance in each node which represents the Kirchhoff equations

$$0 = P_{bus}(\Theta, V_m) + P_d - P_g \tag{3.3a}$$

$$0 = Q_{bus}(\Theta, V_m) + Q_d - Q_g \tag{3.3b}$$

where $P_{bus}(\Theta, V_m)$ and $Q_{bus}(\Theta, V_m)$ are the sum of the active and reactive power flows, $P(d)$ and $Q(d)$ the reactive power demand and P_g and Q_g are the sum of active and reactive power injections in each node.

Additional inequality constraints are line flow limits representing the thermal line limits

$$F_{min} \ \leq \ F_f(\Theta, V_m) \leq \ F_{max} \tag{3.4a}$$

$$F_{min} \ \leq \ F_t(\Theta, V_m) \leq \ F_{max} \tag{3.4b}$$

where F_{min} and F_{max} are the upper and lower power flow limits and $F_f(\Theta, V_m)$ and $F_t(\Theta, V_m)$ are the power flows in both positive and negative direction respectively.

Also voltage magnitude and angle limits are constrained in order to account for insulation limits and static stability

$$\theta_i^{i,min} \ \leq \ \theta_i \ \leq \ \theta_i^{i,max} \quad \forall i \tag{3.5a}$$

$$v_m^{i,min} \ \leq \ v_m^i \ \leq \ v_m^{i,max} \quad \forall i \tag{3.5b}$$

where $\theta_i^{i,min}$ and $\theta_i^{i,max}$ are the upper and lower phase angle limits, θ_i the actual phase phase angle, $v_m^{i,min}$ and $v_m^{i,max}$ the upper and lower voltage magnitude limits and v_m^i the actual voltage magnitude.

Another constraint concerns generator active and reactive power limits to account for current and voltage limits in generators as well as the limits for mechanical and thermal stress of generation units

$$P_g^{i,min} \leq P_g^i \leq P_g^{i,max} \quad \forall i \tag{3.6a}$$

$$Q_g^{i,min} \leq Q_g^i \leq Q_g^{i,max} \quad \forall i \tag{3.6b}$$

where $P^{i,min}$ and $P^{i,max}$ are the maximum and minimum allowable active power generation, P_g^i the actual active power generation, $Q^{i,min}$ and $Q^{i,max}$ are the maximum and minimum allowable reactive power generation and Q_g^i is the actual reactive power generation of node i.

Equations (3.4a) and (3.4b) show that the power flow on each line is a function of the bus voltage magnitude and phase angle. On the other hand, bus voltage magnitudes and phase angles are determined by the active and reactive power injections (3.3a) and (3.3b) and the resulting voltage drops in the transmission lines. Therefore, the power flow problem has to be solved using an iterative approach. Additionally, convergence problems may occur in case the starting point for the iterative calculation is not chosen wisely or if the system matrix is close to singularity [91].

If all voltage magnitudes are assumed to be equal and the sine of voltage angle differences is approximated by the angle differences themselves, the power flow equations can be linearised. This simplification is called DC power flow calculation [91]. If DC power flow calculation is used, the equations regarding reactive power can be eliminated from the objective function and the constraints of the OPF formulation result in:

$$min \sum_{i=1}^{ng} f_p^i(p_g^i) \tag{3.7a}$$

$$s.t.\ 0 = P_{bus}(\Theta) + P_d - C_g P_g \tag{3.7b}$$

$$F_{min} \leq F_f(\Theta) \leq F_{max} \tag{3.7c}$$

$$F_{min} \leq F_t(\Theta) \leq F_{max} \tag{3.7d}$$

$$\theta_i^{i,min} \leq \theta_i \leq \theta_i^{i,max} \tag{3.7e}$$

$$P_g^{i,min} \leq p_g^i \leq P_g^{i,max} \tag{3.7f}$$

This simplification is justified in transmission grids as the voltage magnitude and angle differences between grid nodes are small. The main advantage of using DC power flow formulation is that the problem is linearised and solved with a matrix multiplication instead of an iterative solution as with AC power flow. The DC power flow calculation always finds a solution as it solved with a matrix multiplication. In the OPF formulation, the optimization constraints are linearised whereby simpler and faster optimization solvers can be used. This reduces the computation time for the optimization drastically and also has a positive influence on convergence of the optimization algorithm.

To calculate the maximum power injection capability to import power into a particular node x, the objective functions as provided by (3.2) and (3.7a) have to be extended. An additional term subtracts the injection in node x from the total generation costs using a conversion factor K.

$$min \sum_{i=1}^{ng} f_p^i(p_g^i) + f_q^i(q_g^i) - Kp_g^x \tag{3.8a}$$

$$min \sum_{i=1}^{ng} f_p^i(p_g^i) - Kp_g^x \tag{3.8b}$$

In case the generation costs in node x are set equal to or lower than all other generators, the injection in node x is maximized while respecting the constraints (3.3a - 3.6b) respectively (3.7b - 3.7f). Such an assumption is acceptable in case node x is selected as connection point of a large wind farm or an interconnector to a neighbouring grid. In case of a wind farm, the marginal generation costs would be near zero and in case of injection from another grid, electricity would be imported, which implies that the costs in the importing grid have to be higher than or equal these of imported energy. The conversion factor K is used to weigh both objectives: minimization of generation costs and the maximization of the injection in node x. Figure 3.3 illustrates the effect of the factor K on the both objectives. If a large value is chosen for factor K, the objective of maximizing the injection outweighs that of minimizing the total generation costs and vice versa. Depending on the chosen value of the factor K, the obtained solution moves along a Pareto front. Hence, the absolute value of K should be chosen carefully, considering cost of generation.

To calculate the maximum power absorption capability, the upper generation limits of the generator in node x has to be set to zero. In that case, a negative value has to be used for the conversion factor K.

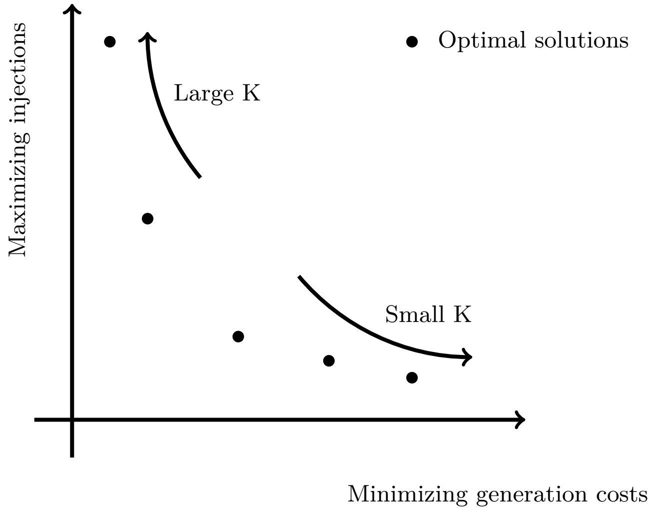

Figure 3.3: Effect of the weight factor K on prioritizing the objectives of minimizing generation costs versus maximizing injections

The result of the optimal power flow calculation delivers the maximum power injection capability. Additionally, the result of the optimal power flow calculation can be used to determine weak paths in transmission grids. Obviously, no line overloads can occur if the optimal power flow calculation converges due to the thermal line limit constraint (3.4a - 3.4b and 3.7c - 3.7d). Nevertheless, the lines operated at or near their thermal limits can easily be identified. The lines operated most frequently near their thermal limits are the most likely ones to be overloaded in case the injection in node x exceeds the calculated maximum power injection capability.

In the following paragraphs a comparison between AC OPF and DC OPF is made while calculating maximum power injection capabilities. The calculations are carried out on a modified version of the IEEE 118 bus test system (figure 3.4). The node x is varied between all nodes in the system in order to compare the maximum power injection capabilities. In this modified version, radial connections are eliminated and the network is reduced to 109 nodes. Thus allowing to consider the N-1 security criterion (section 3.5). In case there are radial connections with single circuit lines, the maximum power injection capability would be zero, as there is always one disconnected node in the N-1 case causing non-convergence during the OPF calculation.

It is assumed that 3 wind generators are situated at buses 10, 57 and 71, with zero marginal costs. Line limits for the lines and transformers are set

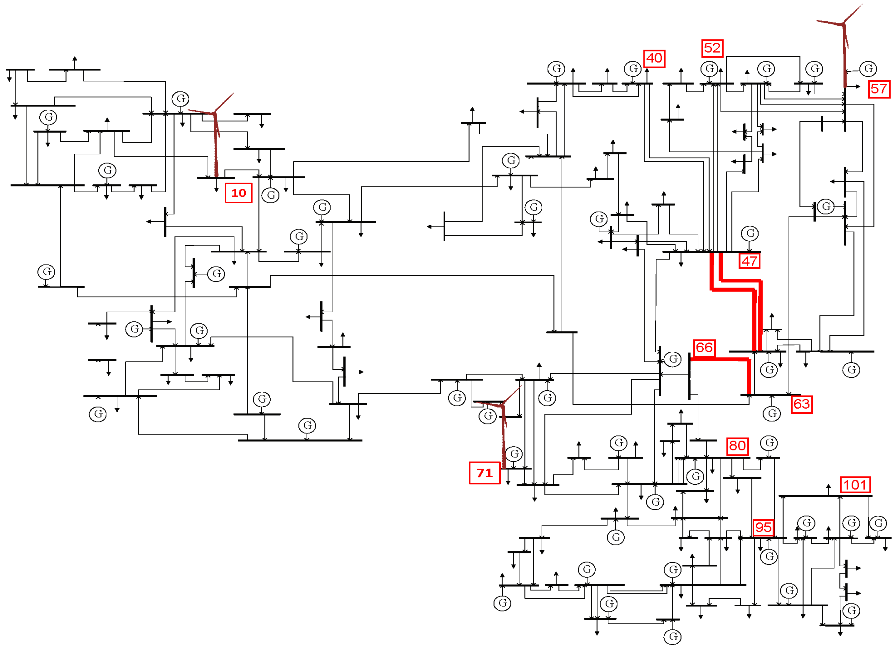

Figure 3.4: Modified IEEE 118 bus system, thick, red lines indicate lines equipped with PSTs respectively replaced by HVDC connections in section 3.6

to 500 MVA and 250 MVA at respectively the 345 kV and 138 kV level. To determine the strongest node, at each iteration, a different node x is equipped with a generator at marginal cost equal to wind generators. The load level of each bus is varied between 75% and 125% of the base values defined for the IEEE 118 bus test system [92], resulting in 50 different load cases.

Figure 3.5 shows the relative difference between the $MPIC$ in each node between using AC and DC OPF calculation. The figure shows that on average 0,46% higher values are achieved with AC OPF. Except for one bus, the relative difference between both methods is below 10%. On the buses with the highest power injection capability, (buses 47, 57, 63, 66 and 77), the differences are negative with the exception of bus 57. This means that in these buses the DC OPF approach delivers higher $MPIC$ values than the AC OPF method.

Especially for long term planning, the load and generation uncertainties can introduce much higher errors than those made using DC power flow. The DC optimal power flow approach is suitable for long term planning purposes in densely meshed networks due to the advantage of better convergence, faster

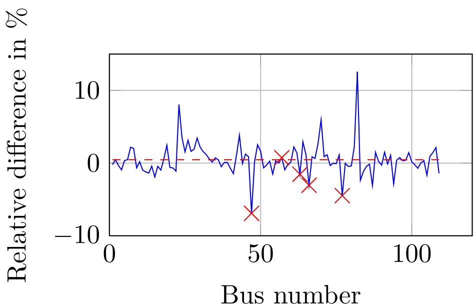

Figure 3.5: Relative difference between AC and DC OPF methods, red line indicates mean value of difference, × marks the difference for buses with highest MPIC

computation and sufficient accuracy. In practise while using DC power flow and optimal power flow calculations, the thermal line limits are set to lower values (typically 90% - 95% of their actual values) in order to account for the difference with the AC power flow approach.

3.4 Probabilistic methods

Power flow or optimal power flow calculations only capture a snapshot of many different generation and demand situations. In reality, demand and generation change constantly. They can vary in two dimensions, time and location. As not all possible combinations of generation and demand can be calculated, probabilistic power flow calculations have been introduced in the 1970s [93, 94]. The idea behind the probabilistic power flow calculation is the representation of power injections and power flows using probability density functions.

3.4.1 Gaussian distributed variables

Using the DC power flow approach with Gaussian distributed power injections, the expected value and standard deviation of branch flows can be calculated using two matrix multiplications [93]:

$$\bar{P}_{flow} = PTDF \cdot (I - L_0 \cdot \epsilon_N) \cdot \bar{P}_{bus} = H \cdot \bar{P}_{bus} \tag{3.9a}$$

$$PTDF = B_f \cdot B^{-1} \tag{3.9b}$$

$$\sigma^2_{flow} = H^2 \cdot \sigma^2_{P_{bus}} \tag{3.9c}$$

The mean values of branch flows ($\bar{P}_{flow}$) are computed using the mean value of power injections in each node ($\bar{P}_{bus}$) (3.9a). PTDF is the power transfer distribution function matrix, defining the change in power flow in each line depending on the change in power injections of each bus (3.9b). The PTDF matrix is calculated using the susceptance matrix of the system B is and B_f mapping the branch susceptances to buses. Each row of B_f represents a branch, whereas the columns represent buses. For a branch connecting buses i and j, the i^{th} element is the positive branch susceptance, whereas the j^{th} element is the negative. I is the identity matrix and $L_0 \cdot \epsilon_N$ defines the distribution of excess power at the slack node(s) [93]. ϵ_N is a unit line vector. L_0 is a column vector with length M. The elements contain values between zero and one depending on how much they contribute to balance the excess power. The sum of the elements of L_0 is one.

In general, the probability distribution of demand is not Gaussian. It depends on the time of day and weather conditions [95]. The consumption behaviour is reflected by the time dependence, whereas the weather conditions determine the quantity. Additionally, there exists a random component reflecting unusual consumption behaviour [95]. The injections of renewable energy sources show a non-Gaussian distribution as well. This means that the above equations cannot be used to calculate probabilistic power flow. Therefore, other possibilities have to be found in order to determine the probability distribution of power flows.

3.4.2 Gaussian Component Combination Method

The Gaussian component combination method [96,97] can be used to represent any probability distribution as a weighted sum of Gaussian distributions (3.10).

$$f_Y(y) = \sum_{i=1}^{L} \omega_i f_N(\mu_i, \sigma_i^2) \tag{3.10}$$

These Gaussian distributions have all different mean values and standard deviations. In (3.10), L is the number of components chosen and $f_N(\mu_i, \sigma_i^2)$ the i^{th} Gaussian (Normal) distribution function with expected value μ_i and standard deviation σ_i^2. ω_i is the weight of the i^{th} component with $\sum_{i=1}^{L} \omega_i=1$.

Figure 3.6 illustrates the principle of the Gaussian component combination method. The probability distribution shown belongs to power output of a wind farm. Although the wind speeds are Weibull distributed, the application of the wind farm power curve results in a distribution which is far away from a Weibull distribution. To construct this distribution, 8760 Weibull distributed random wind speed samples are created and applied to the wind turbine power output curve (figure 3.7). For the sake of simplicity it is assumed that all wind turbines experience the same wind speed. The samples are created such that the capacity factor of the wind farm equals 43% which is usual for offshore wind farms. Figure 3.6 shows that the wind farm power output is either 0 or 1 pu most of the time. The distribution is reconstructed as a sum of four Gaussian distributions ($L = 4$) using the "gmdistribution" function of Matlab. The Gaussian components of wind power injections can reach into negative injections or higher injections than 1 pu (Figure3.6). In such cases values under 0 pu and above 1 pu need to eliminated.

The Gaussian component combination method (GCCM) to calculate power flows is applied as follows. First, power injections and loads in all buses are approximated using the GCCM. As such, each component is now Gaussian distributed so that according probabilistic flows can be calculated (3.9). In this case, the Gaussian components of each injection or load have to be combined. The required number of calculations is,

$$N_r = \prod_{j=1}^{N_{inj}} L_j \tag{3.11}$$

where N_{inj} is the number of injections and L_j is the number of Gaussian components of each injection or load. For instance, if all injections would be represented with one Gaussian component, only one power flow calculation has to be performed. In case there are two injections represented with two components each, the number of necessary calculations is 4.

The probability distribution of power flows (PDF_{flows}) can be calculated using

$$PDF_{flows} = \sum_{i=1}^{N_r} \hat{\omega}_i \cdot PTDF \cdot P_N^{inj}\left(\hat{\mu}_i, \hat{\sigma}_i^2\right) \tag{3.12}$$

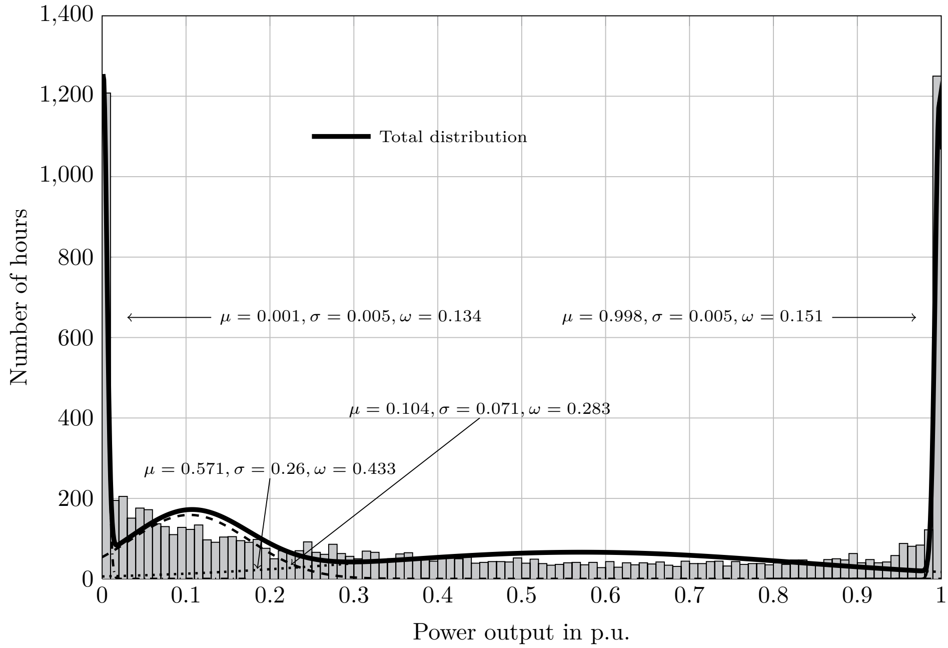

Figure 3.6: Probability distribution of the power output of a wind farm and its approximation using GCCM

The weight of each Gaussian component $\hat{\omega}_i$ is calculated with $\hat{\omega}_i = \prod_{j=1}^{N_{inj}} \omega_j$ where the sum of the weight for all components must add to $\sum_{i=1}^{N_r} \hat{\omega}_i = 1$.

In larger grids, with hundreds of buses this can still result in a large number of power flow calculations. Nevertheless, the number can be limited by reducing the number of used Gaussian components for the probability density functions. One method is the pair merging approach with integral square differences [98–100]. In this method, the integral square difference between the original combination $f(y)$ and the combination with the reduced number of components $g(y)$

$$J_s = \int (f(y) - g(y))^2 dy \tag{3.13}$$

is calculated for all possible combinations of Gaussian components. The pair of components i and j which deliver the smallest value of J_s are merged to one new component. The resulting weight of the merged component is

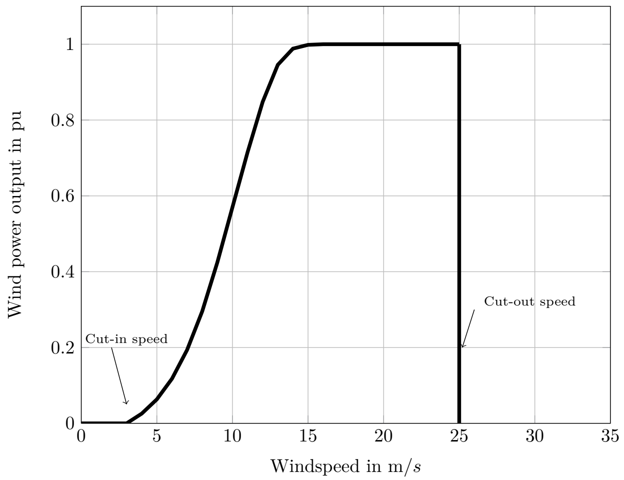

Figure 3.7: Typical power output curve of a wind turbine

$$\omega_{ij} = \omega_i + \omega_j \tag{3.14}$$

where ω_i and ω_j are the weights of components i and j respectively. The mean value and standard deviation of the combined component are calculated with

$$\mu_{ij} = \frac{1}{\omega_i + \omega_j} \cdot (\omega_i \cdot \mu_i + \omega_j \cdot \mu_j) \tag{3.15}$$

and

$$\sigma_{ij}^2 = \frac{1}{\omega_i + \omega_j} \cdot \left(\omega_i \cdot \sigma_i^2 + \omega_j \cdot \sigma_i^2 + \frac{\omega_i \cdot \omega_j}{\omega_i + \omega_j} \cdot (\mu_i - \mu_j)^2 \right) \tag{3.16}$$

where μ_i and μ_j are the mean values and σ_i^2 and σ_j^2 are the standard deviations of components i and j respectively.

3.4.3 Monte Carlo Simulation

The most popular approach to deal with non-Gaussian probabilities is the Monte Carlo simulation. The general principle of Monte Carlo simulation is illustrated in figure 3.8. A large number of data samples for network injections (load and generation) is created. Based on the created data samples, deterministic power flow calculations are performed for each sample. Using the results of all power flow calculations, a probability density function (PDF) for a given confidence interval can be created. The number of sufficient samples depends on the number of injections as well as the probability distribution of samples. For larger systems with hundreds of nodes, the computational burden can be very high.

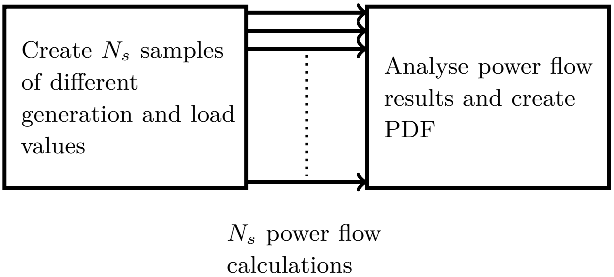

Figure 3.8: General principle of Monte Carlo simulation

3.4.4 Comparison of Monte Carlo Simulation and GCCM

The comparison between Monte Carlo simulation and the GCCM is discussed, based on the calculation of the maximum power injection capability. As case study, the IEEE 118 bus system as illustrated in the previous section is used (figure 3.4). In this example, power injections and loads are considered to be uncorrelated. If the injections are treated as uncorrelated, more extreme combinations between injections and loads are taken into account. This results in higher variances in branch flows and more distinctive maximum and minimum flows than in case of correlated injections.

For the case studied, three generators are modelled as wind generators (3.6). The wind generators are located at buses 10, 57 and 71. The probability distribution functions of the wind injections are approximated using the four Gaussian components. To limit the number of calculations, the number of Gaussian components is reduced to three using the pair merging approach with integral square differences [98–100]. The probability distribution of loads is derived from real load profiles obtained from [101]. The load profiles are set in per unit and applied to all loads of the IEEE 118 bus test system [92]. All load profiles are approximated first with 2 Gaussian components. Except in six buses, the number of components is reduced to one. This results in $N = 3^3 \cdot 2^6 = 1728$ optimal power flow calculations. For the comparison, a

Monte Carlo Simulation with 10000 samples of uniformly distributed values is used.

Figure 3.9 shows the results achieved with the GCCM method and the MCS for the 5 buses with the highest power injection capability. The mean value of the $MPIC$, its standard deviation, the branch most likely to be overloaded (critical branch, CB) and the probability that the critical branch reaches its limits (line limit frequency LLF) are illustrated. With the Gaussian component combination method a good approximation of the distribution of the maximum power injection capability can be achieved. There is one difference visible concerning node 57. The figure shows that the standard deviation with Monte Carlo Simulation is significantly higher than in the case of GCCM. The reason therefore is that a wind farm is situated at node 57 (figure 3.4). During the calculation of the Gaussian components, the parts of the Gaussian distributions which are lower than 0 pu and higher than 1 pu have been discarded (figure 3.6). Due to the characteristic of the wind injection, components with mean values close to 0 pu and 1 pu respectively occur. Due to the error made by discarding parts of the distribution, the standard deviation becomes smaller in comparison to the MC simulation. At the other buses situated further from the wind farms, these effects are not visible as the injected power is distributed over several paths. The computation time of the maximum power injection capabilities require 2 hours and 33 minutes with the GCCM in comparison to 12 hours and 51 minutes with the Monte Carlo simulation achieving approximately 5 times higher computational speed.

In practice, it is not necessary to calculate the $MPIC$ of every single node in the observed power system. Due to geographic restrictions, already a subset of investigated nodes can be preselected. Additionally, it is possible to exclude nodes whose connection capability is not large enough:

$$P_{con,i} = \sum_{j=1}^{N_{br}} \frac{P^2_{max,j}}{\bar{P}_{N,max}} \tag{3.17}$$

$P_{con,i}$ is the connection capacity of bus i, N_{br} is the number of branches connected to bus i, $P_{max,j}$ is the rating of branch j and $\bar{P}_{N,max}$ is the average of all branch ratings. Obviously, the connection capability is not a strict selection criterion as the distribution of the maximum power injection capability depends on the connected loads and generators as well. The connection capability should be used as indication and for automated calculation procedures where the there is no user interaction during the selection of candidate nodes, the number of candidate notes should be chosen higher than actually required.

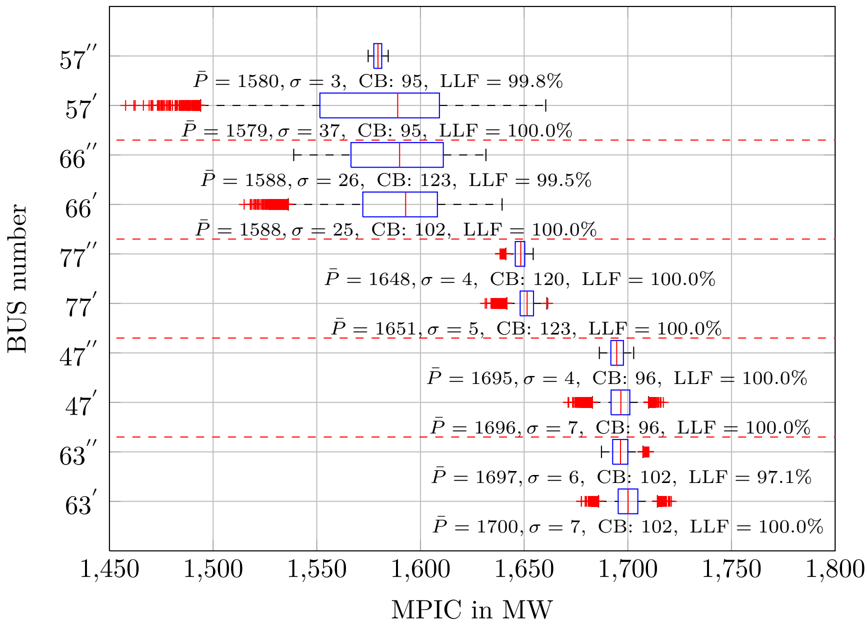

Figure 3.9: Comparison of GCCM and MC simulation, ′ indicates MC simulation while ″ indicates the GMMC method. The five buses with highest $MPIC$ are depicted

3.5 Effect of N-1 security

The N-1 approach is widely used in transmission system planning to take possible outages of equipment in the transmission system into account. The N-1 criterion states that the power system must still be safe if one major element in the power system faces an outage. For large power systems, the calculation of all N-1 cases requires large computation time as the outage of each element is investigated separately. If there are N elements in the system (e.g. lines, generators,...), N power flow (or optimal power flow) calculations have to be performed. In case probabilistic methods are used, the number of calculations would be $N \cdot N_s$ where N_s the number of samples used, clearly a very large number.

In order to limit the computational effort, the set of the investigated elements can be reduced. One possibility is based on the expertise of the system planner who is able to point out the most critical elements in his system.

To identify the set of most critical elements in a generalized way, line overload distribution factors (LODF) can be used [102]. The LODFs indicate the change in power flow in a set of monitored lines M in case of outage of a defined set of lines O.

If monitored and outaged lines are investigated one by one, a matrix γ can be built, representing the effect of outage of each branch on all remaining branches in the system:

$$\gamma = \begin{bmatrix} 0 & LODF_{1,2} & \cdots & LODF_{1,N_{br}} \\ LODF_{2,1} & 0 & \cdots & LODF_{2,N_{br}} \\ \vdots & \vdots & \vdots & \vdots \\ LODF_{N_{br},1} & \cdots & LODF_{N_{br},N_{br}-1} & 0 \end{bmatrix} \tag{3.18}$$

The elements of γ are,

$$\gamma_{i,j} = LODF_{i,j} = PTDF^0_{i,j} \left(I - PTDF^0_{j,j} \right)^{-1} \tag{3.19a}$$

$$\gamma_{i,i} = 0 \tag{3.19b}$$

where i are the affected branches (monitored branches), j branches with outage and I the identity matrix. The zero values in the main diagonal are chosen arbitrarily, as the effect of outage of a branch on itself is unidentified. $PTDF^0$ is the pre-contingency PTDF matrix [102].

The effect of a line outage on remaining lines depends on the initial power flow situation. For instance, if the power flow on a tripped line is not high, the power can be distributed amongst different paths without causing overload. In case of a large power flow, overload situations on other branches might occur. Using the γ-matrix after each optimal power flow calculation, a set of lines can be determined which cause overload on other lines in case of outage. This way, the N-1 calculation can be reduced only to the lines expected to cause problems.

While calculating the maximum power injection capability, it is not necessary to use the whole set of lines which cause an overload. The maximum power injection capability is calculated using the minimum value obtained in the N-1 calculation as all other injection capabilities would result in an overload. As such, it is sufficient to use only the lines causing the most critical situations in case of outage. In general, these are the lines with the highest value in the γ-matrix. This way, it is possible to further reduce the number of calculations to a smaller set while investigating in N-1 security.

The calculation procedure to take into account the N-1 security criterion in the developed methodology is depicted in figure 3.10. First, the OPF calculation is performed to calculate the maximum power injection capability in the N state for one combination of Gaussian components (or for one sample of the Monte Carlo simulation). The result of the OPF calculation delivers the branch flows in the N state. Using the branch flows in the N state and the γ-matrix, potential overloads are determined. The branches are ranked after the severity of overloads they are cause. Based on the ranking, a sub-set of lines causing the highest overloads is chosen. Sequentially, each branch in this sub-set is deactivated and the maximum power injection capability in each N-1 state is determined. The minimum value of power injection capabilities among each N-1 case is used as the final maximum power injection capability of the sample used. This procedure has to be repeated for each combination of Gaussian components or each sample of the Monte Carlo simulation.

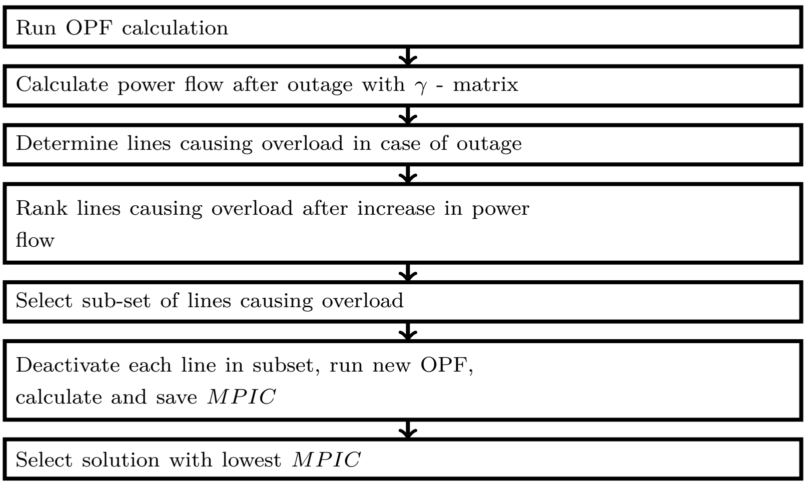

Figure 3.10: Line selection procedure for N-1 criterion

Figure 3.11 illustrates the change in the maximum power injection capability if the N-1 security criterion is considered. The maximum power injection capability of investigated nodes decreases significantly. The decrease in $MPIC$ is different for each node considered (figure 3.11). The ranking of the "strongest" buses changes. Also the most critical branches which reach their limits most frequently are different in the N and N-1 case. As such, the neglection of security criteria can lead to wrong assumptions in the identification of strong grid nodes. These strong nodes are the basis for the optimization process of future lines and therefore have high importance.

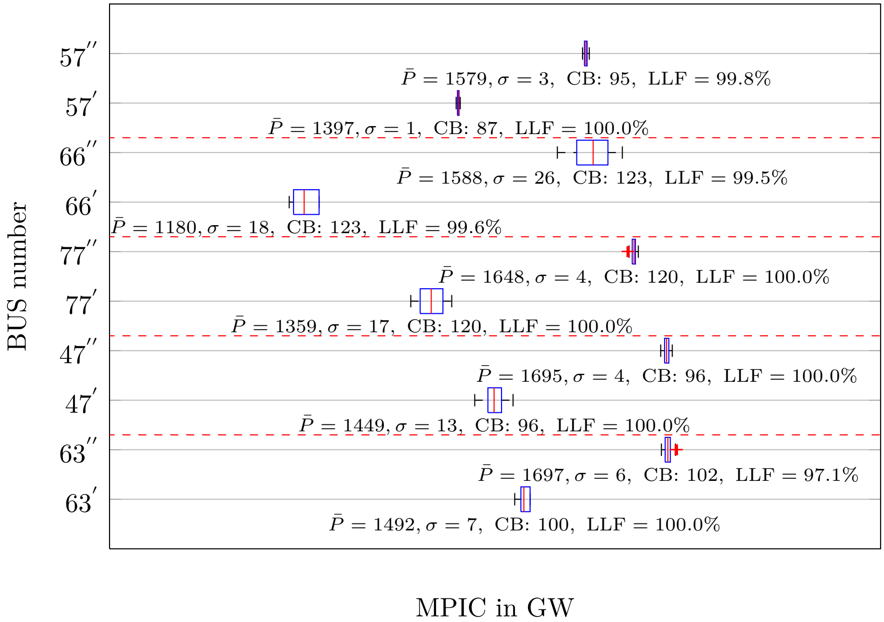

Figure 3.11: Comparison of $MPIC$ between N and N-1 case on the modified IEEE 118bus network, $'$ indicates N-1 case and $''$ indicates the base case

3.6 Effect of power flow controlling devices

The maximum power injection capability depends on the temporal and spatial distribution of generation and demand as well as the network characteristics. Eventually, the power flows are distributed according to the injection pattern and the impedances of network elements. As their name states, power flow controlling devices can change the power flow in the lines they are installed in but also influences the flows in neighbouring lines. This controllability can be used to increase the maximum power injection capability in case such devices are already installed in the grid. This section investigates the effect of power flow controlling devices. Two common types of power flow controlling devices, namely phase shifting transformers (PSTs) and high voltage direct current (HVDC) links are used.

3.6.1 PST devices

Phase shifting transformers induce a voltage in quadrature of the line voltage in order to change the voltage magnitude and phase angle. The power flow through a line with a PST can be controlled [91]. Using series compensation devices, such as thyristor controlled series compensation (TCSC) or static synchronous series compensator (SSSC) performances similar to PSTs can be achieved [103].

As stated in [104–106], during power flow calculation, a transmission line i, j equipped with a PST can be modelled using an additional impedance having two additional injections with opposite signs on both sides (figure 3.12). The additional power injections $\Delta P_{eq}^{ij}(\phi)$ and $-\Delta P_{eq}^{ij}(\phi)$ create a change in the power flow through line i, j caused by the phase angle change of the PST situated at line i, j. X_{ij} is the reactance of the line i, j and X_{pst} is the reactance of the phase shifting transformer respectively. Appropriate values for X_{pst} can be found in [107, 108].

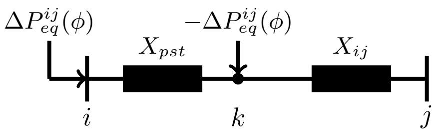

Figure 3.12: Modelling of PSTs with additional equivalent power injections

In the DC OPF calculation, the additional injections $\Delta P_{eq}^{ij}(\phi)$ and $-\Delta P_{eq}^{ij}(\phi)$ can simply be modelled using two additional generators in the system, connected to nodes i and a new created node k (figure 3.12). This way the optimal values $\Delta P_{eq}^{ij}(\phi)$ and $-\Delta P_{eq}^{ij}(\phi)$ can be found by the OPF algorithm, maximizing injection capabilities of grid nodes and respecting power flow limits of each transmission line in the system by changing the power flow on line i, j . In the OPF formulation, the sum of injections from both additional generators has to be zero being an additional constraint to the optimization. The generation costs of these additional generators is zero[1]. Therefore, the optimization solver prefers the control function of the PST above other generators. Obviously, the additional injections $\Delta P_{eq}^{ij}(\phi)$ and $-\Delta P_{eq}^{ij}(\phi)$ have to be limited in order to account for the maximum and minimum phase angles of the installed PSTs. The maximum and minimum equivalent injection

[1]Costs can be assigned to the additional generators, if additional costs, such as transmission losses of the PST, have to be considered.

$P_{eq}^{max,ij}$ and $P_{eq}^{min,ij}$ can be calculated using

$$\Delta P_{eq}^{max,ij} = \frac{\phi_{pst}^{max}}{X_{pst}} \tag{3.20a}$$

$$\Delta P_{eq}^{min,ij} = \frac{\phi_{pst}^{min}}{X_{pst}} \tag{3.20b}$$

where X_{pst} is the reactance of the phase shifting transformer and ϕ_{pst}^{max} and ϕ_{pst}^{min} are the maximum and minimum phase angles of the PST respectively.

For the results (figure 3.13), three PSTs are added to the system, two PSTs on branches 96 and 97, connecting buses 47 and 64, one PST on branch 102 connecting bus 63 with bus 66. These branches are the critical branches obtained in the previous calculations (figure 3.9). For the maximum phase angle shift of the transformers, $\pm$ 30° is used. The power system can be operated closer to its limits when power flow controlling devices are used. The mean value of the maximum power injection capability is in all cases higher than in the case without PSTs. Another positive effect is observed in bus 47 where the line limit frequency, indicating how frequent lines are operating at their limit, of the critical branch decreases.

3.6.2 HVDC connections

By changing the power set points of HVDC converters, the power flow through an HVDC link can be controlled. This controllability can be used to increase the maximum power injection capability of selected grid nodes. Similar to PSTs, HVDC links can be included in DC optimal power flow calculations [109]. In this case, a DC link is represented by two generators which are connected at the buses where the DC link is connected. A new optimization constraint has to be included enforcing opposite signs of injected power (figure 3.14). A power flow through the new branches equals the optimal power flow through the HVDC link. If HVDC transmission losses must be taken into account, the constraint can be rewritten as $P_g = -P_{g1} + f_l(P_g)$, where $f_l(P_g)$ represents the HVDC transmission losses as a function of transmitted power through the link. The costs of the additional generators can be set to a value representing the costs of using the HVDC link.

In figure 3.15, the effect of HVDC links on the maximum power injection capability is shown. The same three lines as in the case with phase shifting transformers have been replaced by HVDC links. The costs of the additional

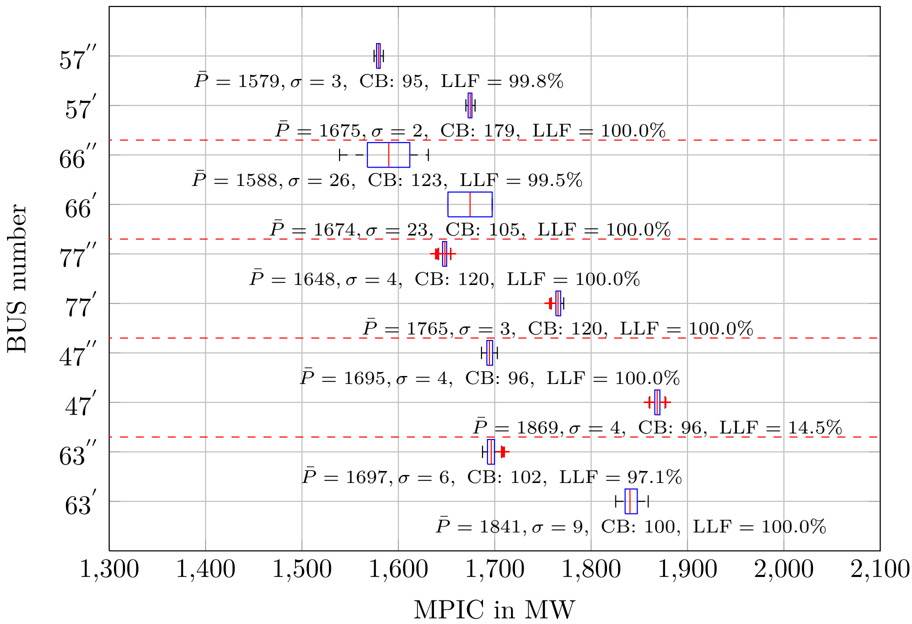

Figure 3.13: Effect of existing PSTs on the $MPIC$, $''$ indicates the base case and $'$ indicates case with PSTs

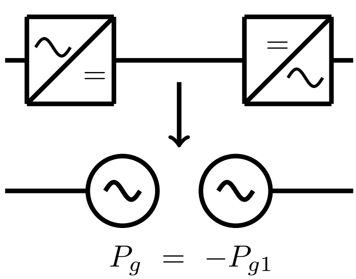

Figure 3.14: Modeling of HVDC connections in the optimal power flow calculation

generators simulating the HVDC link have been set to zero to allow maximum flexibility in the use of the links. Figure 3.15 depicts that the additional controllability of HVDC links increases the maximum power injection capability of grid nodes. As the set points of HVDC converters is determined by the OPF with the objective of maximizing injections in the investigated nodes, the power flow is distributed such that higher injections become feasible.

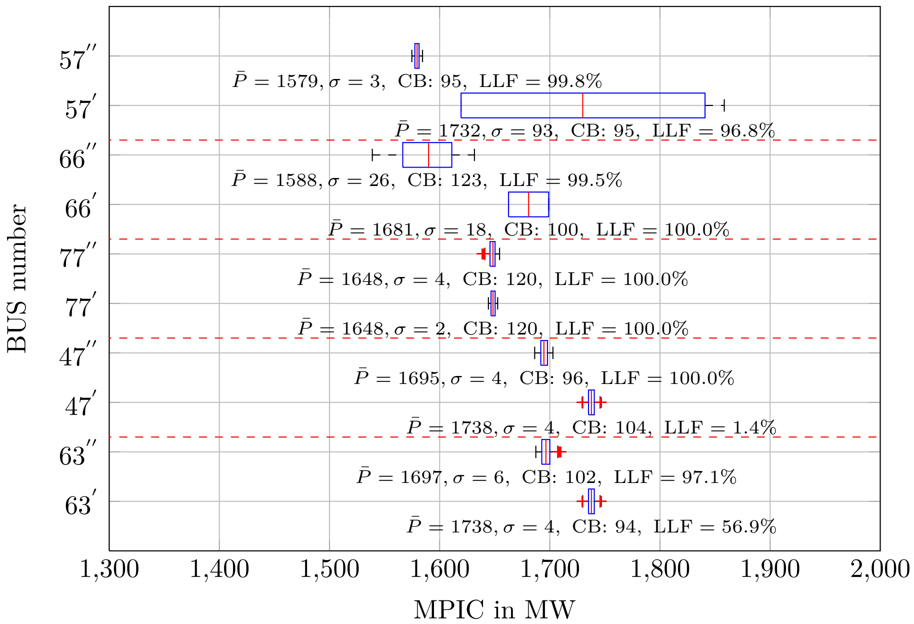

Figure 3.15: Effect of existing HVDC lines on the maximum power injection capability, ″ indicates the base case and ′ indicates case with HVDC lines

3.7 Conclusions

In this chapter a methodology is discussed, combining different calculation and modelling techniques in a different way to quantify maximum power injection capabilities. The maximum power injection capabilities indicate how much power in a certain node can be injected without causing overload situations in the investigated network. These capabilities are used as input parameters for the optimization of transmission system investments which is elaborated in the following chapters. The use of maximum power injection capabilities allows an abstraction from the existing grid, in order to reduce optimization and state variables in the further optimization process.

The methodology allows TSOs to assess strong connection points in their grid which can serve to connect power plants or interconnectors. Besides TSOs, this methodology can also be used by power generators in order to assess the sizing of their investments. As the calculation of the maximum power injection capability uses cost information of existing generators, power generation companies can use this methodology to estimate their future revenues and conduct a cost benefit analysis for their investments in case they have sufficient information about their competitors.

The maximum power injection capabilities depend on the temporal and spatial distribution of generation and demand, as well as network characteristics. As such, these capabilities have to be calculated in a probabilistic way. This chapter has provided an application of the Gaussian component combination method to approximate probability distribution functions. Using the Gaussian component combination method, savings in computation time can be achieved without compromising accuracy.

Security constraints limit the power injection capability in certain nodes setting limits on new transmission system investments. The methodology includes a procedure to efficiently assess N-1 security during the determination of maximum power injection capabilities. The assessment shows that the consideration of the N-1 security constraint changes the ranking of grid nodes in terms of injection capability. A node which is the strongest one in the N case does not necessarily have to be the strongest one in the N-1 case. The investigated nodes serve as future connection points for large scale transmission system investments and possibly a future overlay grid. As such, the candidate nodes have to be chosen very carefully as the topology of the future transmission grid depends on the candidate nodes.

This chapter further shows that power flow controlling devices help to use the existing grid better allowing higher injections into the grid. With increased flexibility in the transmission grid, the maximum power injection capability increases as well, as the transmission lines can be utilized more efficiently. By increasing flexibility connection of larger power plants or links with higher power ratings might become feasible increasing the overall social benefits as larger single power units or links are economically more feasible.

Chapter 4

Optimization of Topology, Technology and Routing

Improvement makes strait roads, but the crooked roads without improvement, are roads of genius. - William Blake

4.1 Introduction

The properties of the optimization variables and constraints make the transmission system investment optimization a non-convex, non-linear and a mixed-integer optimization problem. Such problems are difficult to solve by existing optimization solvers.

In the literature, a large number of transmission expansion optimization methodologies exist considering different levels of detail. With the level of detail, also the level of complexity varies. Detail and complexity have a direct influence on the computational efficiency.

This chapter is based on [22] and illustrates an optimization methodology to determine the economically most feasible transmission topology, route, technology and power ratings for system expansion. The remainder of this chapter is outlined as follows. The optimization methodology is described in general. The mixed integer linear program and the shortest path calculation are illustrated which are used iteratively in the developed algorithm. Further, the interface between both building blocks is described. The chapter concludes with illustrative examples demonstrating the capabilities of the developed methodology.

4.2 Structure of the optimization methodology

As elaborated in section 2.6, the optimization methodology aims to find the best transmission topology, transmission technology and transmission route for a given interconnection capacity using the maximum power injection capability of the underlying grid. The optimal topology (starting and terminating substations of new links) and power ratings are determined in such a way that investment costs of new links are minimized. The transmission route and the technology selection of a certain link is easy to determine if the rated power and the topology are known. The difficulty is that the used costs for the topology and rating optimization depend on the route and technology selection which in turn is a result on the selected topology and rating.

One way of solving this optimization problem is to determine the best technology and route for each possible transmission path and power rating. If all the optima per path and power rating are known, the global optimal topology enabling the desired interconnection power can be determined using linear integer programming (brute force approach). It is a time intensive prospect to calculate the optimal route, technology and cabling option for every possible power rating and every possible path. The method proposed in this chapter separates the coupled problem into two dependent sub-problems: selection of topology and rating of an electrical network, and discovery of a least cost path which combines the factors of routing, technology and cabling (overhead lines versus underground cabling). The two problems are solved iteratively in a separate way. Topology and rating are first optimized using mixed-integer linear programming (MILP), but based only on fixed average costs per branch. Only the branches chosen in the first stage for a given iteration are optimally routed using shortest path algorithms. Sequentially, the average costs used in the first stage are updated based on the results of the optimal routing algorithm for the next iteration. This way, the computation time can be decreased significantly. The case study in Section 4.6 shows that global optimal solutions are still approached.

Figure 4.1 depicts the proposed optimization methodology. To solve the optimization problem, the maximum power injection capabilities of a selected set of buses have to be provided as input parameter. Additionally, the change in maximum power injection capabilities due to injections and absorptions in different candidate nodes are needed. The calculation procedure of these input parameters has been described in chapter 3.

Initially, average costs for each possible branch are determined, which are used as input for the MILP optimization. To save computation time, these costs are determined using the optimal routing algorithm with a low spatial resolution. The average costs have the dimension $€/MW$. A detailed explanation of the cost calculation is given in section 4.4.

In the first step, the transmission system topology is optimized using MILP. In this step the rating of each branch is optimized, using the average costs and the distance between buses. The objective function and constraints of the MILP optimization are described in section 4.3.

In the second step, the optimal routing, technology and cabling option of each selected path is determined. Spatial information of the investigated area is required. Based on this information, different sub-areas with different spatial weights for each technology and cabling option are defined. These spatial weights are translated into costs to be used by the optimal routing algorithm. Two optimal routing algorithms are described and compared in section 4.5. The output of the optimal routing algorithm delivers minimum costs, optimal route, transmission technology and cabling option for each selected transmission path and power rating.

In the third step, the average costs of selected paths are updated using the output of the optimal routing algorithm. The obtained topology is saved and the routine is repeated until the objective function value of the MILP algorithm and the optimal routing algorithm converge or a certain maximum number of iterations is reached. After the iterative optimization, an N-1 analysis is performed and additional necessary circuit additions are proposed.

The reason for choosing this specific iterative structure rather than including technology selection, transmission routing and security constraints in the MILP optimization is to avoid a complex and non-linear integer problem (MINLP) formulation. Commercial and non-commercial solvers for this type of problems often have problems in terms of convergence and computation time, especially for large scale problems with thousands of variables. The iterative structure of the proposed methodology further allows to obtain a set of feasible solutions instead of one particular solution in the case that the entire problem is solved in one optimization step.

The methodology is implemented in MATLAB. The commercial CPLEX and the open source SCIP solvers are used to solve the MILP problem both delivering different computational efficiency in depending on the size of the MILP problem [110–113]. For smaller scale problems the SCIP solver proves to be more efficient whereas for large scale problems as shown in Chapter 6 the CPLEX solver delivers better efficiency and convergence.

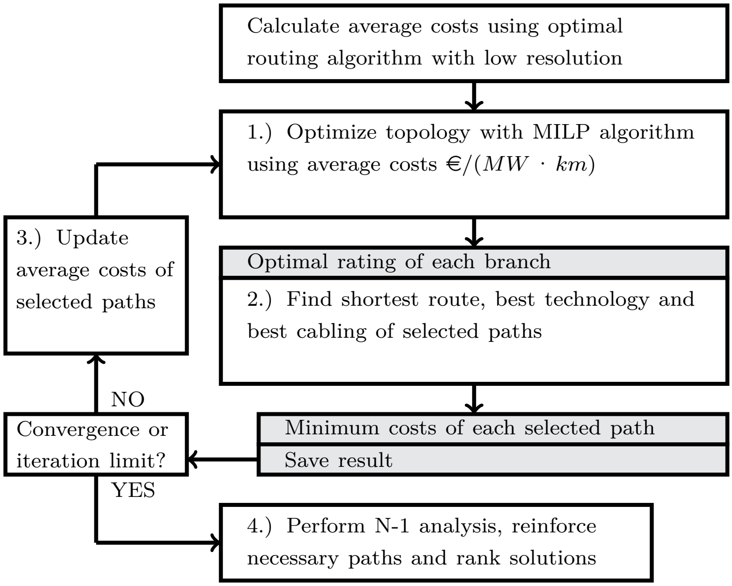

Figure 4.1: Iterative optimization of transmission topology, technology, cabling and routing

4.3 MILP optimization of Topology and Rating

The goal of the MILP optimization is to find the rating of branches in a given set of possible branches which minimize the total investment costs while enabling the desired interconnection P^{inter} between two zones. Possible power ratings are restricted to discrete values given by the $1 \times N_k$ vector

$$\mathbf{k} = [k_1, k_2, \ldots, k_{N_k}] \tag{4.1}$$

where N_k is the number of possible ratings allowed. All possible branches between candidate nodes are considered in the optimization. This means, if there are N_n candidate nodes, $N_b = N_n!/(2 \cdot (N_n - 2)!)$ possible branches exist to invest in.

The interconnector can be comprised of multiple tie-lines and branches, and the final optimal configuration may require flows in different directions. Each branch may affect maximum possible injections of other nodes in a manner unsymmetrical with direction. To account for asymmetry and flow cancellation, two decision matrices of size $N_b \times N_k$ are used in the formulation to indicate a given topology and capacity design. This results in a search space consisting of $N_s = 2 \cdot N_b \cdot N_k$ variables. The definition for positive paths is

$$U^+ = \begin{cases} u_{i,j} = 1 & \text{if branch } i \text{ with rating } j \text{ selected} \\ 0 & \text{otherwise} \end{cases} \tag{4.2}$$

The definition of negative paths (U^-) is similar. Each branch can have at most one capacity specified and a path cannot be selected to be both forward and backward.

$$\sum_{j}^{N_k} U_{ij}^+ + U_{ij}^- = 1 \; \forall \; i \tag{4.3}$$

The actual selected capacities are a $N_b \times 1$ vector

$$K = \left(U^+ - U^-\right) \cdot \mathbf{k} \tag{4.4}$$

where the sign of K indicates intended direction of flow to achieve the desired interconnection capability P^{inter}.

Branches situated inside one zone do not contribute directly to the desired interconnection capability. They are rather local reinforcements necessary to avoid overload situations in case the interconnectors are built. Therefore, tie-lines are marked by the $N_b \times 1$ indicator vector l,

$$\mathbf{l} = \begin{cases} 1 & \text{if branch } i \text{ is a tie line} \\ 0 & \text{otherwise} \end{cases} \tag{4.5}$$

Using the above definitions, the topology optimization problem is formulated as the minimization of a total capacity cost C_{cap} while meeting or exceeding the desired interconnection power and not exceeding maximum injection capabilities of candidate nodes.

$$
\begin{aligned}
\min_{\substack{\forall\, U^+, U^- \\ \in\, B^{N_b \times N_k}}} \quad C_{cap} &= \left(U^+ + U^-\right) : \left(\vec{1} \otimes \mathbf{k}\right) \ \cdot \tilde{C} : L && (4.6) \\
&= \sum_i \sum_j \left(U^+_{ij} + U^-_{ij}\right) \ \cdot K_{ij} \ \cdot \tilde{C}_{ij} L_{ij} \\
s.t. \\
P^{inter} &\leq \left(U^+ + U^-\right) : \mathbf{l} \otimes \mathbf{k} && (4.7) \\
P_{MPIC} &\geq \Delta^{tot}_{MPIC} \ \cdot \ \left(U^+ + U^-\right) \ \cdot \mathbf{k} && (4.8) \\
\overline{K},\ \forall\, i \in [1, N_b] &\geq K_i && (4.9)
\end{aligned}
$$

$\tilde{C}_{ij}$ and L_{ij} denote an average cost and length respectively for every possible branch i and rating j, P_{MPIC} is a column vector with the nodal maximum power injection and absorption capability and Δ_{MPIC} a matrix defining the change in maximum power injection and absorption capabilities due to flows on selected candidate branches. $\overline{K}$ is the maximum allowable capacity of a single line dictated by reliability concerns. This value indicates the power rating of the strongest link within a transmission grid allowed to face an outage and is defined by the TSO according to its specific security constraints. As indicated in the expansion (4.6), the ":" operator in (4.6) and (4.7) is the sum over an element-wise product or Frobenius product, while " $\cdot$ " denotes a regular matrix multiplication or inner product and $\otimes$ the outer product.

Constraint (4.7) states that the sum of power ratings of interconnecting branches has to be more than or equal to the total interconnection power P^{inter}. Constraint (4.8) describes Kirchhoff's current law and states that the maximum power injection capability of connected nodes may not be exceeded. P_{MPIC} is a vector containing maximum power injection and absorption capabilities of candidate buses. If there is a power injection or withdrawal in one node, the maximum power injection capabilities of other nodes change, which is expressed by

$$
\Delta^{tot}_{MPIC} = \begin{bmatrix}
\Delta_{1,1,1} & \Delta_{1,2,1} & \dots & \Delta_{1,N_b,1} & \dots & \Delta_{1,N_b,N_k} \\
\Delta_{2,1,1} & \Delta_{2,2,1} & \dots & \Delta_{2,N_b,1} & \dots & \Delta_{2,N_b,N_k} \\
\vdots & \vdots & \vdots & \vdots & \vdots & \vdots \\
\Delta_{N_n,1,1} & \Delta_{N_n,2,1} & \dots & \Delta_{N_n,N_b,1} & \dots & \Delta_{N_n,N_b,N_k}
\end{bmatrix} \qquad (4.10)
$$

Δ^{tot}_{MPIC} is constructed using the matrices $\Delta^{i,i}_{MPIC}$, $\Delta^{i,a}_{MPIC}$,$\Delta^{a,i}_{MPIC}$ and $\Delta^{a,a}_{MPIC}$ described in section 3.2. The first index indicates the affected node, the second the number of the branch affecting the maximum power injection capability and the third the possible power rating of the branch.

Constraint (4.9) states that the power rating of a selected branch i must not exceed a defined maximum rating $\overline{\mathbf{K}}$, as determined by the technology associated with that branch in the current iteration.

4.4 Calculation and update of average costs

The average transmission system costs in €$/MW$ are inversely proportional to the rating of the transmission system. This is due to the fact that installation costs of equipment are independent of the power rating, once the voltage level, the technology and the location of the installation are defined. Additionally, investment costs also have a fixed part which is independent of the power rating as parts of the production and transportation costs are independent of the power rating.

A given technology achieves a desired link capacity by using an integer number of lines. This introduces a discontinuity in the dependence of cost on link capacities (figure 4.2a). In case different technologies and cabling options for new investments are considered, multiple discontinuities can be found near a given link capacity value. In fact, either technology is cheapest in the neighbourhood of its maximal capacity per circuit (figure 4.2a). A local minimum in the MILP optimization always comes next to such discontinuities, and this complicates the optimization of the topology. Figure 4.2a demonstrates that there can be multiple break-even values to guide a choice of technology 1 or 2. Figure 4.2b is based on the equipment and installation costs used for the case study (section 4.6). The figure shows that for different power ratings of a certain inter-connector, different technologies might provide the cheapest solution. As such, the technology selection has to be performed for each possible power rating separately, rather than based on a predefined break-even power rating.

The costs per used power of transmission equipment for each possible power rating have to be provided. In order to save computation time, the costs for each possible path at the maximum power rating of one system are calculated to provide cost information in the first iteration. The calculation is performed for four different possibilities: AC underground cables (AC UGC), AC overhead lines (AC OHL), DC underground cables (DC UGC) and DC overhead lines (DC OHL), using the optimal routing algorithm with a low spatial resolution. In the same way, the costs at the maximum power rating of a single path, $\overline{K}$

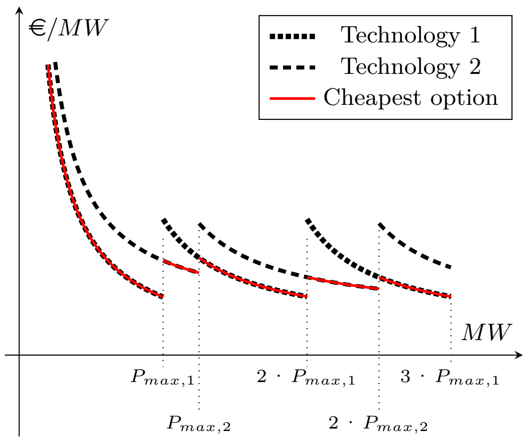

(a) Average transmission system costs as a function of the power rating fro two different technologies.

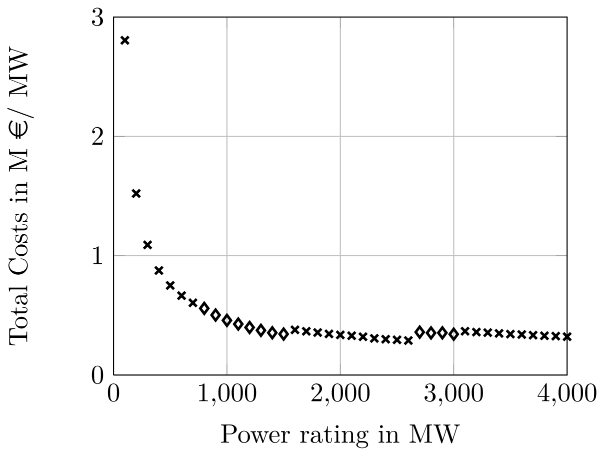

(b) Costs per MW for a possible branch of the case study depicted in figure 4.7. The cheapest technology option for each power range is indicated. Crosses indicate that HVDC technology is preferred, diamonds indicate that HVAC technology is preferred.

Figure 4.2: Average transmission system costs in €/ MW as a function of rated power in MW.

(e.g. on one tower of overhead transmission lines) are calculated. The costs at power ratings other than the aforementioned ratings are obtained using a linear approximation of the calculated costs (figure 4.3a).

After each iteration, the costs of selected paths and power ratings are updated using the costs calculated with the optimal routing algorithm with desired spatial resolution. The costs at all other power ratings are recalculated using linear interpolation and extrapolation of the updated costs (figure 4.3b). In case the obtained average costs after the second iteration are lower than the initially calculated ones, the MILP algorithm chooses the same paths and power ratings again. The optimization algorithm has found a local minimum. As there is no guarantee that the local minimum is a global one, penalty functions are applied while updating the average costs. Therefore, if the costs after the route optimization are lower than the assumed average costs, the average costs of not selected branches are decreased as well. In contrary, if the costs after route optimization are higher, the costs for the selected branch are increased for all power ratings. This way, new branches and power ratings become more attractive in the following iterations and bigger parts of the search space are analysed, increasing the chance of finding the global optimal solution.

4.5 Optimal Routing Formulation and Solution From Cost Graph

The route and transmission technology are interdependent. Additionally, the installation costs for different technologies depend on the type of soil, land acquisition costs and other factors. It is therefore important to optimize the cabling option (OHL vs. UGC), technology (HVAC vs. HVDC) and the transmission route at the same time.

The investment and installation costs for transmission equipment depend on spatial properties of the area of focus. In the developed algorithm, a map of the considered installation area containing all candidate nodes is discretized to a grid of spatial points $p_i = [x_i, y_i]$ of size $N_x \times N_y$ (figure 4.4). The number of chosen nodes and their horizontal and vertical position depend on the desired spatial resolution and the size of the area. All points $p_i = [x_i, y_i]$ are distributed at equal distance. The mesh size for discretization is defined by the user and kept constant during the optimization process for the sake of simplicity. If higher spatial resolutions are needed to investigate a specific area or connection, a different type of map would be needed, requiring the intervention of the user anyhow.

To be able to optimize the technology together with the cabling option, the four technologies of AC OHL, AC UGC, DC OHL and DC UGC must also be represented, as well as the effect of creating hybrid options such as AC with DC and OHL with UGC. Therefore, the optimal routing and technology problem

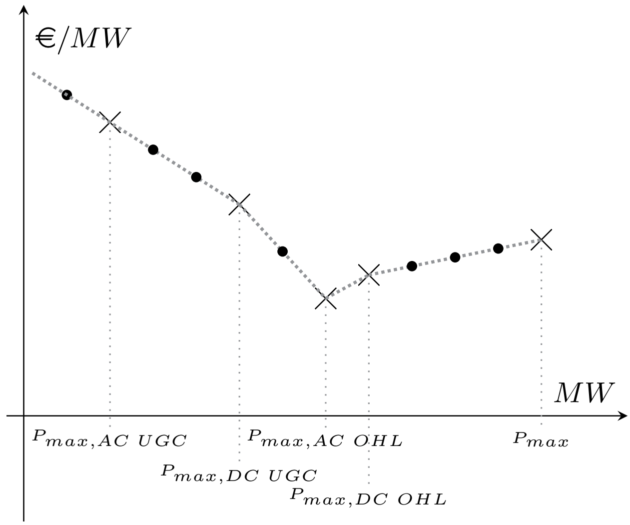

(a) Calculation of average costs for initial MILP

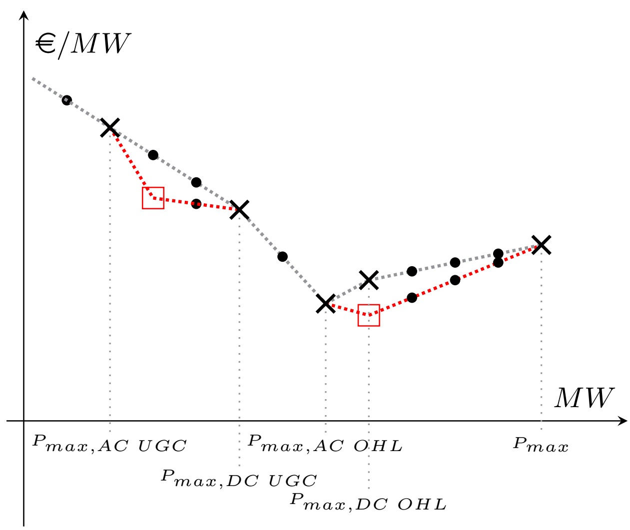

(b) Update of average costs after each iteration.

Figure 4.3: Calculation of initial and updated average costs for the MILP optimization. Crosses indicate costs calculated by the optimal routing algorithm in the first iteration. Squares indicate costs calculated by the optimal routing algorithm in further iterations. Dots indicate extrapolated costs.

Figure 4.4: Creation of a weighted directed graph by discretizing a spatial map

is formulated around a weighted graph $\mathcal{G} = (\mathcal{V}, \mathcal{E})$ having four technology layers and weighted edges signifying costs. For each technology option a separate discretization is performed. For every spatial point p, there are four associated vertices $\mathcal{V}$ representing possible technologies (figure 4.5). A full set of edges $\mathcal{E}$ between vertices associated with adjacent spatial points correspond to cables or lines of a given technology. There are also edges between the vertices associated with different technologies at the same spatial point p that correspond to mechanical or electrical conversions necessary to join dissimilar technologies. This means that for a graph with $N_x \cdot N_y$ nodes, $(10 \cdot N_x \cdot N_y - 3 \cdot (N_x + N_y) + 2)$ edges exist [1].

The graph cost function $\mathcal{W}(p_i, \mathcal{E}_j)$ can take a different positive value for every edge j and represents the cost associated with progressing spatially or switching between technologies:

$$\mathcal{W}(p_i, \mathcal{E}_j) = \left(c^{inv}(p_i, \mathcal{E}_j) + c^{inst}(\mathcal{E}_j) \cdot w(p_i)\right) d(\mathcal{E}_j) + w^{switch}(\mathcal{E}_j) \qquad (4.11)$$

where $c^{inv}(p_i, \mathcal{E}_j)$ and $c^{inst}(p_i, \mathcal{E}_j)$ correspond to both location and technology dependent investment and installation costs, respectively. $w(p_i)$ is a spatial weighting factor to take the change of installation costs in different areas into account. $d(\mathcal{E}_j)$ is the spatial distance associated with the edge, and $w^{switch}(\mathcal{E}_j)$ is a technology conversion cost. The cost factors also depend on the optimal capacity K determined by the other sub-problem, but is omitted as the quantity is fixed for a given iteration.

In (4.11), $c^{inv}(p_i, \mathcal{E}_j)$ and $c^{inst}(\mathcal{E}_j)$ are given in €$/km$ for a defined reference area. The spatial weight $w(p_i)$ defines the relative difference of installation costs in a certain area compared to the reference. In case of offshore cabling, a different $c^{inv}(p_i, \mathcal{E}_j)$ is used to take price differences between on- and offshore cables into account. For HVAC onshore applications, three single phase cables

[1] The total number of edges consist of $[2 \cdot ((N_x - 1) \cdot (N_y - 1)]$ edges connected nodes at the borders of the map, $[(N_x - 1) \cdot N_y + (N_y - 1) \cdot N_x]$ for edges connecting the remaining nodes and $[6 \cdot N_x \cdot N_y]$ nodes for the edges connecting the 4 technology layers.

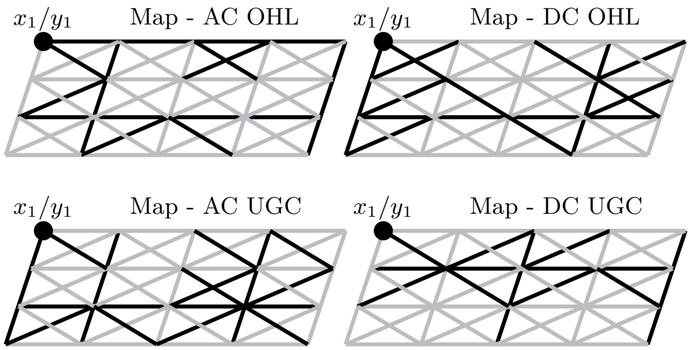

(a) Illustration of the weighted graphs for the 4 technologies, different colors indicate different weights

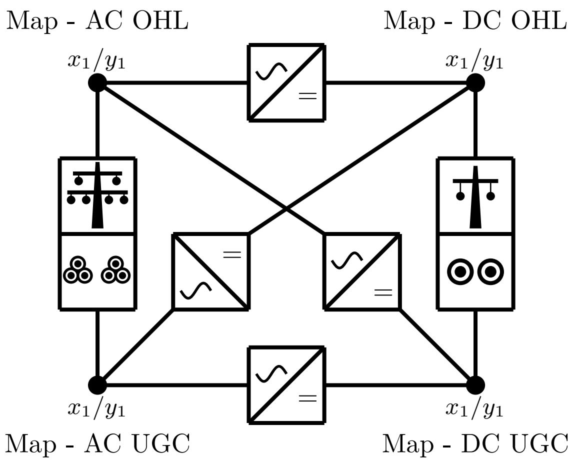

(b) Connection of the four weighted graphs at each edge to enable the technology switch

Figure 4.5: Creation of a weighted directed graph containing four technologies as input for the shortest path algorithm

per circuit are used. On the other hand, three phase cables are used for HVAC offshore applications, as the installation becomes easier. This results in a different number of cables for the same power rating of the link, reflected in the investment costs. For HVDC cables, the number of offshore and onshore cables can be the same. Nevertheless, a cost difference between on- and offshore HVDC cables has to be taken into account, as the armouring of both cables are different. In the same manner, different prices are used for on- and offshore HVDC converters to take the significant offshore platform costs into account.

In case of overhead lines, it is assumed that 2 systems can be installed on one transmission tower both for AC and DC overhead lines such that the cost increase from one system to two systems does not result in doubled costs.

When there is a switch in transmission technology, additional costs occur. The weighting factor $w^{switch}(\mathcal{E}_j)$ is assigned to each edge of the graph to represent such costs in the weighted graph. Figure 4.5 shows how the technology switch is realized. The four technology maps (figure 4.5a) are connected at each vertex x_i/y_i. In case of a switch from AC to DC or DC to AC, the edge is weighted with the cost of an HVDC converter. In case of a switch within the same technology to a different cabling option, the weight is determined using the necessary number of cable systems and conductors per cable system (figure 4.5b). The parameter w^{switch} can be updated by the grid planner in order to adjust the additional costs of technology switch for operational issues and additional necessary equipment for protection. If there is no switch in technology or cabling option, w_i^{switch} is zero.

To calculate the investment costs for the four transmission options, the number of conductors and their cross sections for a given power rating have to be known. The minimum number of conductors and their cross section are calculated using a database with available cable cross sections and their according rating. The necessary number of overhead lines and cables are determined using the rated power of the transmission path delivered by the MILP algorithm and the rated voltage of the link. In the developed algorithm, the available voltage levels for each technology can be defined by the user as input. The defined voltage level is considered to be fixed. In case multiple voltage levels for different transmission technologies are used, the number of technology maps can be increased. In such cases following additional costs have to be included while using w_i^{switch} between technology layers.

- Transformer cost for voltage level changes between AC and AC, with additional costs for transition from OHL to cables.
- HVDC converter station costs for voltage level changes between AC and DC, with additional costs for transition from OHL to cables.
- DC-DC converter station costs for voltage level changes between DC and DC, with additional costs for transition from OHL to cables.

High voltage AC UGC have a high capacitance resulting in high charging currents. This imposes a maximum distance on a cable without compensation. It is therefore assumed that the cable has to be compensated after each cable section of the length $\overline{d}_{ac-ugc}$, such that the active and reactive current in the cable are the same.

$$\overline{d}_{ac,ugc} = \frac{\sqrt{3} I_N}{\sqrt{2} \cdot \omega \cdot C \cdot U_N} \tag{4.12}$$

I_N is the rated current of one conductor, C the capacitance of the conductor per km and U_N the rated voltage of the conductor. Using the charging current, the rating and cost of the necessary compensation equipment is determined and added to the investment costs of AC cables.

Offshore cables can only be compensated at both ends as intermediate offshore compensation stations are too expensive. This means, that AC UGC transmission paths having a longer total offshore cable length than $\overline{d}_{ac-ugc}$ must pass through an onshore area for the compensation station. Therefore, a distinction between on- and offshore edges of the weighted AC UGC graph is included in the shortest path algorithm. Every time an edge located offshore is chosen, the offshore length of the selected path is compared to the maximum AC offshore length $\overline{d}_{ac,ugc}$. If the maximum offshore length of one path is reached, the weights of the next candidate offshore AC edges are multiplied by a large number, so that they are not chosen by the algorithm. After a switch from offshore AC to onshore AC or to HVDC technology, the offshore length of the path is set to zero again to enable further possible offshore segments within the same path.

Including the above mentioned costs and restrictions into a weighted graph, the shortest distance between starting and termination point of a path can be determined using shortest path algorithms. If the weights assigned to the edges of the graph are costs per km of transmission line, the shortest path algorithm delivers the minimum transmission system cost between two vertices.

$$\min_{S} C_{equip} = \sum_{\mathcal{E} \in \mathcal{S}} \mathcal{W}(\mathcal{E}) \tag{4.13}$$

As all four technology layers are interconnected, the shortest path algorithm delivers the minimum transmission system cost where S is a sequence of edges corresponding to the lowest cost or "shortest" path. Two different shortest path algorithms are implemented in the developed methodology, the deterministic shortest algorithm of Dijkstra and the heuristic A* algorithm.

4.5.1 Dijkstra's shortest path algorithm

The Dijkstra algorithm is an iterative algorithm which determines the shortest path between a starting point X and an end point Y in a weighted graph [114].

The algorithm divides all nodes of the weighted graph in three sets which are updated in each iteration.

- Set A contains all nodes from which the minimum path to the starting point X is known.
- Set B contains all nodes which to added to set A in the coming iteration step, being all nodes connected with at least one edge to a node of set A.
- Set C contains all remaining nodes.

All edges of the weighted graph are divided in three sets as well.

- Set I contains all edges which occur in the minimal paths from to the starting point X to the nodes in set A.
- Set II contains all edges which could be added to set I in the coming iteration step. Only one branch of this set is chosen to be added to set I
- Set III contains all remaining branches.

At the start of the algorithm, all nodes and edges are put in set C and set III respectively. The algorithm assumes an infinite distance between all nodes in the start. Then the starting node X is transferred into set A and deleted from set C. Iteratively the following two steps are applied until the shortest path is found (until the end point Y is reached).

- Step 1: All branches connecting the node currently moved into set A with the nodes in sets B and C are investigated. If a branch b delivers a longer path between its corresponding node in set B and the starting point, it is rejected and put in set III. If the branch b connects a node in set C and delivers a shorter path, the branch is put in set II and the corresponding node is moved to set B.
- Step 2: As set I contains minimum paths between the starting point and the points in set A, every node in B can only be connected to starting point in one way and has therefore only one distance to the starting point. The node with the minimum distance from the starting point is moved to set A and the corresponding branch is moved to set I.

Steps 1 and 2 are repeated until the end point Y is transferred into set A, which means that the shortest path is found.

As the shortest path is created using the actual distances between the visited nodes, this algorithm always finds the shortest path between the start node and the end node.

4.5.2 A* shortest path algorithm

The heuristic A* shortest path algorithm determines the shortest path between a starting point X and an end point Y by estimating the distance of candidate nodes and the end point [115]. The algorithm is greedier and therefore faster than the Dijkstra approach.

Starting from X, the set of nodes connected to the starting node are found and included in set A. Sequentially for each node in set A, a distance estimation is performed given in (4.14):

$$h(X,Y) = d(X,A) + h(A,Y) \tag{4.14}$$

d(X,A) is the known distance between node X and the nodes in set A. $h(A,Y)$ is an estimate of the distance between the nodes in set A and the end point Y.

From the nodes in set A, the one with the lowest distance estimate $h(X,Y)$ is chosen as the next node A_{next} in the path. The actual distances of all other nodes in set A to the starting point are saved in set B. These distances are the minima. In the next iteration, A_{next} is defined as the new starting point and set A is recalculated. The estimates are recalculated for the nodes in set A. As some nodes of set A can be part of set B, also the new estimates for these nodes are calculated using the distances in the separate set.

As long $h(A,Y)$ underestimates the distance between the actual node in set A and the end node (e.g. by using the Euclidean distance), the algorithm converges to the shortest possible path. The A* algorithm performs faster if the weights of the graph edges have a large difference as the estimate $h(A,Y)$ has similar values for all nodes in set A if the Euclidean distance is used. The algorithm also performs faster if $h(A,Y)$ overestimates the distance between node A and the end node Y. In this case there is no guarantee of finding the shortest path.

Figure 4.6 shows the relative difference between the computation time of the Dijkstra and the A* algorithm compared to the relative accuracy. The heuristic estimator has been varied for the A* algorithm in order to speed up computation. The horizontal axis shows the length of the shortest path obtained with the A* algorithm divided by the length obtained by the Dijkstra algorithm. The vertical axis shows the computation time of the A* algorithm divided by the computation time of the Dijkstra algorithm. The calculations are performed for different possible transmission paths and power ratings of the illustrated case study in section 4.6.

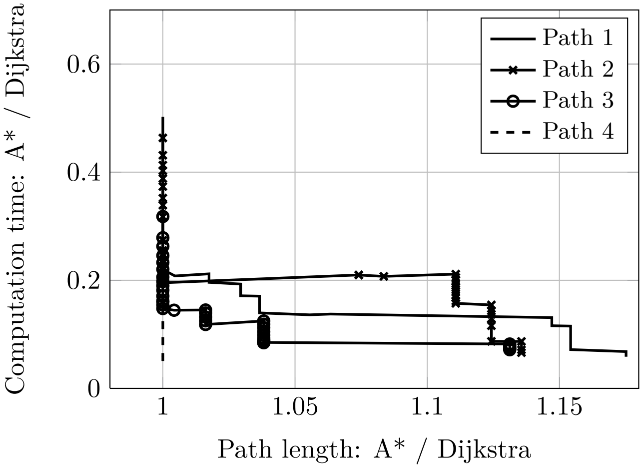

Figure 4.6: Comparison of computation time of the Dijkstra and A* shortest path algorithm

The figure shows that the A* star algorithm reaches 5 to 10 times improvement in computational efficiency without compromising the accuracy. Graphs with a higher number of nodes can be analysed using the same computation time as with the Dijkstra algorithm. This allows the analysis of larger areas and the use of higher spatial resolutions during the analysis.

4.6 Case study

In this section, the application of the developed optimization methodology is shown. The case study is based in IEEE 24 bus test system [116]. During the calculation of the maximum power injection capabilities, the line limits, the maximum generation capacity and the load values of the network are increased. The line impedances are kept constant. The network data of the modified IEEE 24 bus test system is provided in appendix A. The network is divided in two different zones between whom the desired interconnection capability is realised. Zone 1 consists of buses 1 to 12 and bus 24 whereas zone 2 consists of buses 13 to 23. As possible connection points for the additional lines, 5 candidate buses are chosen in each zone which are depicted in figure 4.7.

The area of focus contains offshore areas and prohibited areas (a 3^{rd} country) and several zones where the installation costs of different equipment types have different values. Table 4.1 shows the used weights to take the varying installation costs into account. These weights are chosen arbitrarily and do not necessarily reflect real installation and land acquisition costs. The values are chosen such that different technology options and line routings become feasible. A complete case study with realistic grid and geographic data is provided in chapter 6.

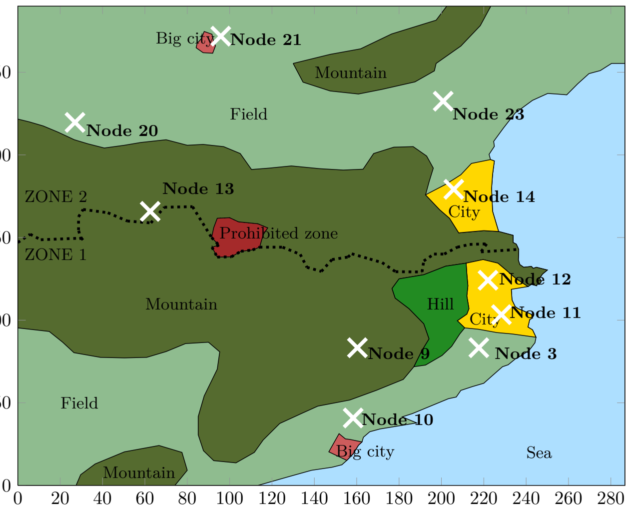

Figure 4.7: Spatial map of area of focus showing candidate nodes in both zones. The case study resembles the eastern border between France and Spain, although no attempt is made to use actual data.

Table 4.1: Spatial weights of the sub areas for the different technology options

Area	AC OHL	DC OHL	AC UGC	DC UGC
Field	1	1	1	1
Hill	2.5	2.5	1	1
Mountain	10	10	4.5	4.5
Sea	40	40	0.75	0.75
City	10	10	2	2
Big city	40	40	2.5	2.5
Prohibited area	40	40	40	40

A number of scenarios with different input parameters are analysed to verify that the proposed methodology converges towards the global optimum. The total interconnection power, P^{inter} and the maximum power per path, $\overline{K}$ are varied in the scenarios. Two different spatial resolutions are considered in the calculations in order to verify the computational efficiency. Possible power ratings of transmission paths are defined as multiples of 100 MW. In this example, a transmission voltage of 400 kV is chosen for AC, whereas ±320 kV is used for DC transmission. The total transmission system cost,

$$C_{tot} = \sum_{N_b} C_{equipment} \tag{4.15}$$

is the final outcome of the iterative optimization methodology where N_b is the number of paths containing transmission equipment and $C_{equipment}$ is the cost of equipment for each path consisting of investment, installation and possible land acquisition costs. The maintenance costs can be added to the investment costs to account for operational costs. The costs for losses are not considered as due to network abstraction actual flows are unknown. Nevertheless, as each feasible solution is delivered as output, a re-ranking can be performed afterwards using the full grid representation including proposed topologies.

Table 4.2 compares the computation time as well as the cost difference between the solutions obtained with the proposed iterative method and global optimum ΔC_{tot}. The global optimum is found using a brute force approach. Therefore, the minimum costs for each possible transmission path and power rating are calculated using both optimal routing algorithms. Once the minimum costs for each path and transmission path are known, the global optimum is determined by applying the MILP optimization as described in section 4.3.

Table 4.2 shows that the iterative approach finds the global optimum or near optimum in a fraction of the computation time required for the brute force approach. The table clearly shows that the savings in computation time are higher in case of higher spatial resolutions. The computation time for the optimal routing algorithm increases exponentially with the resolution, whereas the computation time for the MILP algorithm is largely unaffected by the spatial resolution. The efficiency of the MILP algorithm depends on the number of optimization variables and the costs used in the objective function formulation. The number of optimization variables is independent of the spatial resolution, whereas the costs only vary insignificantly due to the spatial resolution.

The weight of an edge is determined using the average of weights of the starting and terminating node. By using a different spatial resolution, the weight of an edge may change depending on the location of different spatial areas (figure 4.8).

Figure 4.9 shows how the obtained final grid topology is affected by the resolution of the spatial map used. Although the choice of the connected nodes and the power ratings of the connections are the same, there is a clear difference

Table 4.2: Comparison of proposed method (PRO) and brute force calculation (BFC), excluding N-1

P^{inter} (MW)	$\overline{K}$ (MW)	Resolution (km)	Algorithm	C_{tot} (M€)	ΔC_{tot} %	Time (min) PRO	BFC
7000	2000	4	Dijkstra	2373	0	111	637
		4	A*	2373	0	59	361
		8	Dijkstra	2258	1.36	19	80
		8	A*	2258	1.36	13	41
7000	3000	4	Dijkstra	2185	0	88	986
		4	A*	2185	0	61	547
		8	Dijkstra	2094	0	19	123
		8	A*	2094	0	18	63
8000	2000	4	Dijkstra	2719	0	87	637
		4	A*	2719	0	57	361
		8	Dijkstra	2582	0	9	80
		8	A*	2582	0	5	41
8000	3000	4	Dijkstra	2503	0	108	986
		4	A*	2503	0	82	547
		8	Dijkstra	2441	0	34	123
		8	A*	2441	0	17	63

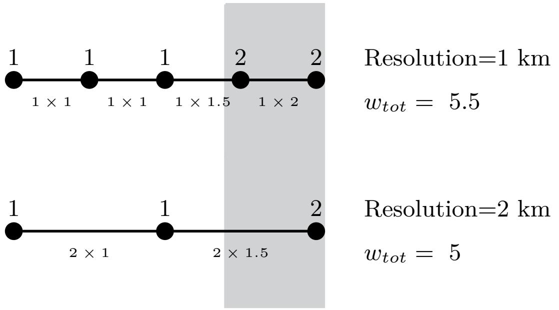

Figure 4.8: Effect of spatial resolution on edge weights

between the line routes and the used technology. For instance, in the HVDC connection between nodes 3 and 21, the optimal routing algorithm with a 8 km resolution delivers a combination of overhead lines and underground cables including an offshore cable section (figure 4.9a). By using a 4 km resolution, the HVDC link is proposed to be built with overhead lines only (figure 4.9b).

Figure 4.10 shows the obtained transmission system in case circuit additions are made to ensure N-1 security of the overlay system. Compared to figure 4.9b, the proposed topology has changed. Although in the N secure case the topology of figure 4.9b is 7% cheaper than the topology of figure 4.10, in the N-1 secure solution that of figure 4.10 becomes 1.3% cheaper. The total investments are approximately 60% higher if the additional transmission system is designed as N-1 secure. In this case, a cost benefit analysis should be conducted taking the expected unavailability and the resulting costs in case of an outage into account. If the expected costs of outages do not justify a cost increase of 60%, the additional system can be designed N secure.

4.7 Conclusions

This chapter provides a methodology to efficiently optimize the transmission system topology, technology, rating and routing taking into account spatial properties. The goal of the optimization is to realise a given interconnection capacity with a minimum on investments consisting of equipment costs and installation costs. The proposed optimization methodology is able to deal with non-linear and discontinuous investment costs to better reflect the lumpiness of transmission system investments.

The main advantage of the demonstrated methodology is that the transmission route and the technology are optimized together. This allows to include area specific installation costs due to soft constraints. For instance, constraints regarding electromagnetic field emissions, visual, environmental and social influencing factors can be reflected in the optimization process. In regions where the effect of these soft constraints is expected to be higher, the area specific weights can be set higher. This way, the transmission route and technology obtained comply with the associated soft constraints. It should be noted that these aspects are difficult to quantify, requiring interaction with the grid planner to analyse different scenarios and sensitivities.

Using an iterative approach, the developed methodology is able to achieve significant computation time savings helping to analyse a larger number of scenarios regarding different input parameters, such as the spatial weights, the maximum power per path, equipment and installation costs.

In this chapter it is shown that the choice of the spatial resolution has an effect on the selection of the route as well as the choice of technology. Therefore it is important to use a routing algorithm which allows a sufficient level of accuracy. This chapter provides two different shortest path algorithms to optimize transmission route and technology. The heuristic A* algorithm proves to be 30 to 50% faster than the Dijkstra algorithm without compromising accuracy.

The chapter also shows that the obtained optimal transmission topologies in the N and N-1 secure cases are generally different. Before designing the additional transmission system N-1 secure, it is important to conduct a cost benefit analysis to compare the extra cost of making the system N-1 secure versus the expected costs due outage for a N secure designed system.

The methodology provided here is only of static nature and considers the transmission system to be built at once. As the development of the system is multi-year process, the methodology has to be modified to assess temporal effects. The following chapter provides the necessary information to improve the developed methodology.

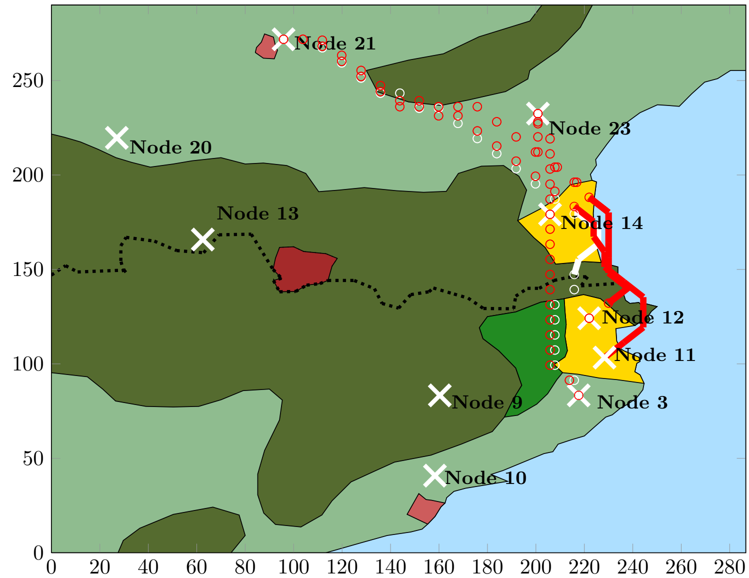

(a) Optimal topology calculated with a resolution of 8km excluding N-1

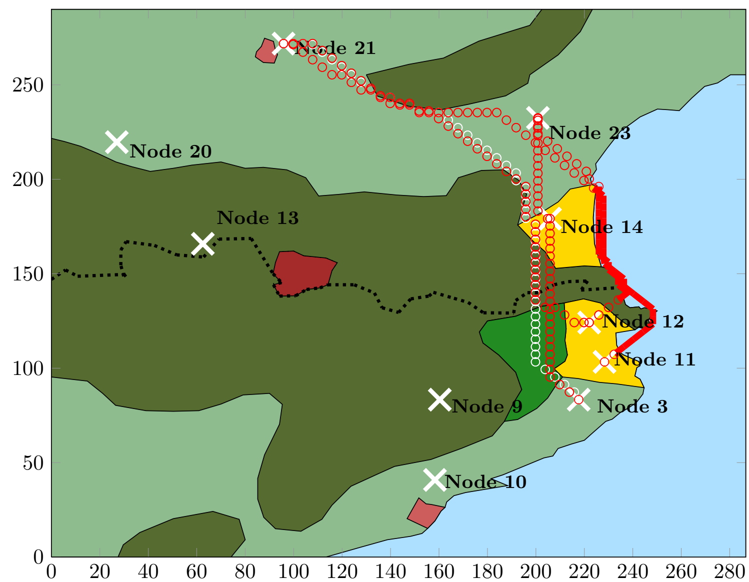

(b) Optimal topology calculated with a resolution of 4km excluding N-1

Figure 4.9: Comparison of different resolutions. Red colour indicates HVAC connections. White colour indicates HVDC connections. Solid lines indicate underground cables. Circles indicate overhead lines. $P^{inter} = 8000\ MW$, $\overline{\mathbf{K}} = 2000\ MW$

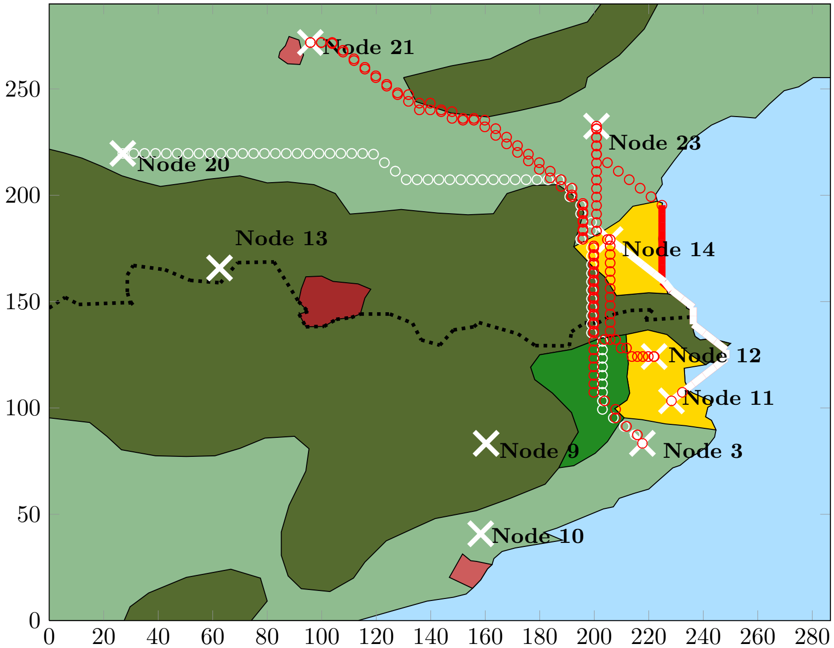

Figure 4.10: Optimal topology calculated with a resolution of 4 km including N-1 for $P^{inter} = 8000\ MW$, $\overline{\mathbf{K}} = 2000\ MW$

Chapter 5

Optimization of Investment Time Points

The future depends on what you do today. - Mahatma Gandhi

5.1 Introduction

Transmission system investment projects are very long lasting infrastructure projects. Transmission lines, cable connections, power transformers or HVDC links built three or four decades ago are still in operation. The planning process of such durable infrastructure is very complex, iterative and time consuming. The transmission system investment process consists of several phases starting from initial planning at the current state of the grid until the construction and commissioning phase (figure 5.1). This entire process usually requires several years up to decades until the assets are built, commissioned and operated. Therefore, large transmission system investments are always planned for long term needs rather than for short term solutions.

While creating an investment plan for future investments, it is very important to align location, type and time point of individual investments. Although postponing investments is economically more feasible in general, it can make sense to overrate transmission lines, in case more generation is planned to be connected in future. The overrating of a transmission line can result in the selection of a different technology and transmission route, as it was shown in chapter 4. Such a behaviour is currently observed for offshore wind farms

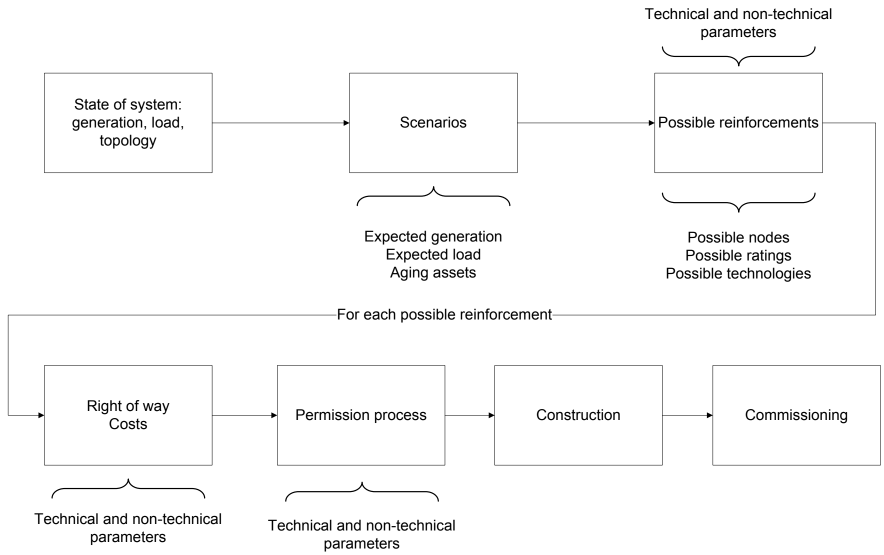

Figure 5.1: The process of transmission system investments [117]

located far from the coast. Although not all offshore wind farms start operation at the same time, offshore wind farms are connected in clusters. The power is transmitted to shore using connections with higher power ratings, decreasing the cost compared to individual connections significantly. Following [11, 117] it is in most cases still economically more beneficial to build clusters even if offshore wind farm projects are severely delayed.

By determining the sequence of investments, a prioritisation of the investments is performed. Assets with the highest priority are built first whereas assets with the lowest priority are postponed as far as possible. The priority of an investment is influenced by different parameters.

System requirements indicate the necessity of building an asset due to expected future generation, demand and power flows. An investment can only be postponed so far, until the system is operated at its limits. If a certain investment is delayed further, shortages of electricity supply can occur.

Technical feasibility indicates the availability of a technology. It can be economically more feasible to postpone an investment until a technology is more mature. This way higher power ratings or lower transmission losses might be achieved without increasing necessary investments.

Economical feasibility indicates that the most expensive assets should be postponed as much as possible. Future investments are in general less expensive in today's currency as future spendings are depreciated.

Investment risk indicates that investments with the lowest risk should be realised first as they are the least likely to fail. The main reason of investment risk is the lack of information and the level of uncertainty. Investments with a higher risk can be postponed in order to obtain more information about the development of the electricity market, demand, generation capacity and technology availability. Additionally there is an uncertainty in terms of permitting and construction of assets. If more and reliable information is available, the investment risk decreases.

The priority of investments may be changed by *political decisions*. For instance, due to the change in energy, climate or environmental policies the priority of investments may need to be adjusted. Besides priority, also the investments might be chosen which comply better with the policy although being not the best technical or economical solution.

This chapter provides an addition to the optimization methodology described in Chapter 4. A time point optimization is included in the optimization methodology in order to analyse and quantify the above discussed parameters. Section 5.2 shows how the objective function and optimization constraints are modified to include time point optimization. Section 5.3 illustrates in detail how the above mentioned parameters influence the final grid topology, technology selection and total investment costs. During the analysis, the case study of Section 4.6 is used as a basis.

5.2 Problem formulation

To include time point optimization, only the MILP problem statement of the optimization methodology is modified. The structure of the optimization methodology where MILP and optimal routing algorithms are used iteratively is kept (figure 4.1). In order to make the optimal routing problem time dependent, the used spatial weights for installation costs can be defined separately for each time point. This way expected changes in the topography, the population density, building density or future natural reserves can be modelled. In the case studies shown in the remainder of the thesis, the spatial weights are kept constant over time as there is little information about the change of these spatial parameters. Eventually, the costs obtained by the optimal routing algorithm have to be depreciated according to investment time points as the optimization of topology and rating considers time dependent costs.

To optimize the topology and power rating, a binary decision variable has been defined for each possible path between candidate nodes and for each possible power rating of the new built assets (section 4.3). In order to include time point optimization, the MILP problem statement has been extended by another dimension, the time. Therefore, the search space has been redefined by using a binary decision variable for possible path, power rating and time point.

In the static case, the number of optimization variables was $N_s = 2 \cdot N_b \cdot N_k$, where N_b is the number of possible branches and N_k the number of possible power ratings. By including optimization time points, the number of optimization variables increases to $N_s = 2 \cdot N_b \cdot N_k \cdot N_t$, where N_t is the number of discrete investment time points during the planning horizon defined by the grid planner.

The objective of the MILP problem statement is the minimization of transmission system costs over the entire planning horizon.

$$\min_{\substack{\forall\, U^+, U^- \\ \in\, B^{N_b \times N_k \times N_t}}} C_{cap} = \left(U^+ + U^-\right) : \left(\vec{1} \otimes \mathbf{k}\right) : \left(\vec{1} \otimes \mathbf{t}\right) \cdot \tilde{C} : L \tag{5.1}$$

$$= \sum_i \sum_j \sum_t \left(U^+_{ijt} + U^-_{ijt}\right) \cdot K_{ijt} \cdot \tilde{C}_{ijt} \cdot L_{ijt} \tag{5.2}$$

The vector $\tilde{C}$ contains the costs for each transmission path and power rating. The elements of $\tilde{C}$ have to be defined separately for each optimization time point t,

$$\tilde{C} = [C_{ij,t=0}, C_{ij,t=1}, \ldots, C_{ij,t=N_t}] \tag{5.3}$$

As future expenses are worth less in today's currency, the elements of the cost vector $\tilde{C}$ have to be depreciated over time

$$C_{ij,t=x} = C_{ij,t=0} \cdot (1-q)^x, \quad 1 \geq q \geq 0 \tag{5.4}$$

where q is a user defined discount rate. As the discount rate is greater than zero, future costs are always lower than at the starting year of the planning horizon. The optimization solver always postpones more expensive investments, as the more expensive solutions have the highest depreciation. The postponement of more expensive investments can only go as far as the optimization constraints allow it. The inclusion of the time point optimization requires the adaptation of existing constraints and the inclusion of several new constraints which are illustrated in (5.5) - (5.10).

$$
\begin{aligned}
P_t^{inter} &\leq \left(U^+ + U^-\right) : \mathbf{l} \otimes \mathbf{k} & \forall\ t \in [1, N_t] \quad (5.5)\\
P_{MPIC,t} &\geq \tilde{\Delta}^{tot}_{MPIC} \cdot \left(U^+ + U^-\right) \cdot \mathbf{k} & \forall\ t \in [1, N_t] \quad (5.6)\\
\overline{\mathbf{C_t}} &\geq \left(U^+ + U^-\right) : \left(\vec{1} \otimes \mathbf{k}\right) \cdot \tilde{C} : L & \forall\ t \in [1, N_t] \quad (5.7)\\
0 &= U^+_{dl} + U^-_{dl} & \forall\ t \leq \mathbf{t_{dl}} \quad (5.8)\\
\vec{1} &\geq E_{hvdc} \cdot \left(U^+_{hvdc} + U^-_{hvdc}\right) & \forall\ t \leq t_{HVDC} \quad (5.9)\\
\overline{K},\ \forall\ i \in [1, N_b] &\geq K_i & (5.10)
\end{aligned}
$$

Constraint (5.5) states that the sum of power ratings of tie lines between zones must be equal or greater than the desired *interconnection capacity*. This constraint has to be fulfilled separately for each time step of the planning horizon. In (5.5), $\mathbf{l}$ is a vector indicating tie lines between the considered zones (eq. (4.5)). As discussed previously in this thesis, the desired interconnection capacity is provided by a market based algorithm calculating the optimal necessary interconnection capacity between zones. The interconnection constraint requires that the desired interconnection capacity is provided for each time step of the planning horizon.

Constraint (5.6) enforces that the *maximum power injection capabilities* of candidate nodes are not exceeded. Similar to the cost matrix $\tilde{C}$, $\tilde{\Delta}^{tot}_{MPIC}$ is defined as a $N_n \times N_t$ matrix, N_n being the number of candidate nodes. The elements of $\tilde{\Delta}^{tot}_{MPIC}$ contain the matrices Δ^{tot}_{MPIC} which indicate the change in the injection capabilities of candidate nodes depending on the power ratings of possible branches,

$$\tilde{\Delta}^{tot}_{MPIC} = \left[\Delta^{tot}_{MPIC,t=0}, \Delta^{tot}_{MPIC,t=1} \ldots, \Delta^{tot}_{MPIC,t=N_t}\right] \quad (5.11)$$

The definition of Δ_{MPIC}^{tot} has been already been provided in equations (4.10) and (3.1) together with the probabilistic calculation procedure for the elements of the matrices.

Usually, transmission system operators have to obtain the necessary *capital for transmission system investments* on the capital market. The amount of available capital for transmission system operators is determined by their financial status and is limited in a certain investment period. Therefore, a new optimization constraint is included to take the limitation of capital availability into account. Constraint (5.7) states that the sum of investments in a particular time step may not be higher than a defined maximum investment $\overline{C}_t$. The $1 \times N_t$ vector $\overline{\mathbf{C}}_\mathbf{t}$ contains the maximum investments per term which can have different values at each investment time point

$$\overline{\mathbf{C}}_\mathbf{t} = \left[\overline{\mathbf{C}}_\mathbf{1}, \overline{\mathbf{C}}_\mathbf{2}, \ldots, \overline{\mathbf{C}}_{\mathbf{N_t}}\right] \tag{5.12}$$

By varying the elements of $\overline{\mathbf{C}}_\mathbf{t}$, several different investment sequences and grid configurations can be obtained. This helps the grid planner to analyse the effects of capital availability on the final grid configuration and the total net present value of investment options. By comparing the different investment sequences, the grid planner can prioritize different investments and reduce investment risks.

Transmission system investment projects face *delays due to internal and external factors.* Internal factors include delays in the supply chain for equipment as well as delays in construction due to unforeseen technical or geographical obstacles. Internal delays occur rarely. External factors occurring often include delays in the planning and permission process, mostly due to public resistance or policy issues. It is important to analyse the effect of possible delays on the final transmission grid topology and the resulting costs in order to identify priority corridors. Constraint (5.8) includes possible delays in the optimization model. The constraint states that certain transmission paths can only be built after a pre-defined time point of the planning horizon. U_{dl}^{+} and U_{dl}^{-} are sub-sets of the binary decision variables U^{+} and U^{-} respectively, defining which transmission paths are the ones facing delays. The vector $\mathbf{t_{dl}}$ assigns time points to each element of U_{dl}^{+} and U_{dl}^{-} from where on connections on these paths may be realised. For instance, to determine how long a line can be postponed from the system point of view, the time point in the delay vector can be increased step by step, until no feasible solution is found or the connection becomes obsolete. Connections which can only be delayed or postponed for a short time period will be the ones with the highest priority and vice versa.

Another interesting aspect in long term planning is *technology availability*. Depending on technology availability, the final grid topology and final investment costs can be different. To analyse the effect of availability of meshed HVDC configurations, constraint (5.9) has been introduced in the MILP optimization problem. The constraint states that for all time points t which are smaller than a defined time point t_{HVDC} no multi-terminal or meshed HVDC configuration is possible. U^{+}_{hvdc} and U^{-}_{hvdc} indicate the decision variables of paths which are established with HVDC and E_{hvdc} is an incidence matrix. E_{hvdc} has the size $N_N \times N_b$, where N_N is the number of candidate nodes and N_b is the number of possible branches. $E_{j,i}$ and $E_{k,i}$ are 1 if branch i is an element of U^{+}_{hvdc} and U^{-}_{hvdc} and connects nodes j and k. All other elements are zero. Constraint (5.9) enforces that only *one HVDC connection can be connected to any node*. The variation of t_{HVDC} helps to determine until when the technological matureness of multi-terminal HVDC configurations must be reached so it is still economically feasible to build such configurations. If the technology maturity is not reached by that time point, only point to point connections are built until the end of the planning horizon.

Constraint (5.10) states that *the maximum power rating* of a connection path may not exceed a pre-defined maximum rating $\overline{K}$.

5.3 Application of the time point optimization

This section shows the application of the time point optimization delivering a stepwise investment plan as output. The calculations are based on the geography and grid data of the example shown in Section 4.6.

Figure 5.2 shows the result of the time point optimization for four chosen time points, $t = [0, 4, 8, 12]$ years. The desired additional interconnection capacity between both zones is 2400 MW in year 0, 2600 MW in year 4, 2600 MW in year 8 and 2400 MW in year 12 equal to additional 10 GW of interconnection capacity at the end of the planning horizon. The maximum power rating for single transmission paths is $\overline{K} = 3000\ MW$. Figure 5.2 depicts the resulting expansion plan for the base case where the constraints for meshed HVDC, line delays and maximum investment per time step are relaxed. The relaxation of these constraints delivers the cheapest possible solution under the taken assumptions. By using more strict constraints on the optimization problem, the obtained solution can only be more expensive.

In the first time step, two AC connections are established between nodes 23 and 12 containing an offshore cable section. Between nodes 23 and 14, a local reinforcement is placed using an AC overhead line configuration. In year 4, an HVDC overhead line connection is established between nodes 21 and 3. In years 8 and 12 HVDC overhead line connections between nodes 21 and 10 and nodes 20 and 3 are established respectively. This results in a multi-terminal HVDC scheme consisting of nodes 3, 10, 20 and 21. In the base case, the total investments over the entire planning horizon equal 2413.4 M€. The power ratings of the connections and their total costs are summarized in table 5.1. The table shows non-discounted ($C_{tot}^{non-disc}$) and discounted costs (C_{tot}^{disc}) using an discount rate of 5 %.

Table 5.1: Cost, length and time points of built links in the base case

From node	To node	Rating	Time point	$C_{tot}^{non-disc}$	C_{tot}^{disc}	Length
		(MW)		(M€)	(M€)	(km)
12	23	2600	1	598.6	598.6	129.7
23	14	200	1	73.7	73.7	54.7
3	21	2600	2	847.9	690.6	253.8
10	21	2600	3	911.2	604.5	303.5
3	20	2200	4	825.2	445.9	299

5.3.1 Variation of meshed HVDC constraint

In this section, the multi-terminal HVDC constraint is enforced during the MILP optimization. The maximum investment and the line delay constraints remain relaxed. In the base case, the first multi-terminal configuration was established after the 8^{th} year of the planning horizon (figure 5.2). Therefore, two cases are analysed. In the first case, multi-terminal HVDC operation is allowed only after the 12^{th} year, whereas in the second case multi-terminal HVDC operation is not allowed throughout the planning horizon.

Figure 5.3 and table 5.2 show the obtained investment sequence and the detailed breakdown of costs for case one. Figure 5.3 depicts that the final grid topology is different to the base case. In the first time step, two HVAC links are established. In the second time step an HVDC overhead line connection is built. In third step, where still no multi-terminal operation is possible, another point to point link is established between nodes 10 and 21. In the last time step, the first multi-terminal link is established between nodes 3 and 10 and 21. The total costs of the obtained system are 47.7 M€ higher than in the base case.

Table 5.2 shows that although the starting and terminating points of the links are not changed, different power ratings are used to fulfil the desired interconnection capability. As mentioned earlier throughout this work,

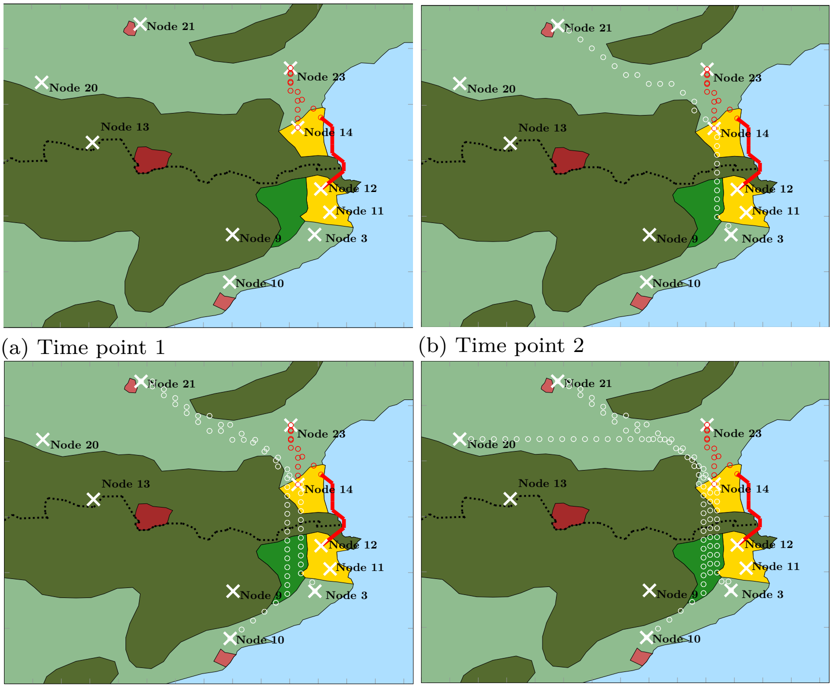

(a) Time point 1
(b) Time point 2
(c) Time point 3
(d) Time point 4

Figure 5.2: Optimal investment plan of base case. Red colour indicates HVAC connections. White color indicates HVDC connections. Solid lines indicate underground cables. Circles indicate overhead lines. $P^{inter} = 10000\ MW$, $\overline{\mathbf{K}} = 3000\ MW$

differences in power ratings may result in different route and technology selections. In this case, we can see that the HVDC link connecting nodes 3 and 21 has a power rating of 2200 MW, resulting in the use of overhead lines combined with underground and submarine cables. In the base case, the same HVDC link has a power rating of 2600 MW and consists entirely of overhead lines using another transmission route. The difference in power ratings requires a different number of circuits and cross sections resulting in the selection of a different transmission route and technology.

Figure 5.4 and table 5.3 show the obtained expansion plan if multi-terminal HVDC operation is not allowed throughout the entire planning horizon. Figure 5.4 depicts that the most HVDC connections are substituted by HVAC connections if multi-terminal HVDC operation is not possible. In this case, only one HVDC link, connecting nodes 10 and 21, is selected in the final grid topology. In the final topology 6 links are established instead of 5 in the previous two cases. The total costs of the obtained system are 98.2 M€ higher

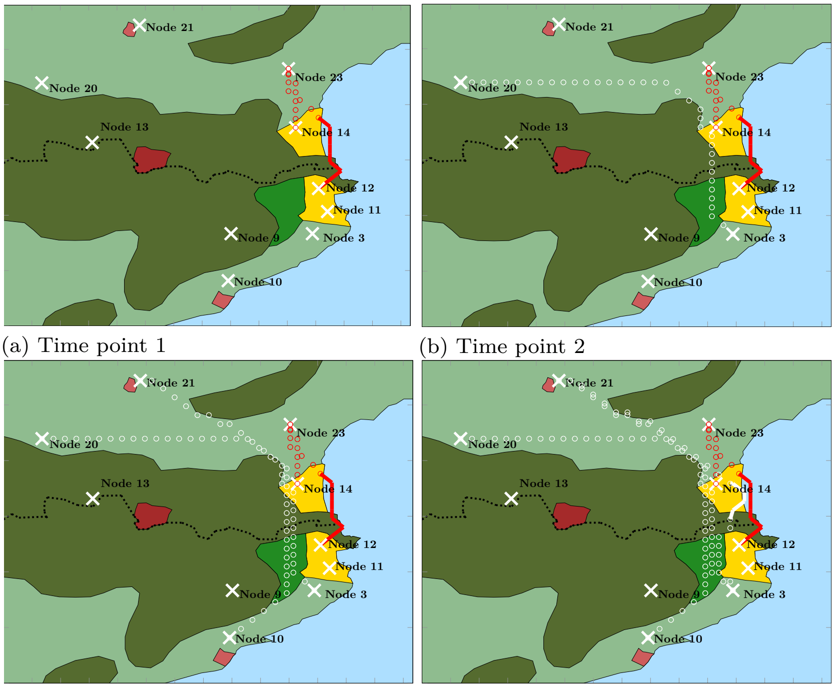

(a) Time point 1
(b) Time point 2
(c) Time point 3
(d) Time point 4

Figure 5.3: Optimal investment plan if multi-terminal HVDC may first be built in time point 4. Red colour indicates HVAC connections. White color indicates HVDC connections. Solid lines indicate underground cables. Circles indicate overhead lines. $P^{inter} = 10000\ MW$, $\overline{\mathbf{K}} = 3000\ MW$

Table 5.2: Cost, length and time points of built links, with constraint on multi-terminal HVDC

From node	To node	Rating	Time point	$C_{tot}^{non-disc}$	C_{tot}^{disc}	Length
		(MW)		(M€)	(M€)	(km)
12	23	3000	1	670.8	670.8	129.7
23	14	600	1	83.5	83.5	54.7
3	20	2200	2	825.2	672.2	299
10	21	2600	3	911.2	604.5	303.5
3	21	2200	4	796	430.1	269.1

than the base case equal to 4.12 %. It should be noted that these costs only reflect the investment and installation costs. In this case, the total length of transmission system is increased to 1193 km compared the 1041 km of the base case. The additional 152 km of lines and cables affect the costs for maintenance which is not considered in this calculation.

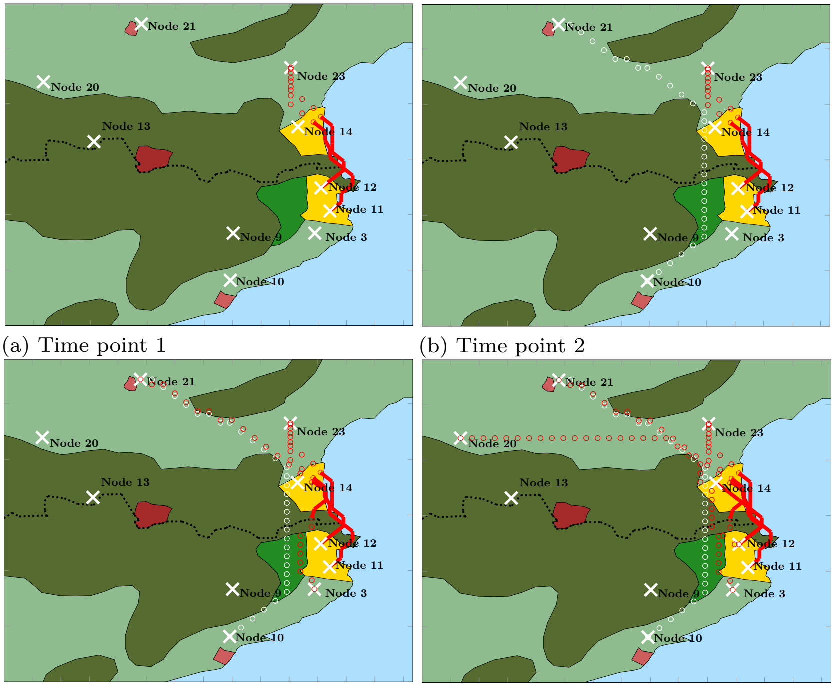

(a) Time point 1 (b) Time point 2

(c) Time point 3 (d) Time point 4

Figure 5.4: Optimal investment plan if multi-terminal HVDC is not allowed. Red colour indicates HVAC connections. White color indicates HVDC connections. Solid lines indicate underground cables. Circles indicate overhead lines. $P^{inter} = 10000\ MW$, $\overline{\mathbf{K}} = 3000\ MW$

Table 5.3: Cost, length and time points of built links if multi-terminal HVDC is not allowed

From node	To node	Rating	Time point	$C_{tot}^{non-disc}$	C_{tot}^{disc}	Length
		(MW)		(M€)	(M€)	(km)
11	23	1400	1	376.4	376.4	153.1
12	23	1000	1	254.5	254.5	129.7
10	21	2600	2	911.2	742.2	303.5
3	21	3000	3	1097.5	728.1	269.1
12	20	1400	4	546.6	295.4	262.5
12	14	600	4	212.9	115.1	75.4

5.3.2 Variation of line delay constraint

This section shows how the optimal grid topology is affected if certain connections cannot be established before a dedicated time point t_{dl} of the planning horizon. During the calculations, the multi-terminal HVDC and the maximum investment constraint have been relaxed. In the analysed cases, so far the HVAC connection between nodes 12-14 and nodes 12-23 have been chosen in the first time step of the planning horizon. Figure 5.5 depicts the investment sequence if these two connections cannot be established in the first time step of the planning horizon, e.g. due to delays in permitting process. In this case we can see that the final grid topology is the same as in the base case as these connections are built in the second time step instead of the first time step. Nevertheless, the total costs are increased by 32.6 M€, due to the difference in the investment sequence.

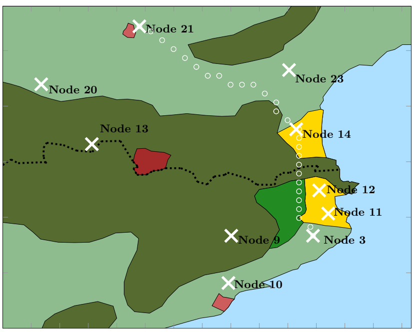

(a) Time point 1

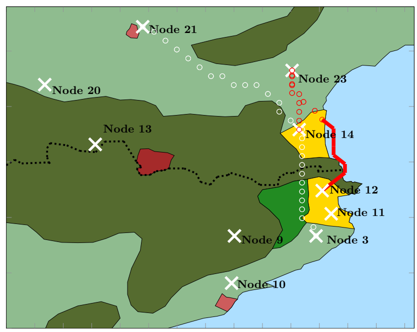

(b) Time point 2

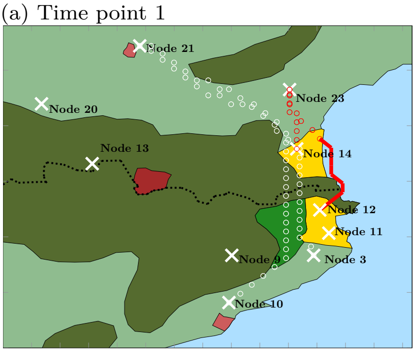

(c) Time point 3

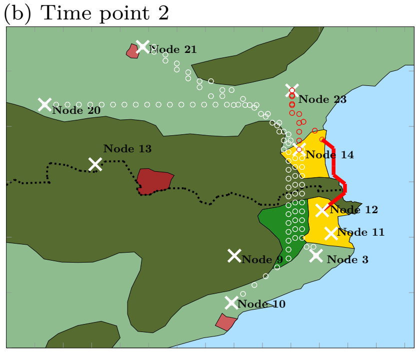

(d) Time point 4

Figure 5.5: Optimal investment plan if connections between 12-14 and 12-23 are allowed in the second time step of the planning horizon. Red colour indicates HVAC connections. White color indicates HVDC connections. Solid lines indicate underground cables. Circles indicate overhead lines. $P^{inter} = 10000\ MW$, $\overline{\mathbf{K}} = 3000\ MW$

Figure 5.6 shows the investment sequence if the connections between nodes 12-14 and 12-23 are delayed until the third time step of the planning horizon. In this case we can see that these connections are not established during the entire planning horizon even although they would have been possible in time steps 3 and 4. This means that after the investments made in the first two time steps, it is not the most economic solution to establish connections between nodes 12-14 and 12-23. The total costs of this configuration are 67.1 M€ higher than the base case.

This simple example shows how important it is to take possible delays in the planning process into account. The example shows that the economical benefits of putting the lines in place is only given until a certain point in time. If the investments cannot be achieved until then, another investment plan should be favoured.

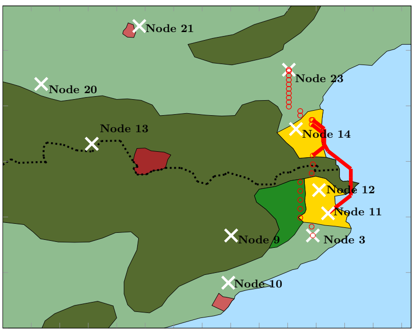

(a) Time point 1

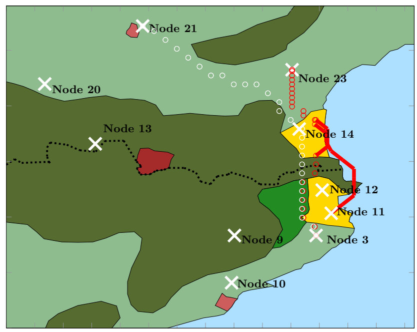

(b) Time point 2

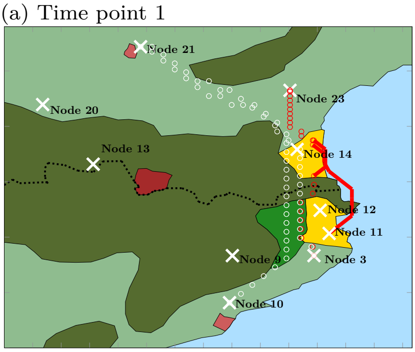

(c) Time point 3

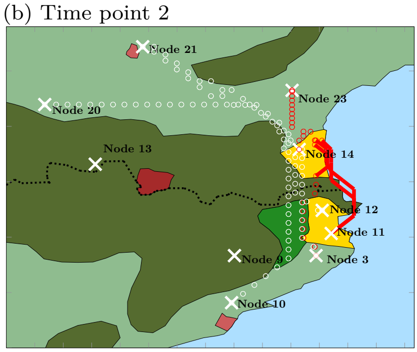

(d) Time point 4

Figure 5.6: Optimal investment plan if connections between 12-14 and 12-23 after the third step of planning horizon. Red colour indicates HVAC connections. White color indicates HVDC connections. Solid lines indicate underground cables. Circles indicate overhead lines. $P^{inter} = 10000\ MW$, $\overline{\mathbf{K}} = 3000\ MW$

5.3.3 Variation of maximum investment constraint

This section shows how the optimal investment sequence is affected if the capital availability is constrained. The meshed HVDC constraint and the line delay constraints are relaxed during this analysis. In the base case which is the cheapest option, 672.3 M€, 690.6 M€, 604.5 M€ and 445.9 M€ were spent in each investment time period (table 5.1). This equals to total transmission system costs of 2413 M€.

Table 5.4 shows the total investment costs obtained for different combinations of capital availability. The table shows that in the first two investment time steps, at least 1400 M€ have to be invested in order to realise the desired interconnection capacity. Cases where less capital is available in the first two steps result in infeasibility. The table shows that the best solutions are found there, where the capital availability is approximately equally divided. The reason is that the desired interconnection capacity is equally divided over the planning horizon. The optimization algorithm places the cheapest connections first. Although the investments in the following time steps are more expensive in future currency, in the currency of time point 1, they have a similar value to the investments of the first time step. In the base case, 1050.4 M€ have been invested in the third and fourth time step. The only way of decreasing the investment costs in the last time steps is to seriously over-invest in the first years of the planning horizon. Table 5.4 shows that more than 1700 M€ have to be invested in the first two time steps to reduce the spendings in the third and fourth time step. Obviously, this results in an overall worse economic performance compared to the case where capital is not constrained.

5.4 Conclusions

This chapter shows how the optimization of investment time points is included in the proposed optimization methodology. The time point optimization is achieved by modifying the problem formulation of the MILP optimization. Therefore decision variables for investment time points are included in the search space. Three new constraints are included in the problem formulation, in order to take capital availability, possibility of multi-terminal HVDC operation and possible line delays into account.

The analysed case study shows the importance of taking the afore-mentioned constraints into account. If technical developments or realization of investment projects are delayed, the optimal grid topology can be different than in the initially assumed investment plan. Uncertainties in technological developments

Table 5.4: Total costs of investments with constraint on capital availability

$\overline{C}_1$ (M€)	$\overline{C}_2$ (M€)	$\overline{C}_1$+$\overline{C}_2$ (M€)	$\overline{C}_3$ (M€)	$\overline{C}_4$ (M€)	$\overline{C}_3$+$\overline{C}_4$ (M€)	$\sum\overline{C}$ (M€)	C_{tot} (M€)
700	1000	1700	400	400	800	2500	nsff
1000	1000	2000	400	200	600	2600	nsff
700	1100	1800	400	400	800	2600	nsff
900	800	1700	700	200	900	2600	nsff
800	800	1600	500	500	1000	2600	nsff
800	700	1500	500	600	1100	2600	nsff
900	600	1500	500	600	1100	2600	nsff
900	600	1500	600	500	1100	2600	2486
1100	400	1500	500	600	1100	2600	nsf
800	650	1450	600	550	1150	2600	2488
700	700	1400	600	600	1200	2600	2490
900	500	1400	700	500	1200	2600	nsff
1000	400	1400	800	400	1200	2600	nsff
700	650	1350	650	650	1300	2650	nsff
900	900	1800	600	300	900	2700	2624
700	1200	1900	400	400	800	2700	2641
1000	500	1500	800	400	1200	2700	2570
1000	500	1500	700	500	1200	2700	2459
1100	1100	2200	400	200	600	2800	nsff
1200	400	1600	800	400	1200	2800	2585
900	400	1300	900	600	1500	2800	nsff
1000	300	1300	900	600	1500	2800	nsff
1200	1100	2300	400	200	600	2900	2813
1200	1200	2400	400	200	600	3000	2783

nsff . . . no feasible solution found

and delays put additional risks on investments which can be reduced by analysing different scenarios and prioritizing connections. The total economical benefit of achieving technology maturity can be quantified and analysed with the provided methodology.

Delays in transmission infrastructure projects are very common, especially if overhead line technology is used. In this chapter a simple case was shown, where a delay in the investment causes that a certain connection becomes economically less beneficial and therefore never built. Other established links can alleviate the requirements for new investments and a new system architecture can become economically more feasible. Especially for transmission system operators this information is very essential. In order to influence regulating bodies and accelerate the permitting procedure, the "point of no return" for certain links can be provided to decision makers. If the establishment of the connection is delayed beyond that point, other expansion options should be considered.

This chapter also shows how the total system costs are affected if capital availability is constrained. If future capital availability is uncertain, transmission system operators can overinvest in short term. The developed algorithm shows the required overinvestment if future spendings are constrained. This helps to quantify measures to avoid or decrease future risks in the capital market.

Chapter 6

Application of the transmission investment optimization methodology

There is no idea so bad that it cannot be made to look brilliant with the proper application of fonts and colour - Scott Adams

6.1 Description of case study

In order to demonstrate the possibilities of application, its capabilities and also functionality, the developed methodology is applied to a larger system for long term transmission system investment optimization. For the case study, public available data is used. Hence, the shown results can only be interpreted as indicative results as a simplified representation of the transmission grid and limited geographic data could be used.

The starting point of the case study is the roadmap for a low-carbon economy in Europe for 2050 established by the European Climate Foundation (ECF) [10, 118]. The roadmap states that additional 33 GW of transmission capacity between the Iberian peninsula and France may enable economically efficient integration of solar and wind resources in the European electricity system (figure 6.1) [10]. As the Iberian peninsula has favourable wind and solar resources, increased transmission capacity to France is needed to export renewable energy on large scale. This way, social welfare in Europe is maximized while reducing greenhouse gas emissions according to the European 2050 climate targets.

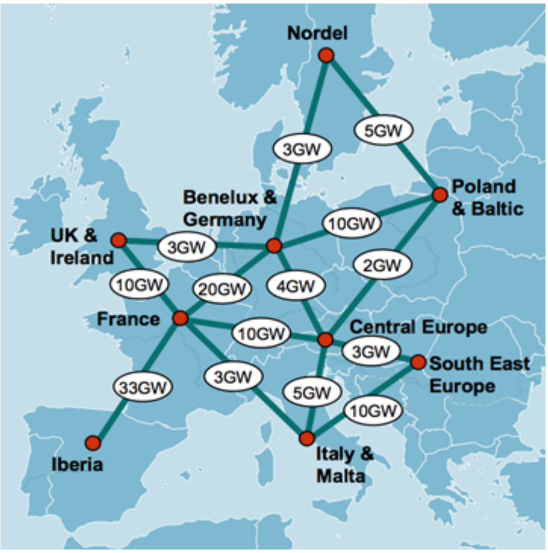

Figure 6.1: Required additional transmission capacity for 2050 according to [10]

The necessary geographic information for the optimization of transmission technology and routes is derived from the Socio-economic Data and Applications Centre (SEDAC). In order to account for social impact, the population density is used whereas elevation is used to reflect topographic properties (figure 6.2).

In order to assign spatial weights to installation costs, the elevation and population density maps are imported as graphical images. Depending on its colour, a different spatial weight is assigned to each pixel of the image. The smallest possible geographic resolution is limited by the graphical resolution of the image. With the available elevation and population density maps, the smallest possible resolution is 2.68 km.

12 different elevation levels have been identified in the used map whereas the population density map consists of 11 different levels. The spatial weights for installation costs of different equipment types are provided in Appendix B. In order to combine both maps, a weighted sum of the population and elevation weights is used

$$\mathcal{W}_{tot} = \frac{a_e \cdot \mathcal{W}_{elevation} + a_p \cdot \mathcal{W}_{population}}{a_e + a_p} \tag{6.1}$$

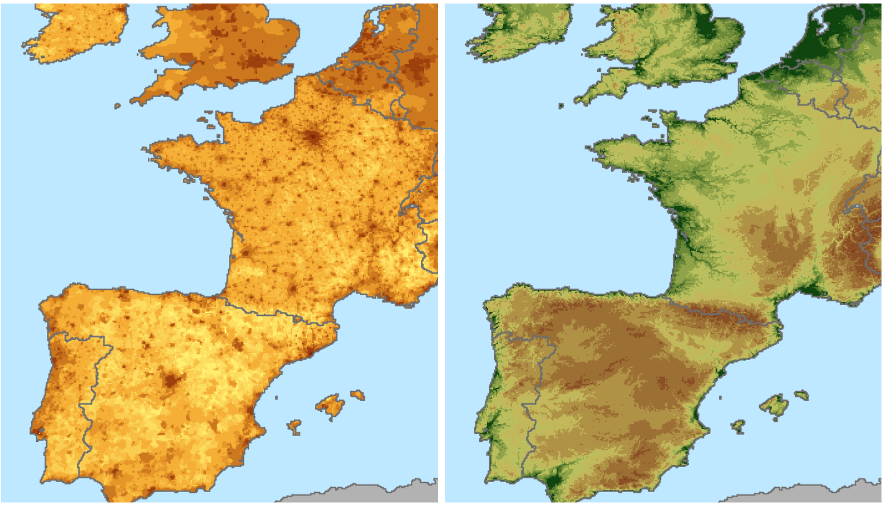

(a) Used population density map [119] (b) Used elevation map [120]

Figure 6.2: Population density and elevation map of the Iberian peninsula and France

where, a_e and a_p indicate how much the elevation and population density contribute to the total spatial weight $\mathcal{W}_{tot}$. In section 6.3, a sensitivity analysis on a_e and a_p is performed comparing the optimal solution and total transmission system costs for different values of a_e and a_p.

6.2 Identification of strong nodes

The European transmission grid model according to [121] provides a sufficiently detailed equivalent representation. The transmission grid model consists of 1494 buses, 2322 branches and 570 generators (figure 6.3). It provides transmission network data (line impedances), power plant locations, fuel types of power plants, locations of load centres and the demand in load centres [121]. It is sufficient to use cost ratios between different generation types for the calculation of maximum power injection capabilities obtained from [122]. The transmission line ratings serve as constraint for the maximum power injection capabilities and need to be estimated as the used transmission grid model does not provide line ratings [121]. Therefore, the number of circuits per branch is calculated using impedance and distance information of lines. The line ratings are calculated using 1500 MW and 800 MW per circuit of 380 kV lines and 220 kV lines respectively.

Figure 6.3: European high voltage transmission grid representation according [121]

To limit the calculation time, only the Spanish and French transmission grids are used consisting of 523 nodes (figure 6.4). The neighbouring transmission grids of Portugal, Italy, Germany, Switzerland, Belgium and UK have been represented using equivalent injections on border nodes. After calculating the connection capability (Section 3.4.4), a total of 34 candidate nodes have been selected. Additionally, the geographic location is taken into account during the selection of candidate nodes. Candidate nodes are geographically distributed in both countries (figure 6.4). Out of the 34 candidate nodes, 18 are situated in France whereas 16 nodes are located in Spain.

For the calculation of maximum power injection (import in one node) and

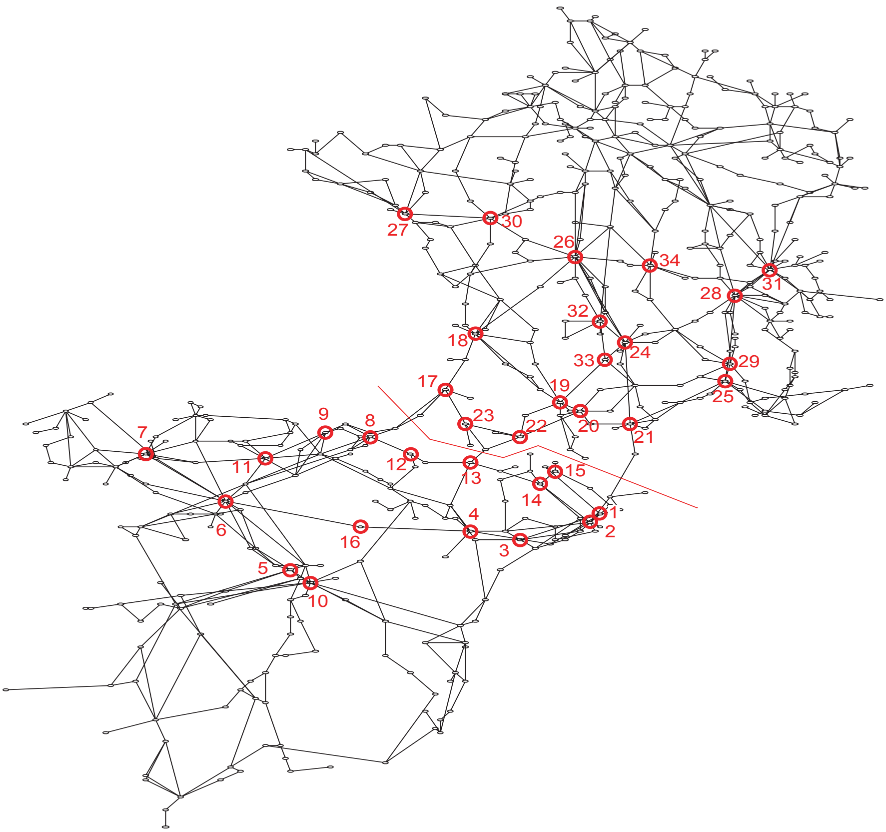

Figure 6.4: Structure of the used network. Circles indicate chosen candidate nodes [121]

maximum power absorption (export from one node) capabilities, different load profiles have been used derived from [101]. Three different load profiles have randomly been applied to each load centre. At nodes containing wind and solar generators, according generation profiles have been applied to account for stochastic renewable generation. After application of the calculation methodology described in chapter 3, maximum power injection and absorption capabilities are obtained (figure 6.5).

Figure 6.5 shows that nodes 26, 28 and 31 have the highest power import capacity. Nodes 6, 10, 26, 28 have the highest power export capacity. The spread of the import and export capacity is different for each node. The most favourable nodes for new connections are the ones, where import and export capacity is high and their spread small. This means that these nodes are less sensitive to volatility of power flows. The figure shows that nodes with a high import capacity also have a high export capacity. In general, the import and export capacity depend on the geographic spread of generation and load centres as well as how well candidate nodes are interconnected. In this specific case, the geographic spread of generation and load centres is more homogeneous so that import and export capacities mainly depend on the level of interconnection.

6.3 Possible future expansion plans

This section shows possible future grid expansion options to establish 30 GW of additional interconnection capacity between Spain and France. Other optimization parameters are:

- The total interconnection power is established in four investment time steps, $\mathbf{t} = [0\ 10\ 20\ 30]$ years
- The cumulative interconnection capacity per time step is $P_t^{inter} = [8\ 16\ 23\ 30]$ GW
- The new connections can be built in multiples of 500 MW
- 400 kV is used for AC transmission, ±320 kV is used fro DC transmission
- DC transmission is assumed to be with VSC technology
- The used discount rate is 3% per year, without accounting for inflation and price increase of equipment

Figure 6.6 shows the optimal investment plan if the maximum power rating per path is restricted to 3 GW. In the first investment time step, strong candidate nodes in southern France and northern Spain are connected first. Four out of five new transmission lines are established using HVAC technology. The longest line section connecting node 15 with node 33 is established using HVDC technology. With advancing time, the total length of new built connections increase as the power injection capability of nodes near the border do not allow the connection of new lines. In the final investment period, line sections up to 1119 km are realised connecting south-east of France with central Spain, using a transmission capacity of 3000 MW. In total, 1301 km, 1530 km, 1658 km and 2835 km of new lines are built at each investment time period.

Under the taken assumptions, most interconnections are established using overhead line technology. During the entire planning horizon, only one

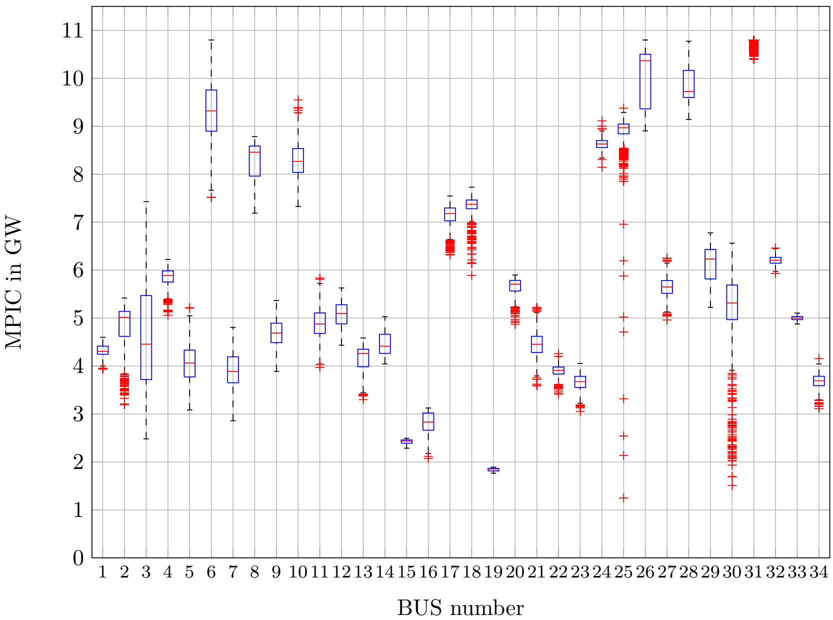

(a) Maximum power import capabilities of candidate nodes

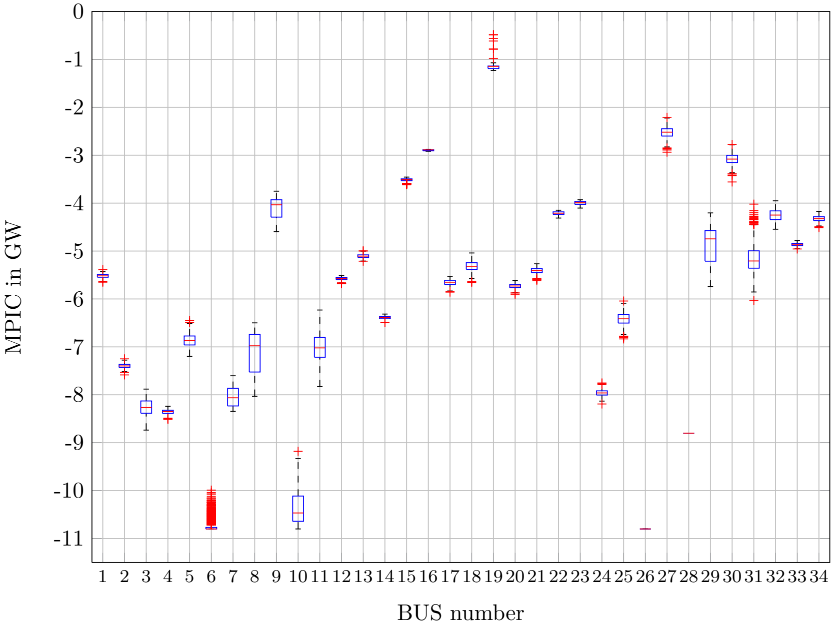

(b) Maximum power export capabilities of candidate nodes

Figure 6.5: Maximum power import and export capabilities of candidate nodes.

underground cable connection appears using HVDC technology (figure 6.6b). HVAC technology is preferred to connect nodes close to each other, whereas for longer distances HVDC technology is used. As HVDC overhead lines require less conductors, the cost per km of HVDC overhead line is less than HVAC overhead lines. Out of 17 new connections built over the entire planning time horizon, 9 are established in HVDC technology. With increasing transmission distance, cost savings of using HVDC overhead lines outweighs costs of HVDC converters making HVDC economically more feasible. The transmission losses are not taken into account during the optimization process.

The total net present value of the grid expansion equals 8223.6 M€. If the costs are broken down by time step, we can see that in the four steps investments worth 1894.8 M€, 2137.5.7 M€, 1863.9 M€, 2327.4 M€ are required. In the obtained investment plan, the net present value of the total investment is spread approximately equally over the planning horizon. On one hand, distances of connections increase with time, on the other hand, investments per km of line decrease due to depreciation. The chosen discount rate of 3% causes that the net present value of investments in year 30 are only worth 40% of year 0.

Figure 6.7 shows the optimal investment plan if links with a maximum power rating of 5 GW can be established. In this case, the number of necessary links is reduced to 15 instead of 17. Figure 6.7 further shows that the majority of long links are built in South-East France and North-East Spain, whereas in the previous case also long connections between Western France and Western Spain were built. This is due to the reason that the larger generation and load centres are situated in South-East France (Lyon area) and North-East Spain (Catalonia). If links with higher capacities can be built, the potential of power injection and absorption in these nodes can be utilized better. Using links with lower capacities mean that other connection points must be found in order to achieve the desired interconnection power. Table 6.1 shows that the total investment cost is decreased if transmission links with 5 GW are used. The total investments decrease to 7.408 G€ equal to a cost saving of 9.91%. Table 6.1 further shows that the required length of new lines is approximately 2000 km less if links with 5 GW are used. This has a positive impact on maintenance decreasing operational costs. With taken assumptions, only overhead lines are used in this configuration. As the proposed line sections are shorter, HVAC technology is preferred more often. Out of 15 connections built over the planning horizon, 10 are established in HVAC technology.

Although any link can be built with 5 GW, only one transmission link is actually built with a capacity of 5 GW connecting nodes 4 and 33 via an HVDC overhead line. The reason is that the use of larger links is restricted by the maximum power injection capability of candidate nodes. In case larger links would be connected, overload situations in the underlying network may

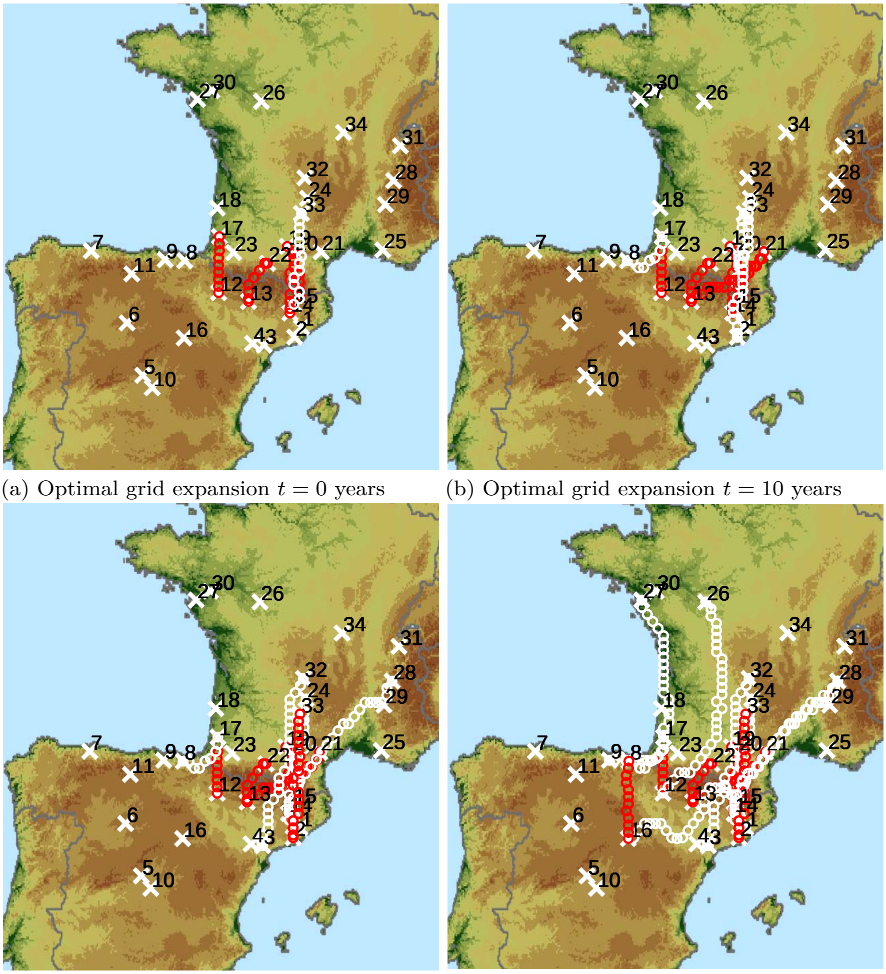

(a) Optimal grid expansion $t = 0$ years
(b) Optimal grid expansion $t = 10$ years
(c) Optimal grid expansion $t = 20$ years
(d) Optimal grid expansion $t = 30$ years

Figure 6.6: Optimal investment plan for $\overline{\mathbf{K}} = 3\ GW$. Red colour indicates HVAC, white colour indicates HVDC. Solid lines indicate underground cables, circles indicate overhead lines

occur. Table 6.1 shows that a further increase in maximum link capacities does not improve the optimal solution. Even if links with a capacity of 8 GW are allowed, the economically best solution is still achieved with the investment plan using 5 GW.

Table 6.1 illustrates that the total investment costs are significantly increased if the use multi-terminal HVDC is delayed. If the use of multi-terminal HVDC is

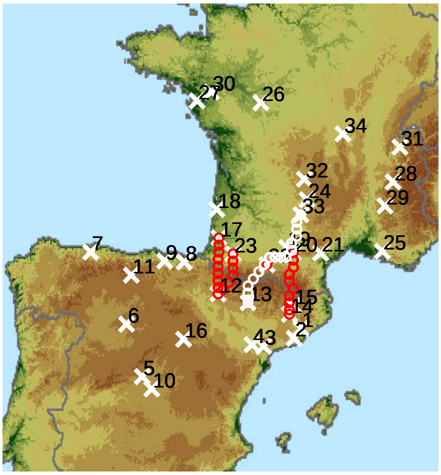

(a) Optimal grid expansion $t = 0$ years

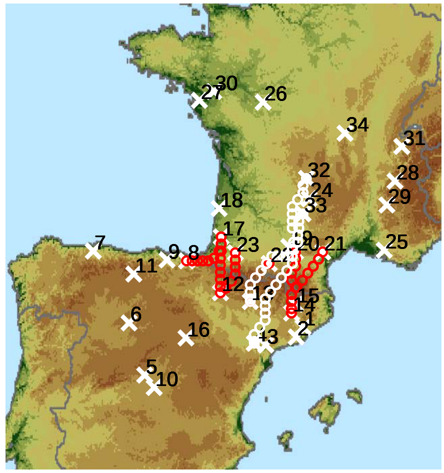

(b) Optimal grid expansion $t = 10$ years

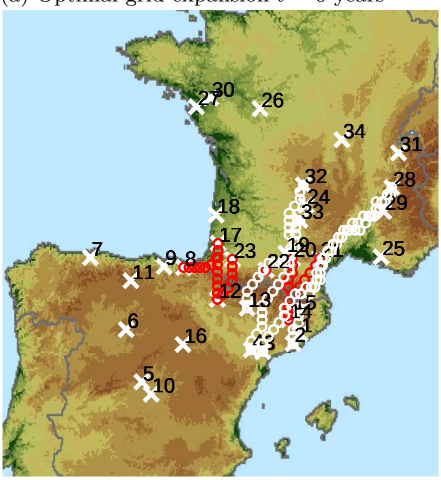

(c) Optimal grid expansion $t = 20$ years

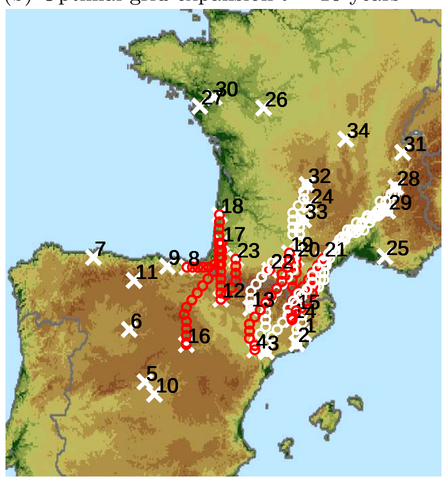

(d) Optimal grid expansion $t = 30$ years

Figure 6.7: Optimal investment plan for $\overline{\mathbf{K}} = 5\ GW$. Red colour indicates HVAC, white colour indicates HVDC. Solid lines indicate underground cables, circles indicate overhead lines

delayed for 20 years, the obtained optimal solution using a maximum capacity of 8 GW performs better than a maximum capacity of 5 GW. In that case, a solution is found where a link of 6.5 GW is established between nodes 10 and 31 using HVDC overhead line technology (figure 6.8). This particular link connects the region of Lyon with the region of Madrid and is longer than 1400 km. Such a long distance, high capacity link can be considered as part of

Table 6.1: Comparison of different maximum power ratings per path

$\overline{\mathbf{K}}$	C_{tot} [M€]			l_{tot} $[km]$		
	t_{HVDC}=0	t_{HVDC}=10	t_{HVDC}=20	t_{HVDC}=0	t_{HVDC}=10	t_{HVDC}=20
3000 GW						
$a_e = 2, a_p = 1$	8223.6	10920	11387	7054	9517	8939
$a_e = 1, a_p = 1$	7898.3	8010.4	8179.2	6789	6846	7334
$a_e = 1, a_p = 2$	8220.2	8220.2	8535.6	7376	7376	7034
5000 GW						
$a_e = 2, a_p = 1$	7408.3	7628.9	8446	5098	4840	5846
$a_e = 1, a_p = 1$	7467.8	7570.1	7755.6	5332	4688	5209
$a_e = 1, a_p = 2$	7547.8	7547.8	7755.0	4913	4913	5291
8000 GW						
$a_e = 2, a_p = 1$	7408.3	7628.9	8061	5098	4840	4847
$a_e = 1, a_p = 1$	7467.8	7570.1	7755.6	5332	4688	5209
$a_e = 1, a_p = 2$	7547.8	7547.8	7755.0	4913	4913	5291

an overlay grid. If the use of multi-terminal HVDC is delayed more than 20 years, the optimization algorithm cannot find any feasible solution under the taken assumptions.

The optimal solution obtained with transmission paths of 5 GW contains 4 HVAC connections established in the first time step of the planning horizon between nodes 12 and 17, 12 and 23, 14 and 20, 13 and 22 (figure 6.7a). In case these connections cannot be built in the first 10 years, it becomes economically more feasible to choose another investment plan (figure 6.9). In this option, the connections between nodes 12 and 17, 14 and 20, 13 and 22 are established in the second step of the planning horizon. The connection between nodes 12 and 23 is not established at all. The total net present value of investments considering line delays equals 7514.8 M€, which is 1.01% higher than the best obtained solution without delay. In the optimal investment plan including line delays, 13 transmission paths are established instead of 15. The total length of new built lines is approximately 300 km less. In this case, a detailed analysis of expected transmission losses and maintenance costs should be conducted in order to assess potential cost savings due to shorter lines versus the 1.01% investment cost increase.

6.4 Conclusions

This chapter shows that the developed methodology can be applied to larger systems. In case sufficient geographic, network and generation information is available, the described building blocks of the developed methodology can be applied in order to obtain a stepwise, long term investment plan.

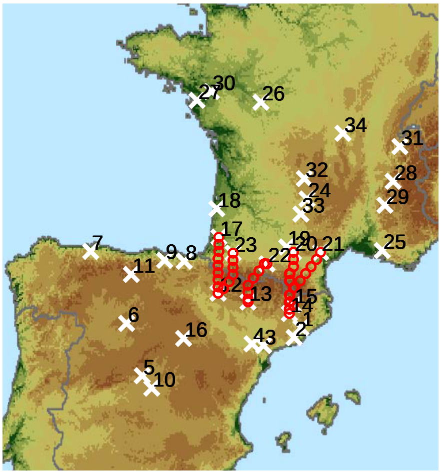

(a) Optimal grid expansion $t = 0$ years

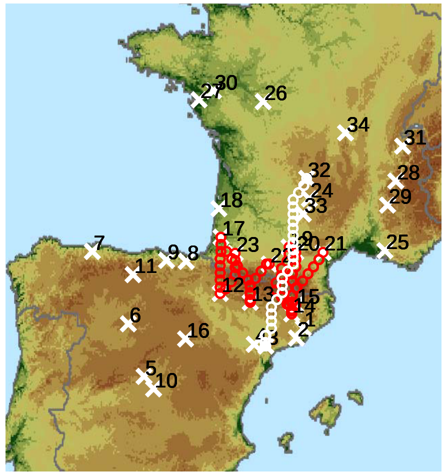

(b) Optimal grid expansion $t = 10$ years

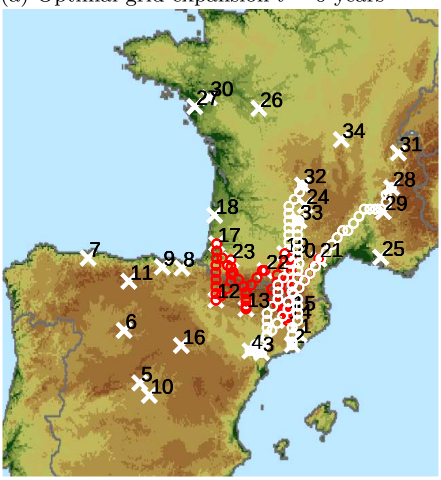

(c) Optimal grid expansion $t = 20$ years

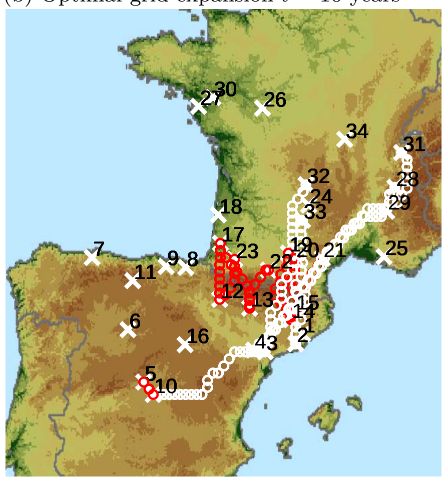

(d) Optimal grid expansion $t = 30$ years

Figure 6.8: Optimal investment plan for $\overline{\mathbf{K}} = 8$ GW and multi-terminal HVDC delayed for 20 years. Red colour indicates HVAC, white colour indicates HVDC. Solid lines indicate underground cables, circles indicate overhead lines

Using the available data and under the taken assumptions, the calculation results show that in the early time steps links with shorter distances and lower power ratings are preferred as they are cheaper. The more expensive, long distance, high power and therefore more expensive links are established at the later stages of the planning horizon. In the considered case study, some of these links can be considered as part of a possible overlay grid. They reach

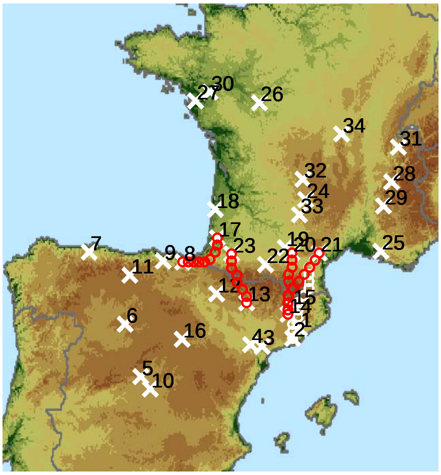

(a) Optimal grid expansion $t = 0$ years

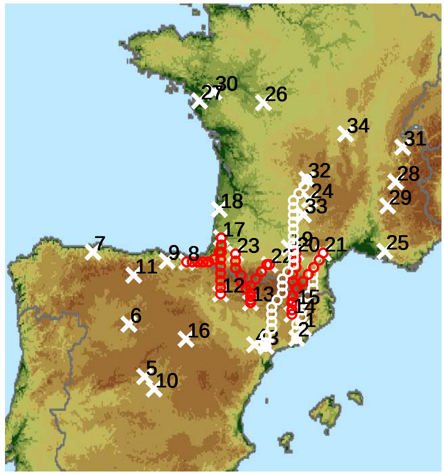

(b) Optimal grid expansion $t = 10$ years

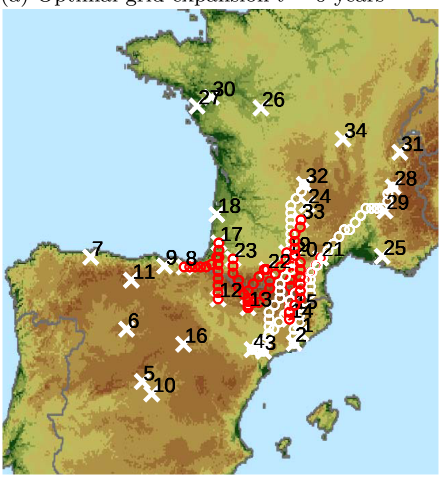

(c) Optimal grid expansion $t = 20$ years

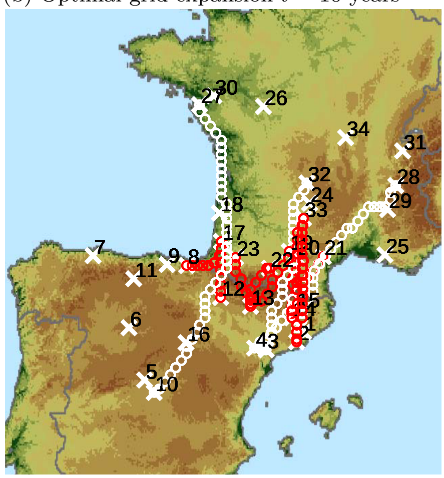

(d) Optimal grid expansion $t = 30$ years

Figure 6.9: Optimal investment plan for $\overline{\mathbf{K}} = 5\ GW$ in case of line delays. Red colour indicates HVAC, white colour indicates HVDC. Solid lines indicate underground cables, circles indicate overhead lines

over several hundred kilometres and directly connect strong grid nodes as the power import capability of nodes close to borders is used in the earlier stages of the planning horizon. For the long distance and high power transmission links, mostly HVDC technology is preferred as the cost savings of cheaper transmission lines outweigh the additional HVDC converter costs.

Cost savings can be achieved using transmission links with higher capacities.

Nevertheless, the underlying transmission grid sets limits to the maximum capacity of such links. Therefore, it is important to consider several scenarios regarding link capacity in order to determine the economically most beneficial option. In the considered case study, significant investment cost savings can be achieved if multi-terminal HVDC operation becomes technically and commercially feasible. Therefore, issues related to protection and control have to be solved in a cost effective way.

It should be noted that obtained results strongly depend on used data. It is important to perform sensitivity analysis on the used data and assumptions. Costs of different investment plans may be close to each other although the obtained grid topologies are very different. In such cases, the operational costs such as transmission system losses and maintenance costs can be the decisive.

Chapter 7

Conclusions and future work

In three words I can sum up everything I've learned about life: it goes on. - Robert Frost

7.1 Overview and overall conclusions

In this thesis, building blocks of a transmission system expansion methodology have been developed which can separately be implemented into existing planning tools or used as a whole. The developed methodology is suitable for long term transmission expansion studies and delivers optimal grid investment plans. The methodology is developed in a modular way allowing user interaction such that it can be integrated in existing planning methodologies.

In order to obtain reliable investment plans, basic assumptions and used data have to be chosen carefully. It is difficult to reliably estimate future power flows, location of generation, cost information and possible delays due to a large number of uncertainties. It is important to analyse a large number of scenarios and perform case studies considering these parameters and by doing so identifying investment options satisfying most of these scenarios. This way, the risk for future investments can be minimized.

In Chapter 3, a network abstraction algorithm using probabilistic optimal load flow has been provided. The methodology allows to identify strong grid nodes and to quantify the amount possible imports and exports in these nodes. Generally, transmission system operators have to provide nodal injection capacities to their customers. Using the proposed abstraction methodology, transmission system operators can provide these capacities taking into account volatile power flows due to renewable power generation. The developed methodology makes use of cost information of existing generators. In case sufficient data is available, generation companies can use this methodology to determine the maximum size of their new investments as well as expected future revenues. This way more reliable cost benefit analysis can be conducted.

In this work, the network abstraction methodology is used as input to optimize future transmission system investments. It is important to investigate different technology options in terms of economics, social and environmental impact in long term, in order to give recommendations to decision makers, transmission system operators and technology providers and minimize investment risks. Chapter 4 provides an optimization methodology for transmission system investments. The optimization methodology allows the consideration of spatial aspects of transmission planning in order to assess the economics, social and environmental impact with sufficient accuracy. The choice of the technology and size of investments and the resulting investment costs depend strongly on spatial aspects. By quantifying area related costs, recommendations for technology development can be provided enabling optimal transmission system design and maximizing social welfare.

Each new investment influences future investments to follow. Chapter 5 shows a possibility to include investment time points into the optimization problem. This way, a sequential investment plan is obtained, delivering the optimal time period for each new investment. This way, temporal effects of line delays, capital availability and technology maturity are analysed. In order to obtain more robust solutions, the transmission investment problem and market model responsible for the generation planning problem should be solved iteratively as shown in Chapter 2.

Delays in transmission system investment projects can cause significant additional costs. The case studies provided in Chapter 6 show that some line delays can be compensated by changing the order of investments. Nevertheless, the calculations show that investments in certain transmission paths may become obsolete in case the order of investments is changed. Using the developed methodology different optimal investment plans can be analysed considering possible delays. This way, connection paths affected most by delays can be identified. Beyond that the point of no return where a certain connection becomes economically less feasible than other connection paths can be determined. This information can be used as an incentive to advise decision makers, accelerate permission procedures or to propose another investment plan in case these delays cannot be avoided.

Chapter 6 shows how the developed methodology can be used as a standalone tool and applied to larger networks in order to conduct long term studies for large scale transmission expansion. As the performed calculations are based on public available data the results can only be considered as indicative. Nevertheless, some main patterns in the results can be observed and some qualitative conclusions can be drawn.

The analysed case study in Chapter 6 shows that it is economically more feasible to establish first shorter connections between border nodes to increase the transmission capacity between two zones as these connections are cheaper. Longer and more expensive links are proposed in later stages of the planning horizon when no more additional power can be injected in border nodes. These more expensive links are postponed as much as possible due to economic reasons. Although larger links are economically more attractive in later stages, the underlying networks are not always able to support such large links, limiting the maximum capacity of such links. This sets limits to the maximum size of links to be built. In the obtained solutions, both HVAC and HVDC technology is used to achieve the desired interconnection power. The calculation results show that HVDC technology becomes more interesting for high power long distance transmission links and underground connections. In the analysed cases significant cost savings could be achieved using multi-terminal or meshed HVDC configurations. This means that in the future, issues related to protection and control of meshed HVDC systems need to be solved in a cost effective way in order to make advantage of these cost savings.

7.2 Future Research

In this thesis, the lumpiness of transmission system investments has been taken into account using an integer formulation of the optimization problem. Available optimization solvers for integer variables face problems in terms of convergence and computational efficiency, especially for large scale problems. In order to achieve numerically more robust results and to handle larger problems, exiting optimization solvers need to be improved.

In case future power flows can be estimated using scenario based or probabilistic approaches, location and size of necessary investments can be determined taking into account several different aspects. In such cases, the investment risk can be reduced by increasing the number of scenarios or using more accurate probabilistic calculations in order to account for volatility of future power flows.

Since the liberalization of electricity markets, generation and transmission investments are carried out by different entities. In order to obtain more robust solutions and better convergence of transmission and generation investments, the interaction between them should be modelled in greater detail. One of the largest investment risks for transmission system operators is delay or cancellation of planned generation investments leading to stranded investments. Current probabilistic criteria only assess volatility of flows based on planned investments as a result of future energy scenarios. Nevertheless, the financial uncertainty of specific planned investments need to be modelled in greater detail in order to avoid stranded investments in both generation and transmission assets.

Although transmission is still a regulated business, transmission system operators have to find the necessary capital for investments on the capital market. In case of delayed or cancelled generation investments, stranded transmission system investments may occur, decreasing social welfare and affecting finances of transmission system operators. In order to reduce or at least quantify this additional risk, probabilistic planning methodologies need to be improved further. The financial uncertainty of planned generation investments should be included in transmission investment models in order to justify specific transmission investments with a certain degree of certainty.

Future research should be conducted in order to develop a methodology, which delivers a stepwise development plan including confidence intervals for proposed investments. This way, decision makers can choose between cheaper options with higher investment risks versus more expensive solution with lower risk.

Another important aspect which should be included in future planning tools is the implementation of probabilistic security criteria. As the flexibility in transmission grids is increasing due to use of phase-shifting transformers, FACTS devices and HVDC links, the future transmission grid may not necessarily be designed for N-1 cases with low probability of occurrence. The welfare loss due to curtailment may be less than the required investments to design the network N-1 secure, especially in case of greater demand flexibility. This way, over-investments can be avoided without compromising security of supply.

In close future transmission system operators will need to invest in the replacement of existing assets as they are approaching the end of their lifetime. In a future transmission planning methodology using probabilistic approaches to model investment uncertainty and probabilistic security criteria, also the age of existing assets and their expected lifetimes should be taken into account in order to find the best expansion solution combining replacement strategies and new investments.

The regulatory framework influences future investment decisions, especially for cross-border investments. In case the regulatory schemes are not aligned, investments can result in sub-optima or in the worst case in cancellation. In future, technical transmission system planning criteria and the design of regulatory frameworks need to be aligned such that a technically and economically optimal system design and a regulatory framework to support such a design can be achieved.

Appendix A

Network data of modified IEEE 24 Bus Test system for MPIC calculation

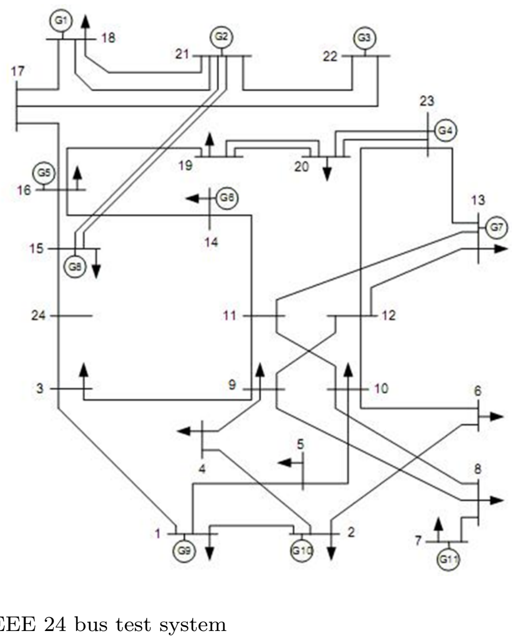

Figure A.1: The IEEE 24 bus test system

Table A.1: Bus data

Bus number	P MW	Q MVar	V kV
1	540	22	400
2	485	20	400
3	900	37	400
4	370	15	400
5	355	14	400
6	680	28	400
7	625	25	400
8	855	35	400
9	875	36	400
10	975	40	400
11	0	0	400
12	0	0	400
13	1325	54	400
14	970	39	400
15	1585	64	400
16	500	20	400
17	0	0	400
18	1665	68	400
19	905	37	400
20	640	26	400
21	0	0	400
22	0	0	400
23	0	0	400
24	0	0	400

Table A.2: Generator Data

Bus number	P_{max} MW	Q_{max} MVar	P_{min} MW	Q_{min} MVar
1	160	160	0	-160
1	160	160	0	-160
1	608	608	0	-608
1	608	608	0	-608
2	160	160	0	-160
2	160	160	0	-160
2	608	608	0	-608
2	608	608	0	-608
7	800	800	0	-800
7	800	800	0	-800
7	800	800	0	-800
13	1576	1576	0	-1576
13	1576	1576	0	-1576
13	1576	1576	0	-1576
15	96	96	0	-96
15	96	96	0	-96
15	96	96	0	-96
15	96	96	0	-96
15	96	96	0	-96
15	1240	1240	0	-1240
16	1240	1240	0	-1240
18	3200	3200	0	-3200
21	3200	3200	0	-3200
22	400	400	0	-400
22	400	400	0	-400
22	400	400	0	-400
22	400	400	0	-400
22	400	400	0	-400
22	400	400	0	-400
23	1240	1240	0	-1240
23	1240	1240	0	-1240
23	2800	2800	0	-2800

Table A.3: Generator Cost Data

Start up cost €	C_2 €/ MW^2	C_1 €/MW	C_0 €
1500	0	130	400,6849
1500	0	130	400,6849
1500	0,014142	16,0811	212,3076
1500	0,014142	16,0811	212,3076
1500	0	130	400,6849
1500	0	130	400,6849
1500	0,014142	16,0811	212,3076
1500	0,014142	16,0811	212,3076
1500	0,052672	43,6615	781,521
1500	0,052672	43,6615	781,521
1500	0,052672	43,6615	781,521
1500	0,00717	48,5804	832,7575
1500	0,00717	48,5804	832,7575
1500	0,00717	48,5804	832,7575
1500	0,328412	56,564	86,3852
1500	0,328412	56,564	86,3852
1500	0,328412	56,5647	86,3852
1500	0,328412	56,564	86,3852
1500	0,328412	56,564	86,3852
1500	0,008342	12,3883	382,2391
1500	0,008342	12,3883	382,2391
1500	0,000213	4,42317	395,3749
0	0	0,001	0,001
1500	0	0,001	0,001
1500	0	0,001	0,001
1500	0	0,001	0,001
1500	0	0,001	0,001
1500	0	0,001	0,001
1500	0	0,001	0,001
1500	0,008342	12,3883	382,2391
1500	0,008342	12,3883	382,2391
1500	0,004895	11,8495	665,1094

Table A.4: Branch Data

From bus	To bus	R p.u.	X p.u.	B p.u.	P_{max} MW
1	2	0,0026	0,0139	0,4611	2000
1	3	0,0546	0,2112	0,0572	2000
1	5	0,0218	0,0845	0,0229	2000
2	4	0,0328	0,1267	0,0343	2000
2	6	0,0497	0,192	0,052	2000
3	9	0,0308	0,119	0,0322	2000
3	24	0,0023	0,0839	0	750
4	9	0,0268	0,1037	0,0281	2000
5	10	0,0228	0,0883	0,0239	2000
6	10	0,0139	0,0605	2,459	2000
7	8	0,0159	0,0614	0,0166	2500
8	9	0,0427	0,1651	0,0447	2000
8	10	0,0427	0,1651	0,0447	2000
9	11	0,0023	0,0839	0	750
9	12	0,0023	0,0839	0	750
10	11	0,0023	0,0839	0	750
10	12	0,0023	0,0839	0	750
11	13	0,0061	0,0476	0,0999	750
11	14	0,0054	0,0418	0,0879	750
12	13	0,0061	0,0476	0,0999	750
12	23	0,0124	0,0966	0,203	750
13	23	0,0111	0,0865	0,1818	2500
14	16	0,01	0,0778	0,0409	1250
14	16	0,01	0,0778	0,0409	1250
15	16	0,0022	0,0173	0,0364	2500
15	21	0,0063	0,049	0,103	2500
15	21	0,0063	0,049	0,103	2500
15	24	0,0067	0,0519	0,1091	750
16	17	0,0033	0,0259	0,0545	2500
16	19	0,003	0,0231	0,0485	2500
17	18	0,0018	0,0144	0,0303	2500
17	22	0,0135	0,1053	0,2212	2500
18	21	0,0033	0,0259	0,0545	2500
18	21	0,0033	0,0259	0,0545	2500
19	20	0,0051	0,0396	0,0833	2500
19	20	0,0051	0,0396	0,0833	2500
20	23	0,0028	0,0216	0,0455	2500
20	23	0,0028	0,0216	0,0455	2500
21	22	0,0087	0,0678	0,1424	2500

Appendix B

Spatial weights for installation costs of equipment

Table B.1: Spacial weights for elevation

Level	AC OHL	AC UGC	DC OHL	DC UGC
Level 1	1	1	1	1
Level 2	1.3	1.1	1.3	1.1
Level 3	1.6	1.2	1.6	1.2
Level 4	1.9	1.3	1.9	1.3
Level 5	2.2	1.4	2.2	1.4
Level 6	2.5	1.5	2.5	1.5
Level 7	2.8	1.6	2.8	1.6
Level 8	3.1	1.7	3.1	1.7
Level 9	3.4	1.8	3.4	1.8
Level 10	3.7	2	3.7	2
Level 11	4	2.1	4	2.1
Offshore	40	0.9	40	0.9

Table B.2: Spacial weights for population

Level	AC OHL	AC UGC	DC OHL	DC UGC
Level 1	1	1	1	1
Level 2	2	1.1	2	1.1
Level 3	3	1.2	3	1.2
Level 4	4	1.3	4	1.3
Level 5	5	1.4	5	1.4
Level 6	6	1.5	6	1.5
Level 7	7	1.6	7	1.6
Level 8	8	1.7	8	1.7
Level 9	9	1.8	9	1.8
Level 10	10	2	10	2
Offshore	40	0.9	40	0.9

Appendix C

Developed Software

In this section the developed software code of the illustrated transmission system investment optimization method is briefly described. Additionally, the description of a software tool to optimize offshore wind farm connections is provided.

C.1 Pesudo-code: Calculation of maximum power injection capabilities

This section provides the pseudo-code for the calculation routine of maximum power injection capabilities.

Process grid data
→ Build data structure in Matpower format, containing bus, branch, generator and generator cost information
→ Add possible HVDC links and PSTs
Process generation and load data
→ Assign a load profile to each bus
→ Assign a generation profile to each renewable generator
Determine Gaussian Components or samples for Monte Carlo Simulation
→ Determine Gaussian components for load and generation profile of each bus
→ Reduce the number of components if possible
Calculate connection capacity and define candidate nodes
Calculate LODF for N-1 calculation

Calculate MPIC - injection

→ for each cadidate node
→→ for each sample of Gaussian component
→→→ solve OPF
→→→ determine important N-1 cases using LODF
→→→→ deactivate each important element
→→→→ recalculate OPF
→→→ save smallest MPIC-value for this sample

Calculate MPIC - absorption

→ for each cadidate node
→→ for each sample of Gaussian component
→→→ solve OPF
→→→ determine important N-1 cases using LODF
→→→→ deactivate each important element
→→→→ recalculate OPF
→→→ save smallest MPIC-value for this sample

Calculate Δ MPIC

→ for i to number of candidate nodes
→→ for j to number of candidate nodes
→→→ for different injection values of node i
→→→→ fix injection of node i
→→→→ calculate MPIC - injection of node j
→→→ for different injection values of node i
→→→→ fix injection of node i
→→→→ calculate MPIC - absorption of node j
→→→ for different absorption values of node i
→→→→ fix injection of node i
→→→→ calculate MPIC - injection of node j
→→→ for different absorption values of node i
→→→→ fix injection of node i
→→→→ calculate MPIC - absorption of node j

C.2 Pesudo-code: Investment optimization

This section provides the pseudo-code for the calculation routine of investment optimization.

Import geographic data

→ Read population density map
→ Read elevation map

→ Define geographic positions of candidate nodes
Define spatial costs
→ For each area of population density define weights for the four technology options
Import MPIC data
→ Import MPIC and Δ MPIC matrices
→ Scale and rearrange matrices
Start optimization block
→ Calculate average costs
→→ For each possible branch
→→→ For power rating of each technology and the maximum power per path
→→→→ Run optimal routing algorithm with low resolution C.2.1
→ Run MILP optimization
→ Until convergence
→→ Run optimal routing algorithm with desired resolution C.2.1
→→ Update average costs
→→ Run MILP optimization
Rank solutions
Plot optimal investment plan

C.2.1 Pseudo code: Optimal routing

Discretise topography map
Assign spatial weights
→ For each technology option
→→ Calculate area dependent costs for each edge of graph
Connect four technology maps
→ Add substation costs or HVDC converters between corresponding nodes
Select algorithm: Dijkstra or A*
Run shortest path algorithm

C.3 Tool to optimize offshore wind farm connections

This software tool is developed to optimize transmission system investments for multiple offshore wind farms [123, 124]. The tool uses rule based heuristics and deterministic optimization to find the transmission layout and technology with the least life cycle costs. The developed tool can be used in the first project

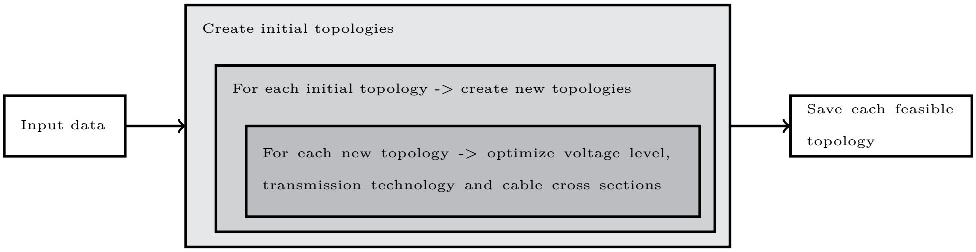

Figure C.1: General methodology of the offshore transmission optimization tool [123]

planning stages, where only little information is available. The tool delivers as output a set of solutions ranked after their life cycle costs which allows further technical assessment of the proposed solutions. The developed tool includes a user friendly interface and databases of equipment costs and equipment ratings which can easily be updated by the user. This way, the tool can be used for different projects, locations and market conditions.

C.3.1 General methodology

The objective of the developed tool is the minimization of the life cycle system costs of transmission systems, connecting multiple offshore wind farms to the onshore electricity grid. The life cycle system costs

$$C_{lcsc} = C_{inv} + \sum_{i=1}^{lifetime} C_{loss,i} + C_{main,i} + C_{nhe,i} \tag{C.1}$$

consist of investment (including installation) costs C_{inv} of transmission equipment, costs of losses during the lifetime C_{loss}, maintenance costs C_{main} and costs of not harvested energy C_{nhe}, caused by the unavailability of the offshore transmission system.

The developed tool uses a multilevel optimization approach (figure C.1). Using specified input data, first, a set of starting topologies are created. The starting topologies consist of radial and ring shaped topologies. Based on the starting topologies, new transmission topologies are created using rule based heuristics.

For each created topology, the transmission technology of each path (AC or DC), the transmission system voltages (AC and/or DC) and cross sections of necessary cables or overhead line are optimized in a deterministic way using power flow calculations.

C.3.2 Rule based heuristics

The creation of new transmission topologies is carried out as follows (figure C.2):

1. In the first generation of topologies, a higher degree of meshing is achieved. Therefore, each node of the transmission system is connected to at least two different nodes. The additional connections are chosen on a random basis to explore different regions of the search space. The feasibility of each new topology is checked using the transmission voltage and equipment ratings of the corresponding starting topology (parent topology). Therefore, an AC power flow calculation is performed using Matpower [90]. If the power flow calculation converges, the topology is investigated further with the deterministic algorithm and saved. In case the power flow calculation does not converge, the topology is discarded.

2. All topologies are modified so that the power flow on a single connection path cannot exceed a maximum value as defined in the input data set. This limit can be set by the TSO in order to maintain system security or can be/is derived from technological or geographical constraints. The limitation of the maximum power flow per path is achieved by iteratively adding new connection paths to the system, until the maximum power flow in the system is smaller than the set limit. Topologies obtained this way are checked for feasibility as explained above and the deterministic algorithm is applied to feasible topologies.

3. In the third generation, topologies resulting in the lowest costs are pairwise crossed with each other. Two basic principles are applied during crossing. First, topologies with higher number of connection paths are created using a union set of both topologies ($T_1 \cup T_2$). Secondly, topologies with a minimum number of connection path are created. Therefore an intersection between both topologies is used, which only contains transmission paths, which both topologies have in common ($T_1 \cap T_2$).

4. Installation costs cause a significant part of the total investment costs of equipment. In connection paths with low power ratings, the installation costs can be significantly higher than the equipment costs. In this part of the algorithm, such connection paths are eliminated. The threshold for the minimum power rating can be defined by the user. Each new topology is checked for feasibility and refined and saved if feasible.

5. In this last step, the crossing algorithm as explained above is used.

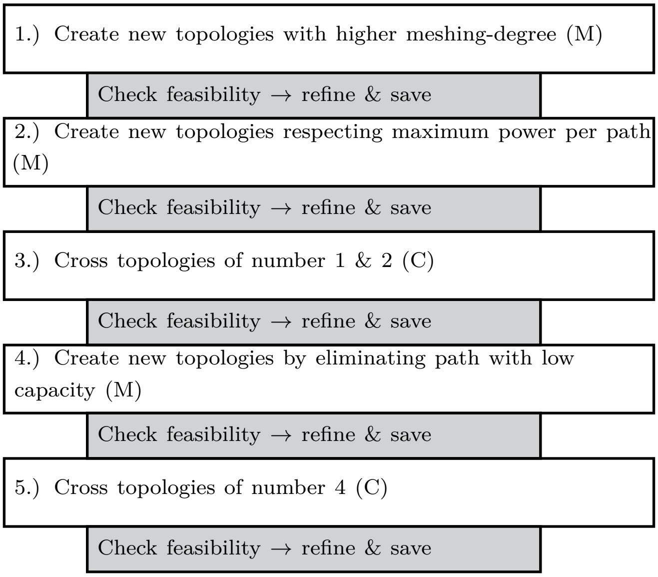

Figure C.2: Rule based heuristics to create new transmission topologies [124]

C.3.3 Optimization of voltage level, technology selection and cable cross sections

Based on the topology determined by the heuristic algorithm, optimal the transmission technology, transmission voltage and cable cross sections are calculated (figure C.3).

Initially, neither the power flows on the connection paths nor the voltage levels of the transmission system are known. Therefore, an initial power flow situation is defined first, based on the topology and the rated power output of the wind farms. Here it is assumed that the total wind power can be transmitted to the shore. Using this initial power flow calculation, the investment costs, the maintenance costs, and the costs of losses are calculated for all possible combinations of AC (30 kV, 70 kV, 150 kV, 220 kV, 400 kV) and DC (±80 kV, ±150kV, ±320kV) voltages in two nested loops. Hence 15 different costs are calculated, whereas the solution with the lowest costs is chosen to be the best. The 5 step calculation procedure is described below.

1. The optimal technology for each transmission path is determined using the empirical function as depicted (figure C.4).

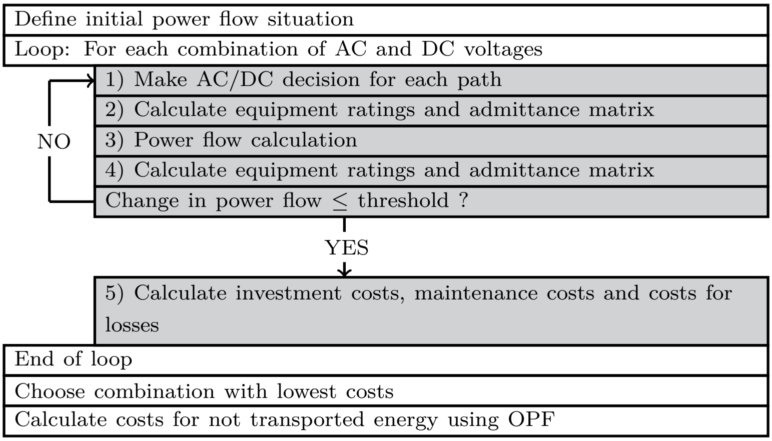

Figure C.3: Optimization routine for voltage, technology and cable cross sections [123]

2. After the selection of the technology, the necessary cross sections are calculated using the specific voltage level. Therefore first the minimum number of cables is calculated using the highest cross section and sequentially, the minimum cross section is determined based on the minimum number. The admittance matrix of the entire system is determined based on the number and cross sections of the cables. If necessary, also impedances of transformers, reactive power compensation devices and HVDC converters are included in the admittance matrix.

3. Using the admittance matrix of the system, a new AC power flow calculation is performed using Matpower [90].

4. Obviously, the power flow calculation is based on an admittance matrix calculated with the power flows of the iteration before. These results are based on the assumed power flows. Therefore, the admittance matrix is recalculated, and the steps 1 to 4 repeated, until the change in power flows is below a certain threshold, or a maximum number of iterations is reached.

5. In the last step, the investment costs, the costs of losses and maintenance costs are determined. For the calculation of losses, the wind power output of wind farms is modelled with an hourly resolution based on Weibull distributed wind speeds.

Using the 5 step calculation procedure, 15 values for the life cycle costs are obtained for each possible combination of AC and DC voltages. To complete

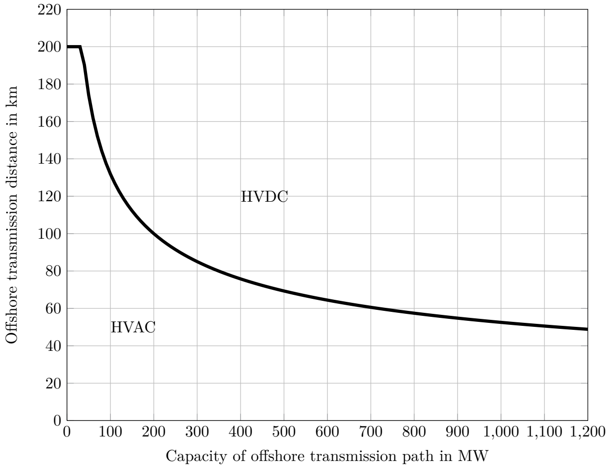

Figure C.4: technology decision function for offshore transmission paths

the life cycle costs, the costs for non-harvested energy due to unavailability of equipment has to calculated. The calculation performed as an N-1 security analysis with optimal power flow calculations considering possible power dispatch between farms. As this calculation is very time consuming, it is only performed for a certain number of topologies which is specified by the user.

C.3.4 Input and output interfaces

The developed software includes user friendly input and output interfaces. The general input interface shows offshore, onshore and prohibited areas as well as positions of wind farms and points of common coupling (figure C.5a). From the general input interface, sub-menus for wind farms, points of common couplings, prohibited areas, onshore areas, options, cable data and cost functions can be opened. In the wind farm interface, the position, power rating, capacity factor (full load hours) and internal voltage level of wind farms can be defined (figure C.5b). In the PCC (point of common coupling) interface, the positions, power injection capability and voltage level of PCCs can be specified (figure C.5c). In the onshore and prohibited area interfaces, geographic positions of these areas can be defined. Additional options such as lifetime, frequency, maximum power and interest rate can be specified in the options interface (figure C.5d). Although default values are provided, in the interfaces cable data and cost functions, user defined values can be entered.

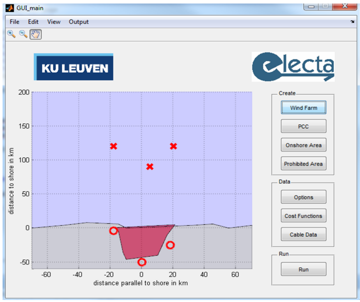

(a) General input interface

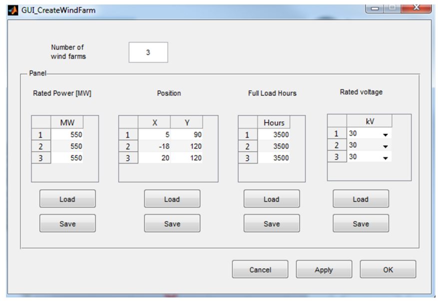

(b) Input interface of wind farms

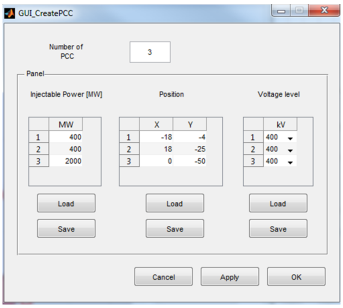

(c) Input interface of points of common coupling

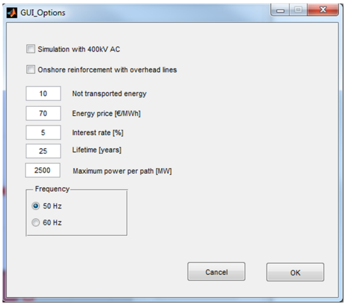

(d) Input interface for additional options

Figure C.5: Input interfaces of developed tool

The output interface shows the transmission system topology for all feasible solutions ranked after their life cycle costs. The graphical interface shows which nodes are connected and which technology is used for each transmission path (figure C.6a). Additional information about the necessary number and cross sections of cables as well as a breakdown of the costs is provided (figure C.6b, figure C.6c).

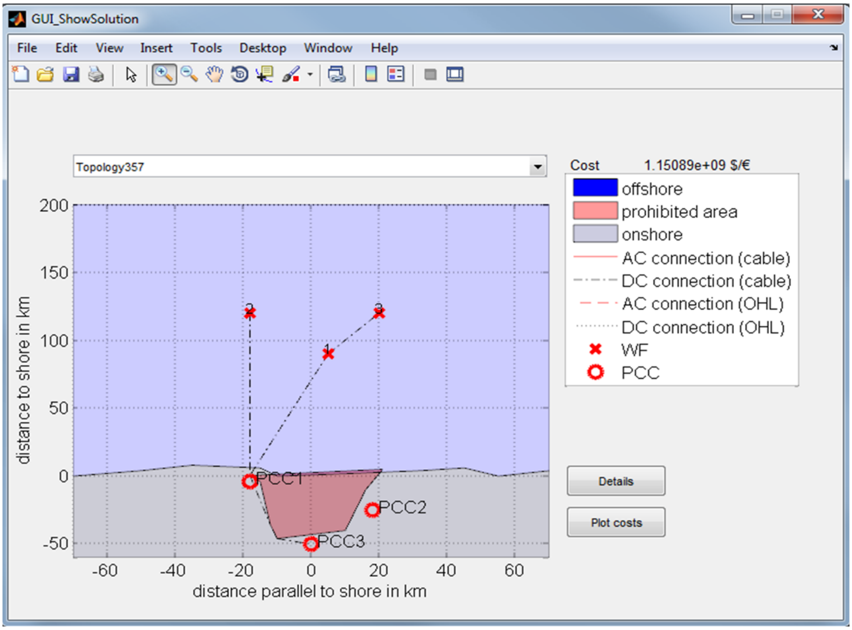

(a) General output interface

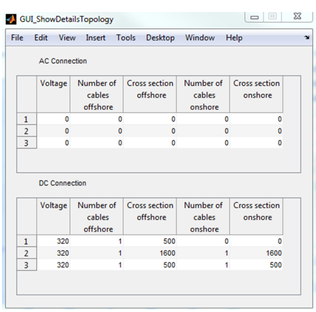

(b) Output interface showing cable details

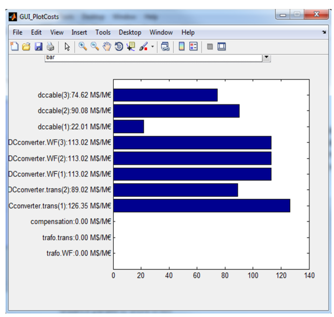

(c) Output interface equipment showing costs

Figure C.6: Input interfaces of developed tool

Bibliography

[1] T. P. Hughes, *Networks of Power, Electrification in Western Society, 1880-1930*. John Hopkins University Press, 1993.

[2] V. Lagendijk, "Electrifying Europe, The power of Europe in the construction of electricity networks," Ph.D. dissertation, Technical University Eindhoven, 2009, ISBN 9789052603094.

[3] O. Oliven. Vorschlag eines Europäischen Großkraftnetzes. http://extras.springer.com/1931/978-3-7091-5155-6/978-3-7091-5155-6_OSFO1.pdf. Last checked: 28.10.2014.

[4] Entso-e. Interconnected System Grid Maps. https://www.entsoe.eu/publications/order-maps-and-publications/electronic-grid-maps/Pages/default.aspx. Last checked: 28.10.2014.

[5] Eurelectric Facts Database. Electricity Generation by Primary Energy. http://www.eurelectric.org/factsfolders/DocLink.asp?DocID=72139. Last checked: 28.10.2014.

[6] ——. Maximum Net Generation Capacity by Primary Energy. http://www.eurelectric.org/factsfolders/factsfolder.asp?FolderID=5245. Last checked: 28.10.2014.

[7] EWEA. (2014, Feb.) Wind in Power - 2013 European Statistics. http://www.ewea.org/fileadmin/files/library/publications/statistics/EWEA_Annual_Statistics_2013.pdf. Last checked: 28.10.2014.

[8] Entso-e. Ten Year Network Development Plan 2012. https://www.entsoe.eu/fileadmin/user_upload/_library/SDC/TYNDP/2012/TYNDP_2012_report.pdf. Last checked: 28.10.2014.

[9] EWEA. (2014, Jul.) Wind Energy Scenarios for 2020. http://www.ewea.org/fileadmin/files/library/publications/scenarios/EWEA-Wind-energy-scenarios-2020.pdf. Last checked: 28.10.2014.

[10] European Climate Foundation (ECF), "Roadmap 2050, A Practical Guide To A Prosperous, Low-Carbon Europe," http://www.roadmap2050.eu/attachments/files/Volume1_fullreport_PressPack.pdf, ECF, Tech. Rep., 2010, last checked: 28.10.2014.

[11] J. De Decker and P. Kreutzkamp, "Offshore Electricity Grid Infrastructure in Europe - Final Report," 3E, Tech. Rep., Oct. 2011.

[12] Desertec Industrial Initiative (DII), "Industrial initiatives dii and medgrid join forces for the development of industrial-scale renewable energy," 2011, last checked: 28.10.2014. [Online]. Available: http://www.dii-eumena.com

[13] L. Moreno, "Concentrated Solar Power (CSP) in DESERTEC - Analysis of technologies to secure and affordable Energy Supply," in *Intelligent Data Acquisition and Advanced Computing Systems (IDAACS), 2011 IEEE 6th International Conference on*, vol. 2, Sep. 2011, pp. 923 – 926.

[14] Desertec Foundation, "Tunisian sun will light european homes by 2016," http://www.desertec.org, 2012, last checked: 28.10.2014.

[15] Greenpeace. (2011) Battle of the Grids. http://www.greenpeace.org/seasia/ph/Global/international/publications/climate/2011/battle%20of%20the%20grids.pdf. Last checked: 28.10.2014.

[16] A. T. Troester E., Kuwahata R. (2011) European Grid Study 2030/2050. http://www.greenpeace.org/seasia/ph/Global/international/publications/climate/2011/battle%20of%20the%20grids.pdf.

[17] Friends of the Super Grid. (2014) Supergrid preparatory phase: review of existing studies and recommendations to move forwards. http://www.friendsofthesupergrid.eu/fosg-report-on-the-preparatory-phase-of-a-supergrid-3/. Last checked: 28.10.2014.

[18] P. E. Morthorst, H. Auer, A. Garrad, and I. Blanco, "Application and Required Developments of Dynamic Models to Support Practical Planning," CIGRE, Technical Brochure 312, Working Group C1.04, Tech. Rep., Feb. 2007.

[19] D. Kirschen and G. Strbac, *Fundamentals of Power System Economics*. Wiley Online Library, 2004.

[20] D. Van Hertem, G.-B. Oriol, and L. Jun, *Building the Grid of the Future Using HVDC*. Wiley, Under Review.

[21] 50-Hertz Transmission GmbH, "Predicted and actual wind infeeds," 2014, last checked: 10.06.2014. [Online]. Available: http://www.50hertz.com/cps/rde/xchg/trm_de/hs.xsl/152.htm?rdeLocaleAttr=de&&rdeCOQ=SID-D779C28B-56985E7F

[22] H. Ergun, B. Rawn, R. Belmans, and D. Van Hertem, "Technology and topology optimization for multizonal transmission systems," *Power Systems, IEEE Transactions on*, vol. 29, no. 5, pp. 2469–2477, Sep. 2014.

[23] P. Buijs and R. Belmans, "Transmission investments in a multilateral context," *Power Systems, IEEE Transactions on*, vol. 27, no. 1, pp. 475–483, Feb. 2012.

[24] G. Latorre, R. Cruz, J. Areiza, and A. Villegas, "Classification of Publications and Models on Transmission Expansion Planning," *Power Systems, IEEE Transactions on*, vol. 18, no. 2, pp. 938 – 946, May 2003.

[25] L. Garver, "Transmission Network Estimation Using Linear Programming," *Power Apparatus and Systems, IEEE Transactions on*, vol. PAS-89, no. 7, pp. 1688 –1697, Sep. 1970.

[26] R. Villasana, L. L. Garver, and S. J. Salon, "Transmission Network Planning Using Linear Programming," *Power Engineering Review, IEEE*, vol. PER-5, no. 2, pp. 36 –37, Feb. 1985.

[27] V. Levi and M. Calovic, "Linear-programming-based decomposition method for optimal planning of transmission network investments," *Generation, Transmission and Distribution, IEE Proceedings C*, vol. 140, no. 6, pp. 516 –522, Nov. 1993.

[28] ——, "A new decomposition based method for optimal expansion planning of large transmission networks," *Power Systems, IEEE Transactions on*, vol. 6, no. 3, pp. 937 –943, Aug. 1991.

[29] R. Chanda and P. Bhattacharjee, "Application of computer software in transmission expansion planning using variable load structure," *Electric Power Systems Research*, vol. 31, no. 1, pp. 13 – 20, 1994.

[30] K. Kim, Y. Park, and K. Lee, "Optimal long term transmission expansion planning based on maximum principle," *Power Systems, IEEE Transactions on*, vol. 3, no. 4, pp. 1494 –1501, Nov. 1988.

[31] Y. Dusonchet and A. El-Abiad, "Transmission Planning Using Discrete Dynamic Optimizing," *Power Apparatus and Systems, IEEE Transactions on*, vol. PAS-92, no. 4, pp. 1358 –1371, Jul. 1973.

[32] H. Youssef and R. Hackam, "New transmission planning model," *Power Systems, IEEE Transactions on*, vol. 4, no. 1, pp. 9 –18, Feb. 1989.

[33] V. A. Levi, "A new mixed-integer methodology for optimal transmission expansion planning," *Electric Power Systems Research*, vol. 32, no. 3, pp. 227 – 238, 1995.

[34] L. Bahiense, G. Oliveira, M. Pereira, and S. Granville, "A mixed integer disjunctive model for transmission network expansion," *Power Systems, IEEE Transactions on*, vol. 16, no. 3, pp. 560 –565, Aug. 2001.

[35] S. Haffner, A. Monticelli, A. Garcia, J. Mantovani, and R. Romero, "Branch and bound algorithm for transmission system expansion planning using a transportation model," *Generation, Transmission and Distribution, IEE Proceedings-*, vol. 147, no. 3, pp. 149 –156, May 2000.

[36] A. Seifu, S. Salon, and G. List, "Optimization of transmission line planning including security constraints," *Power Systems, IEEE Transactions on*, vol. 4, no. 4, pp. 1507 –1513, Nov. 1989.

[37] J. dos Santos, A., P. Franca, and A. Said, "An optimization model for long-range transmission expansion planning," *Power Systems, IEEE Transactions on*, vol. 4, no. 1, pp. 94 –101, Feb. 1989.

[38] A. Sharifnia and H. Aashtiani, "Transmission Network Planning: A Method for Synthesis of Minimum-Cost Secure Networks," *Power Apparatus and Systems, IEEE Transactions on*, vol. PAS-104, no. 8, pp. 2025 –2034, Aug. 1985.

[39] A. Meliopoulos, R. Webb, R. Bennon, and J. Juves, "Optimal Long Range Transmission Planning with AC Load Flow," *Power Apparatus and Systems, IEEE Transactions on*, vol. PAS-101, no. 10, pp. 4156 – 4163, Oct. 1982.

[40] S. Lee, K. Hicks, and E. Hnyilicza, "Transmission Expansion by Branch-and-Bound Integer Programming with Optimal Cost - Capacity Curves," *Power Apparatus and Systems, IEEE Transactions on*, vol. PAS-93, no. 5, pp. 1390 –1400, Sep. 1974.

[41] S. Binato, M. Pereira, and S. Granville, "A New Benders Decomposition Approach to Solve Power Transmission Network Design Problems," *Power Systems, IEEE Transactions on*, vol. 16, no. 2, pp. 235 –240, May 2001.

[42] S. Siddiqi and M. Baughman, "Value-Based Transmission Planning and the Effects of Network Models," *Power Systems, IEEE Transactions on*, vol. 10, no. 4, pp. 1835 –1842, Nov. 1995.

[43] R. Romero and A. Monticelli, "A zero-one Implicit Enumeration Method for Optimizing Investments in Transmission Expansion Planning," *Power Systems, IEEE Transactions on*, vol. 9, no. 3, pp. 1385 –1391, Aug. 1994.

[44] M. Pereira, L. Pinto, S. Cunha, and G. Oliveira, "A Decomposition Approach To Automated Generation/Transmission Expansion Planning," *Power Apparatus and Systems, IEEE Transactions on*, vol. PAS-104, no. 11, pp. 3074 –3083, Nov. 1985.

[45] R. Romero and A. Monticelli, "A Hierarchical Decomposition Approach for Transmission Network Expansion Planning," *Power Systems, IEEE Transactions on*, vol. 9, no. 1, pp. 373 –380, Feb. 1994.

[46] W. Puntel and R. Fischl, "Computer Aided Design of Electric Power Transmission Networks," *IEEE Winter Power Meeting*, Jan. 1972.

[47] M. Pereira and L. Pinto, "Application Of Sensitivity Analysis Of Load Supplying Capability To Interactive Transmission Expansion Planning," *Power Apparatus and Systems, IEEE Transactions on*, vol. PAS-104, no. 2, pp. 381 –389, Feb. 1985.

[48] A. Ekwue and B. Cory, "Transmission System Expansion Planning by Interactive Methods," *Power Apparatus and Systems, IEEE Transactions on*, vol. PAS-103, no. 7, pp. 1583 –1591, Jul. 1984.

[49] A. Ekwue, "Investigations of the transmission system expansion problem," *International Journal of Electrical Power; Energy Systems*, vol. 6, no. 3, pp. 139 – 142, 1984.

[50] A. Monticelli, A. Santos, M. Pereira, S. Cunha, B. Parker, and J. Praca, "Interactive Transmission Network Planning Using a Least-Effort Criterion," *Power Apparatus and Systems, IEEE Transactions on*, vol. PAS-101, no. 10, pp. 3919 –3925, Oct. 1982.

[51] R. Bennon, J. Juves, and A. Meliopoulos, "Use of Sensitivity Analysis in Automated Transmission Planning," *Power Apparatus and Systems, IEEE Transactions on*, vol. PAS-101, no. 1, pp. 53 –59, Jan. 1982.

[52] C. Dechamps and E. Jamoulle, "Interactive computer program for planning the expansion of meshed transmission networks," *International Journal of Electrical Power; Energy Systems*, vol. 2, no. 2, pp. 103 – 108, 1980.

[53] C. Serna, J. Duran, and A. Camargo, "A Model for Expansion Planning of Transmission Systems A Practical Application Example," *Power Apparatus and Systems, IEEE Transactions on*, vol. PAS-97, no. 2, pp. 610 –615, Mar. 1978.

[54] Latorre-Bayona, G. and Perez-Arriaga, I.J., "CHOPIN, a Heuristic Model for Long Term Transmission Expansion Planning," *Power Systems, IEEE Transactions on*, vol. 9, no. 4, pp. 1886 –1894, Nov. 1994.

[55] E. da Silva, H. Gil, and J. Areiza, "Transmission Network Expansion Planning under an Improved Genetic Algorithm," in *Power Industry Computer Applications, 1999. PICA '99. Proceedings of the 21st 1999 IEEE International Conference*, Jul. 1999, pp. 315 –321.

[56] E. Da Silva, H. Gil, and J. Areiza, "Transmission Network Expansion Planning under an Improved Genetic Algorithm," *Power Systems, IEEE Transactions on*, vol. 15, no. 3, pp. 1168 –1174, Aug. 2000.

[57] K. Yoshimoto, K. Yasuda, and R. Yokoyama, "Transmission expansion planning using neuro-computing hybridized with genetic algorithm," in *Evolutionary Computation, 1995., IEEE International Conference on*, vol. 1, Dec. 1995, p. 126.

[58] R. Gallego, A. Monticelli, and R. Romero, "Comparative studies on nonconvex optimization methods for transmission network expansion planning," *Power Systems, IEEE Transactions on*, vol. 13, no. 3, pp. 822 –828, Aug. 1998.

[59] ——, "Transmission system expansion planning by an extended genetic algorithm," *Generation, Transmission and Distribution, IEE Proceedings-*, vol. 145, no. 3, pp. 329 –335, May 1998.

[60] A. Escobar, R. A. Gallego, R. L. Romero, and S. A. de Oliveira, "Hybrid model analysis and constructive algorithms in the performance of a genetic algorithm for the planning of an electric power transmission system," *Proc. 17th Int. Conf. CARS and FOF*, 2001.

[61] H. Gil and E. da Silva, "A reliable approach for solving the transmission network expansion planning problem using genetic algorithms," *Electric Power Systems Research*, vol. 58, no. 1, pp. 45 – 51, 2001.

[62] R. Romero, R. Gallego, and A. Monticelli, "Transmission system expansion planning by simulated annealing," in *Power Industry Computer Application Conference, 1995. Conference Proceedings., 1995 IEEE*, May 1995, pp. 278 –283.

[63] R. Gallego, A. Alves, A. Monticelli, and R. Romero, "Parallel simulated annealing applied to long term transmission network expansion planning," *Power Systems, IEEE Transactions on*, vol. 12, no. 1, pp. 181 –188, Feb. 1997.

[64] R. Teive, E. Silva, and L. Fonseca, “A Cooperative Expert System for Transmission Expansion Planning of Electrical Power Systems,” *Power Systems, IEEE Transactions on*, vol. 13, no. 2, pp. 636 –642, May 1998.

[65] R. Teive, A. Hawken, and M. Laugthon, “Knowledge-based System for Electrical Power Networks Transmission Expansion Planning,” in *Transmission and Distribution Conference and Exposition: Latin America, 2004 IEEE/PES*, Nov. 2004, pp. 435 – 440.

[66] J.-R. Shin and Y.-M. Park, “Optimal long-term Transmission Planning by Expert System Approach,” in *TENCON ’93. Proceedings. Computer, Communication, Control and Power Engineering.1993 IEEE Region 10 Conference on*, Oct. 1993, pp. 713 –717 vol.2.

[67] H. Sun and D. Yu, “A Multiple-objective Optimization Model of Transmission Enhancement Planning for Independent Transmission Company (ITC),” in *Power Engineering Society Summer Meeting, 2000. IEEE*, vol. 4, 2000, pp. 2033 –2038 vol. 4.

[68] R. Gallego, R. Romero, and A. Monticelli, “Tabu search algorithm for network synthesis,” *Power Systems, IEEE Transactions on*, vol. 15, no. 2, pp. 490 –495, May 2000.

[69] E. Da Silva, J. Ortiz, G. De Oliveira, and S. Binato, “Transmission network expansion planning under a Tabu Search approach,” *Power Systems, IEEE Transactions on*, vol. 16, no. 1, pp. 62 –68, Feb. 2001.

[70] F. Wen and C. Chang, “Transmission network optimal planning using the tabu search method,” *Electric Power Systems Research*, vol. 42, no. 2, pp. 153 – 163, 1997.

[71] P. Sensarma, M. Rahmani, and A. Carvalho, “A comprehensive method for optimal expansion planning using particle swarm optimization,” in *Power Engineering Society Winter Meeting, 2002. IEEE*, vol. 2, 2002, pp. 1317 – 1322 vol.2.

[72] P. Maghouli, S. Hosseini, M. Buygi, and M. Shahidehpour, “A Multi-Objective Framework for Transmission Expansion Planning in Deregulated Environments,” *Power Systems, IEEE Transactions on*, vol. 24, no. 2, pp. 1051 –1061, May 2009.

[73] H. Kakuta and H. Mori, “A Multi-objective Memetic Algorithm for probabilistic transmission network expansion planning,” in *Systems Man and Cybernetics (SMC), 2010 IEEE International Conference on*, Oct. 2010, pp. 1414 –1419.

[74] J. Contreras and F. Wu, "A kernel-oriented algorithm for transmission expansion planning," *Power Systems, IEEE Transactions on*, vol. 15, no. 4, pp. 1434 –1440, Nov. 2000.

[75] ——, "Coalition formation in transmission expansion planning," *Power Systems, IEEE Transactions on*, vol. 14, no. 3, pp. 1144 –1152, Aug. 1999.

[76] J. Contreras, "A cooperative game theory approach to transmission planning in power systems," *Ph.D., Univ. California Berkeley*, 1997.

[77] A. Orths and Z. Styczynski, "Game theoretical approach to power network planning," in *Power Tech Proceedings, 2001 IEEE Porto*, vol. 1, 2001, p. 6 pp. vol.1.

[78] O. Azadegan, R. Hager, F. Leuthold, K. Reich, T. Schreier, G. Layr, C. Todem, C. von Hirschhausen, O. Wadosch, and H. Weigt, "Price, Cost and Financial Aspects of Network Expansion in the European Context," *RealiseGrid Project Report*, Apr. 2010, last checked: 28.10.2014. [Online]. Available: http://realisegrid.rse-web.it/content/files/File/Publications%20and%20results/Deliverable_REALISEGRID_3.2.2.pdf

[79] J.-C. Kaltenbach, J. Peschon, and E. Gehrig, "A Mathematical Optimization Technique for the Expansion of Electric Power Transmission Systems," *Power Apparatus and Systems, IEEE Transactions on*, vol. PAS-89, no. 1, pp. 113 –119, Jan. 1970.

[80] J. Dodu and A. Merlin, "Dynamic Model for long-term Expansion Planning Studies of Power Transmission Systems: the Ortie Model," *International Journal of Electrical Power; Energy Systems*, vol. 3, no. 1, pp. 2 – 16, 1981.

[81] S. Binato and G. C. Oliveira, "A Heuristic Procedure to Cope with multi-year Transmission Expansion Planning," *IEEE/KTH Stockholm Power Tech. Conf.*, Jun. 1995.

[82] Entso-e. Ten Year Network Development Plan 2014. https://www.entsoe.eu/Documents/TYNDP%20documents/TYNDP%202014/141031%20TYNDP%202014.pdf. Last checked: 11.12.2014.

[83] ——. Guideline for Cost Benefit Analysis of Grid Development Projects. https://www.entsoe.eu/fileadmin/user_upload/_library/events/Workshops/CBA/131114_ENTSO-E_CBA_Methodology.pdf. Last checked: 11.12.2014.

[84] A. R. Ciupuliga and M. Gibescu, "Report on extension and harmonisation of transmission planning criteria," *RealiseGrid Project Report*, Nov. 2010.

[85] R. Calisti and M. V. Cazzol, "Tool for the assessment of benefits given by the expansion of transmission infrastructures," *RealiseGrid Project Report*, Jun. 2011.

[86] European University Institute. Cost Benefit Analysis in the Context of the Energy Infrastructure Package. http://www.eui.eu/Projects/THINK/Research/Topic10.aspx. Last checked: 11.12.2014.

[87] O. Gjerde, L. Warland, L. Aleixo, and I. H. Doskeland, "Integrated approach for reliability of electricity supply analysis studies of demonstration network," *Cigre Session*, Aug. 2012.

[88] S. P. Vajjhala and P. S. Fischbeck, "Quantifying siting difficulty: A case study of us transmission line siting," *Energy Policy*, vol. 35, no. 1, pp. 650 – 671, 2007. [Online]. Available: http://www.sciencedirect.com/science/article/pii/S0301421506000048

[89] H. Ergun, D. Van Hertem, and R. Belmans, "Identification of Power Injection Capabilities for Transmission System Investment Optimization," *10th IEEE PowerTech Conference*, Jun. 2013, Grenoble, France.

[90] R. D. Zimmerman and C. E. Murillo-Sánchez, "MATPOWER: Steady-State Operations, Planning, and Analysis Tools for Power Systems Research and Education," *IEEE Transactions on Power Systems*, vol. 26, pp. 12 – 19, 2011.

[91] D. Oeding and B. Oswald, *Elektrische Kraftwerke und Netze*, 6th ed. Springer-Verlag, 2004, ISBN 3-540-00863-2.

[92] D. University of Washington. Power System Test Case Archive, 118 Bus Power Flow Test Case. http://www.ee.washington.edu/research/pstca/pf118/pg_tca118bus.htm.

[93] B. Borkowska, "Probabilistic Load Flow," *IEEE Transactions on Power Apparatus and Systems*, vol. 3, pp. 752–759, 1974.

[94] R. Allan, B. Borkowska, and C. Grigg, "Probabilistic Analysis of Power Flows," *Proceedings of the Institution of Electrical Engineers*, vol. 121, pp. 1551–1556, 1974.

[95] W. Charytoniuk and J. Niebrzydowski, "Confidence interval construction for load forecast," *Electric Power Systems Research*, vol. 48, no. 2, pp. 97 – 103, 1998. [Online]. Available: http://www.sciencedirect.com/science/article/pii/S0378779698000935

[96] G. Valverde, A. Saric, and V. Terzija, “Probabilistic load flow with non-Gaussian correlated random variables using Gaussian mixture models,” *IET Generation, Transmission & Distribution*, vol. 6, no. 7, pp. 701–709, 2012. [Online]. Available: http://link.aip.org/link/?GTD/6/701/1

[97] H. Sirisena and E. P. M. Brown, “Representation of non-gaussian probability distributions in stochastic load-flow studies by the method of gaussian sum approximations,” *Generation, Transmission and Distribution, IEE Proceedings C*, vol. 130, no. 4, pp. 165–171, Jul. 1983.

[98] G. Valverde, A. T. Saric, and V. Terzija, “Stochastic Monitoring of Distribution Networks Including Correlated Input Variables,” *Power Systems, IEEE Transactions on*, vol. PP, no. 99, p. 1, 2012.

[99] A. Runnalls, “Kullback-leibler approach to gaussian mixture reduction,” *Aerospace and Electronic Systems, IEEE Transactions on*, vol. 43, no. 3, pp. 989–999, Jul. 2007.

[100] J. Williams and P. Maybeck, “Cost-function-based gaussian mixture reduction for target tracking,” in *Information Fusion, 2003. Proceedings of the Sixth International Conference of*, vol. 2, Jul. 2003, pp. 1047–1054.

[101] Elia. Hourly system loads 2012. http://www.elia.be/en/grid-data/data-download.

[102] J. Guo, Y. Fu, Z. Li, and M. Shahidehpour, “Direct Calculation of Line Outage Distribution Factors,” *IEEE Transactions on Power Systems*, vol. 24, pp. 1633–1634, Aug. 2009.

[103] N. G. Hingorani and L. Gyugyi, *Understanding FACTS*. IEEE Press, New York-USA, 2000, ISBN 0-7803-3455-8.

[104] N. Srinivasan, K. Prakasa Rao, C. Indulkar, and S. Venkata, “On-line computation of phase shifter distribution factors and lineload alleviation,” *Power Apparatus and Systems, IEEE Transactions on*, vol. PAS-104, no. 7, pp. 1656 –1662, Jul. 1985.

[105] Han, Z.X., “Phase Shifter and Power Flow Control,” *Power Apparatus and Systems, IEEE Transactions on*, vol. PAS-101, no. 10, pp. 3790–3795, Oct 1982.

[106] J. Verboomen, D. Van Hertem, P. Schavemaker, W. Kling, and R. Belmans, “Border-flow control by means of phase shifting transformers,” in *IEEE Power Tech, Lausanne*, Jul. 2007, pp. 1338 –1343.

[107] W. Kling, D. Klaar, J. Schuld, A. Kanters, C. Koreman, H. Reijnders, and C. Spoorenberg, "Phase shifting transformers installed in The Netherlands in order to increase available international transmission capacity," in *Cigre Sessions 2004*, 2004.

[108] J. Rimez, R. V. D. Planken, D. Wiot, E. Jottrand, G. Claessens, and J. Declercq, "Grid Implementation of a 400MVA 220/150kV $15°/+3°$ Phase Shifting Transformer For Power Flow Control in the Belgian Network: Specification and Operational Considerations," in *Cigre Sessions 2006*, Paris, 2006.

[109] R. D. Zimmerman and C. E. Murillo-Sánchez, "Matpower 4.1 User's Manual," Dec. 2011. [Online]. Available: http://www.pserc.cornell.edu/matpower/manual.pdf

[110] T. Achterberg, "Constraint integer programming," Ph.D. dissertation, Technische Universität Berlin, 2009. [Online]. Available: scip.zib.de

[111] SCIP. (2014) Solving Constraint Integer Programs. http://scip.zib.de. Last checked: 10.12.2014.

[112] Industrial Information and Control Centre New Zeeland. (2014) Opti Toolbox. http://www.i2c2.aut.ac.nz/Wiki/OPTI/. Last checked: 10.12.2014.

[113] IBM. (2014) CPLEX Optimizer. hhttp://www-01.ibm.com/software/commerce/optimization/cplex-optimizer/. Last checked: 10.12.2014.

[114] E. Dijkstra, "A Note on Two Problems in Connexion with Graphs," *Numerische Mathematik*, vol. 1, no. 1, pp. 269–271, 1959.

[115] R. Dechter and J. Pearl, "Generalized Best-first Search Strategies and the Optimality of A*," *J. ACM*, vol. 32, no. 3, pp. 505–536, Jul. 1985. [Online]. Available: http://doi.acm.org/10.1145/3828.3830

[116] C. Grigg, P. Wong, P. Albrecht, R. Allan, M. Bhavaraju, R. Billinton, Q. Chen, C. Fong, S. Haddad, S. Kuruganty, W. Li, R. Mukerji, D. Patton, N. Rau, D. Reppen, A. Schneider, M. Shahidehpour, and C. Singh, "The IEEE Reliability Test System-1996. A report prepared by the Reliability Test System Task Force of the Application of Probability Methods Subcommittee," *Power Systems, IEEE Transactions on*, vol. 14, no. 3, pp. 1010–1020, 1999.

[117] H. Ergun, D. Van Hertem, and R. Belmans, "Building A New OVerlay Grid For Europe," in *IEEE PES General Meeting*, Jul. 2012.

[118] European Climate Foundation (ECF), "Power Perspectives 2030 - On the road to a decarbonised power sector," http://www.roadmap2050.eu/attachments/files/PowerPerspectives2030_FullReport.pdf, ECF, Tech. Rep., 2011.

[119] Socio-economic Data and Applications Center. (2014) Population density map of Europe. http://sedac.ciesin.columbia.edu/maps/gallery/search/2?facets=theme:population&facets=region:europe. Last checked: 28.10.2014.

[120] ——. (2014) Elevation map of Europe. http://sedac.ciesin.columbia.edu/maps/gallery/search?facets=region%3Aeurope&contains=elevation. Last checked: 28.10.2014.

[121] Q. Zhou and J. Bialek, "Approximate model of european interconnected system as a benchmark system to study effects of cross-border trades," *Power Systems, IEEE Transactions on*, vol. 20, no. 2, pp. 782–788, May 2005.

[122] Wikipedia. (2014) Cost of electricity by source. http://en.wikipedia.org/wiki/Cost_of_electricity_by_source. Last checked: 28.10.2014.

[123] H. Ergun, D. Van Hertem, and R. Belmans, "Transmission system topology optimization for large-scale offshore wind integration," *Sustainable Energy, IEEE Transactions on*, vol. 3, no. 4, pp. 908–917, 2012.

[124] ——, "Optimization Tool for Offshore Wind Connections," *CIGRE Symposium - Innovation for Secure and Efficient Transmission Grids*, 2014, (art. nr. 3A - 122), Brussels-Belgium.

List of publications

Journal Publications

- Ergun, H., Rawn, B., Belmans, R., Van Hertem, D. Investment Plan Optimization for Long Term, Large Scale and Multizonal Transmission System Expansion. *Submitted to IEEE Transactions on Power Systems*
- Ergun, H., Rawn, B., Belmans, R., Van Hertem, D. (2014). Technology and Topology Optimization for Multizonal Transmission Systems. IEEE Transactions on Power Systems, 29 (5), 2469-2477.
- Ergun, H., Van Hertem, D., Belmans, R. (2012). Transmission System Topology Optimization for Large-Scale Offshore Wind Integration. IEEE Transactions on Sustainable Energy, 3 (4), 908-917.
- De Rijcke, S., Ergun, H., Van Hertem, D., Driesen, J. (2012). Grid Impact of Voltage Control and Reactive Power Support by Wind Turbines Equipped With Direct-Drive Synchronous Machines. IEEE Transactions on Sustainable Energy, 3 (4), 890-898.

Conference Publications

- Ergun, H., Van Hertem, D., Belmans, R. Optimal Design of a North Sea Transmission Grid Considering Spatial and Temporal Aspects *Abstract submitted to IEEE PowerTech Conference 2015*
- Ergun, H., Van Hertem, D., Belmans, R. (2014). Optimization Tool for Offshore Wind Connections. CIGRE Belgium 2014 - Innovation for Secure and Efficient Transmission Grids, 12-13 March 2014 (art.nr. 3A - 122).

- Ergun, H., Van Hertem, D., Belmans, R. (2013). Identification of Power Injection Capabilities for Transmission System Investment Optimization. IEEE PowerTech Conference. Grenoble - France, 16-20 June 2013.

- Tielens, P., Ergun, H., Van Hertem, D. (2012). Techno-economic Analysis of Large-scale Integration of Solar Power Plants in the European Grid. International Solar Integration Workshop. Lisbon, Portugal, 12-13 November 2012.

- Ergun, H., Beerten, J., Van Hertem, D. (2012). Building a new overlay grid for Europe. Proceedings of the IEEE PES General meeting 2012. IEEE PES General Meeting. San Diego, 22-26 July 2012 (pp. 1-10).

- Ergun, H., Van Hertem, D., Belmans, R. (2011). Multi level optimization for offshore grid planning. Cigrè International Symposium THE ELECTRIC POWER SYSTEM OF THE FUTURE Integrating supergrids and microgrids. Bologna-Italy, 13-16 September 2011.

- De Rijcke, S., Ergun, H., De Vos, K., Driesen, J. (2011). Grid Integration of Large-scale Wind Turbines Equipped With Full Converters: Belgian Case Study. . EWEA Event. Brussels, 14-17 March 2011.

- Ergun, H., Van Hertem, D., Belmans, R. (2010). CoST Of Wind - Appropriate Connection Selection Tool for Offshore Wind Farms. International Workshop on Large-Scale Integration of Wind Power into Power Systems as well as on Transmission Networks for Offshore Wind Power Plans. Quebec, 18-19 October 2010.

- Ergun, H., Renner, H., Friedl, K. (2010). Characteristic Spectra of Harmonic Currents in Austrian Electricity Transmission an Distribution Networks. The 7th Conference 2010 electric Power Quality and Supply Reliability. Electric Power Quality and Supply Reliability. Tallinn, 16-18 June 2010.

Curriculum Vitae

Hakan Ergun

Born on February, the 16^{th}, 1983 in Leoben, Austria

1998 - 2003	Secondary school HTBL Kapfenberg, Austria Technical secondary school for electrical engineering
2003 - 2004	Military service in Zeltweg, Austria
2004 - 2009	Master of science in electrical engineering Graz University of Technology, Austria
2010 - 2015	Ph.D in electrical engineering Department of Electrical Engineering - ESAT Division, Electrical Energy and Computer Architectures, ELECTA KU Leuven, Belgium

FACULTY OF ENGINEERING SCIENCE
DEPARTMENT OF ELECTRICAL ENGINEERING
DIVISION OF ELECTRICAL ENERGY AND COMPUTER ARCHITECTURES (ELECTA)
Kasteelpark Arenberg 10, Bus 2445
B-3001 Heverlee
hakan.ergun@esat.kuleuven.be
http://www.esat.kuleuven.be/electa